**INSTITUTE**

FOR

**COSMIC RAY RESEARCH**

UNIVERSITY OF TOKYO

# ANNUAL REPORT
# (APRIL 2007 – MARCH 2008)

# TABLE OF CONTENTS

# PREFACE

This report summarizes the scientific activities of the Institute for Cosmic Ray Research (ICRR) of the University of Tokyo in the Japanese FY 2007.

ICRR is an inter-university research institute for studies of cosmic rays. The headquarters of ICRR is located in Kashiwa, Chiba prefecture, Japan. In order to promote various cosmic-ray-related studies efficiently, ICRR has three research divisions; Neutrino and Astroparticle division, High Energy Cosmic Ray division, and Astrophysics and Gravity division. ICRR has 3 observatories in Japan; Kamioka Observatory (Kamioka underground, Gifu prefecture), Norikura Observatory (2770 meters asl, Mt. Norikura, Gifu prefecture), and Akeno Observatory (Yamanashi prefecture). In addition, there are 3 major experimental facilities outside of Japan. They are located in Utah in USA, Yangbajing in Tibet, China, and Woomera in Australia.

More than 300 researchers from various Japanese institutions are involved in the research programs of ICRR. It should be noted that most of the scientific outputs from this institute are the results of the collaborative efforts by many institutions. In order to produce outstanding results, it is very important to carry out an experiment by an international collaboration composed of top-level researchers all over the world. Hence, most of the experimental collaborations that ICRR is involved are international ones. For example, the number of collaborators in the Super-Kamiokande experiment is about 130; among them 60 are from abroad (USA, Korea, China and Poland).

Many exciting scientific activities are described in this report. One of the highlights is the start of the Telescope Array experiment, which is a very large scale cosmic ray experiment to study the highest energy cosmic rays. We hope that this report is useful for the understanding of the current research activities of ICRR. Finally, we appreciate very much the strong support of our colleagues in this research field, the University of Tokyo and the Japanese Ministry of Education, Culture, Sports, Science and Technology. They are indispensable for the continuing, and exciting scientific outcome of ICRR.

Takaaki Kajita,
Director,
Institute for Cosmic Ray Research,
The University of Tokyo

The ICRR building at Kashiwa, Chiba, Japan.
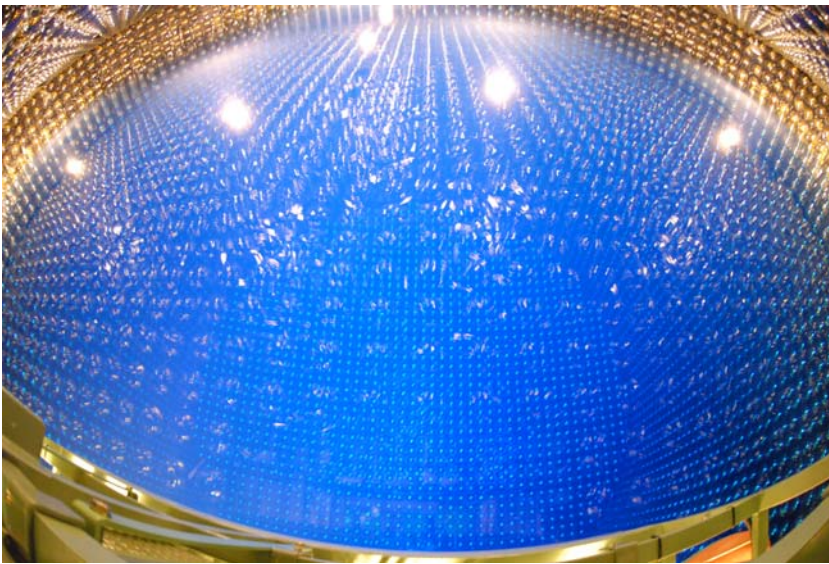


The inner detector of Super-Kamiokande-III during the full reconstruction. The purified water is under filling.



The system of four imaging atmospheric Cherenkov telescopes of 10m diameter of CANGAROO project for detection of very high energy gamma-rays The whole system is in operation since March 2004 in Woomera, South Australia.

Tibet-III air shower array (37000 m$^2$) at Yangbajing, Tibet (4300 m in altitude).



Air fluorescence telescopes (left) and a scintillator surface detector (right) of the Telescope Array experiment under construction in Utah, USA for the study of extremely high energy cosmic rays.
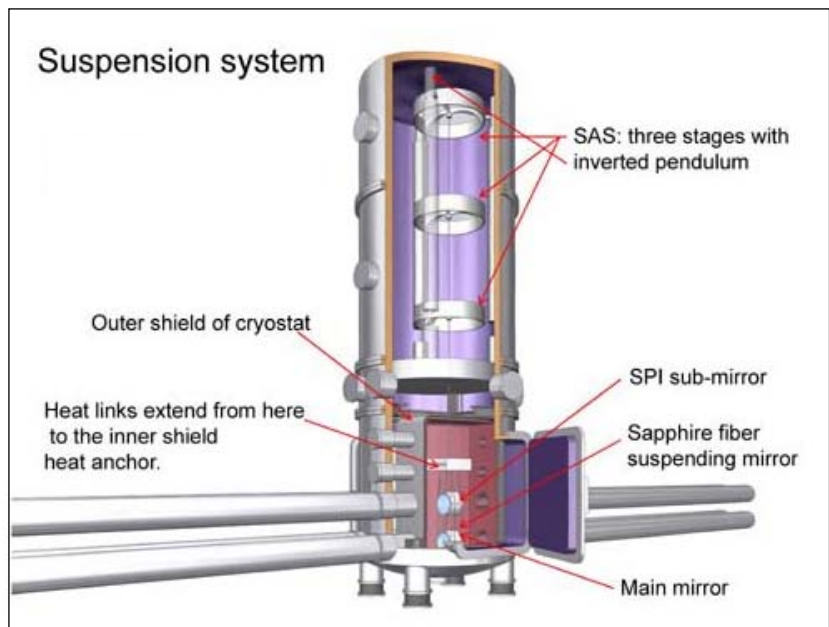


Cryogenic mirror suspension system for Large Scale Cryogenic Gravitational Wave Telescope.

Wide-view telescope of 2.5 m diameter (left telescope) in Arizona, USA for the Sloan Digital Sky Survey project.



A public lecture held by Research Center for Cosmic Neutrinos.

# Organization

```
Board of Councillors ──┬── Faculty Council          ┌── Research Division
                       │                            │      ├─ Neutrino and Astroparticle Division
Director ──────────────┤                            │      ├─ High Energy Cosmic Ray Division
                       │                            │      └─ Astrophysics and Gravity Division
Vice-Director ─────────┴── Advisory Committee        ├── Facilities
                              │                      │      ├─ Kamioka Observatory
                              └── User's Committee    │      ├─ Akeno Observatory
                                                      │      ├─ Norikura Observatory
                                                      │      └─ Research Center for Cosmic Neutrinos
                                                      │            └─ Low-level Radioisotope Measurement Facility
                                                      └── Administration Division
```
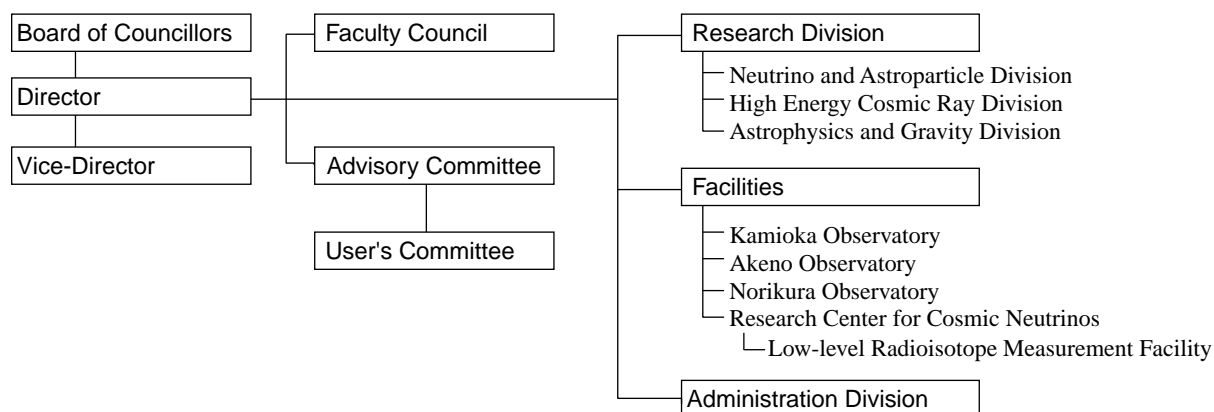
## Number of Staff Members in 2007

|  | Scientific Staff | Technical Staff | Research Fellows | Administrators and Secretaries |  |
|---|---|---|---|---|---|
| Neutrino and Astroparticle Div. | 18 | 5 | 3 | 13 | 39 |
| High Energy Cosmic Ray Div. | 13 | 11 | 10 | 4 | 38 |
| Astrophysics and Gravity Div. | 8 | 0 | 4 | 1 | 13 |
| Administration | 0 | 0 | 1 | 13 | 14 |
| Total | 39 | 16 | 18 | 31 | 104 |

## FY 2002–2007 Budget

|  | 2002 | 2003 | 2004 | 2005 | 2006 | 2007 |
|---|---|---|---|---|---|---|
| Personnel expenses | 460 332 | 434 874 | 539 000 | 465 000 | 566 000 | 624 000 |
| Non-personnel expenses | 1 518 065 | 1 785 449 | 1 902 000 | 1 822 000 | 812 000 | 1 253 000 |
| Total | 1 978 397 | 2 220 323 | 2 441 000 | 2 287 000 | 1 378 000 | 1 877 000 |

(in 1 000 yen)

# RESEARCH DIVISIONS

## Neutrino and Astroparticle Division

**Overview**
**Super-Kamiokande Experiment**
**K2K Experiment**
**T2K Experiment**
**XMASS Experiment**

## High Energy Cosmic Ray Division

**Overview**
**CANGAROO-III Project**
**TA: Telescope Array Experiment**
**Tibet AS$\gamma$ Project**
**Ashra Project**

## Astrophysics and Gravity Division

**Overview**
**TAMA Project**
**LCGT Project**
**CLIO Project**
**Sloan Digital Sky Survey**
**Theory Group**
    Lepton Flavour Violating $\tau$ Decays in the Left-Right Symmetric Model
    Probing Majorana Phases and Neutrino Mass Spectrum in the Higgs Triplet Model at the LHC
    Unitarity bounds in the Higgs model including triplet fields with custodial symmetry
    Neutralino Dark Matter in Light Higgs Boson Scenario
    Relic abundance of dark matter in universal extra dimension models with right-handed neutrinos
    Primordial Non-Gaussianity in Multi-Scalar Slow-Roll Inflation
    Non-Gaussianity in the modulated reheating scenario
    Primordial Non-Gaussianity in Multi-Scalar Inflation
    Non-Gaussianity, Spectral Index and Tensor Modes in Mixed Inflaton and Curvaton Models
    "Flavored" Electric Dipole Moments in Supersymmetric Theories
    Stability of Metastable Vacua in Gauge Mediated SUSY Breaking Models with Ultra Light Gravitino
    Cosmological constraints on neutrino injection
    Affleck-Dine leptogenesis via multiscalar evolution in a supersymmetric seesaw model
    Formation of IMBHs as PBHs in the inflationary cosmology with running spectral index
    Increasing effective number of neutrinos by decaying particles
    Baryon Asymmetry in Heavy Moduli Scenario
    Nonthermal dark matter in mirage mediation
    Cosmological implications of supersymmetric axion models
    Space laser interferometers can determine the thermal history of the early Universe
    Cosmological Constraints on Isocurvature and Tensor Perturbations
    Primordial Helium Abundance from CMB: a constraint from recent observations and a forecast

    Probing the Effective Number of Neutrino Species with Cosmic Microwave Background

# NEUTRINO AND ASTROPARTICLE DIVISION

## Overview

This division aims to study particle physics that is not accessible within accelerator facilities, with prime interests in physics of neutrinos and proton decay, and astroparticle physics with the use of underground experimental facilities.

Our most important facility is the Super-Kamiokande (SK) detector. It is a 50 kton water Cherenkov detector using 11,146 50 cm-diameter photomultipliers (PMTs) for its inner detector and 1,885 20 cm-diameter PMTs for its outer detector. The data taking of SK started in April 1996. The most important physics results are the discovery of neutrino oscillation in atmospheric neutrinos in 1998 and thereby demonstrating that neutrinos have a finite mass, and the accurate measurement of the solar neutrino flux from the decay of $^8$B which served to confirm the long-conjectured neutrino oscillation hypothesis in solar neutrinos beyond doubt. The search for nucleon decay at SK gives the current best limit which strongly constrains the grand unification scenario of particle interactions. SK has been monitoring for neutrinos from supernova bursts. If a supernova burst occurs at a distance from the center of our galaxy, SK will be able to detect about 8,000 neutrino events. A high intensity neutrino beam experiment at J-PARC (T2K) is expected to start in 2009 with the SK detector as the far detector of the experiment. High precision measurement of oscillation parameters and the third oscillation pattern (the effect of the mixing angle $\theta_{13}$) will be investigated by T2K.

Another activity of the Neutrino and Astroparticle division is a multi-purpose experiment using liquid xenon aiming at the detection of cold dark matter, neutrino absolute mass using neutrinoless double beta decay, and low energy solar neutrinos. An R&D study for the liquid xenon detector had been performed at the underground laboratory and the construction of the 800 kg detector was started from 2007.

Recent progress of research activities in the Neutrino and Astroparticle division is presented here.

## Atmospheric neutrinos

Cosmic ray interactions in the atmosphere produce neutrinos. The prediction of the absolute flux has an uncertainty of at least $\pm 20\%$. However, the flavor ratio of the atmospheric neutrino flux, $(\nu_\mu + \bar{\nu}_\mu)/(\nu_e + \bar{\nu}_e)$, has been calculated to an accuracy of better than 5%. Another important feature of atmospheric neutrinos is that the fluxes of upward and downward going neutrinos are expected to be nearly equal for $E_\nu >$(a few GeV) where the geomagnetic effect on primary cosmic rays is negligible.

SK-I observed 12,180 fully-contained (FC) events and 911 partially-contained (PC) events during 1489 days of data taking and SK-II observed 6605 FC events and 427 PC events during 804 days. FC events deposit all of their Cherenkov light in the inner detector, while PC events have exiting tracks which deposit some Cherenkov light in the outer detector. The

Table 1. Summary of the atmospheric $(\mu/e)_{data}/(\mu/e)_{MC}$ ($\equiv R$) ratio measurement.

| | SK-I | | SK-II | |
|---|---|---|---|---|
| | Data | MC | Data | MC |
| Sub-GeV | | | | |
| $e$-like | 3353 | 2879.8 | 1842 | 1554.5 |
| $\mu$-like | 3227 | 4212.8 | 1723 | 2215.4 |
| $R$ | $0.658 \pm 0.016 \pm 0.035$ | | $0.656 \pm 0.022 \pm 0.033$ | |
| Multi-GeV | | | | |
| $e$-like | 746 | 680.5 | 417 | 426.2 |
| $\mu$-like(FC+PC) | 1562 | 2029.5 | 806 | 1103.8 |
| $R$ | $0.702^{+0.032}_{-0.030} \pm 0.101$ | | $0.746^{+0.047}_{-0.044} \pm 0.056$ | |

neutrino interaction vertex was required to have been reconstructed within the 22.5 kiloton fiducial volume, defined to be $> 2$ m from the PMT wall.

The FC events were classified into "sub-GeV" ($E_{vis} < 1330$ MeV) and "multi-GeV" ($E_{vis} > 1330$ MeV) samples. The numbers of observed and predicted events for sub- and multi-GeV energy regions in SK are summarized in Table 1. The prediction is based on the recent precise measurements of primary cosmic rays by BESS, AMS and a three dimensional calculation of the neutrino flux by Honda *et al*. The hadronic interaction model of cosmic rays is also improved in the calculation.

Among FC events, single-ring events are identified as $e$-like or $\mu$-like based on a Cherenkov ring pattern. All the PC events were assigned to be multi-GeV $\mu$-like. Using the number of $e$-like and $\mu$-like events, the ratio of $(\mu/e)$ was obtained and it is significantly smaller than the expectation as shown in the table. The momentum resolution of SK-II is slightly worse than SK-I. This is because the number of ID PMTs in SK-II is about half that of SK-I. However, the performance of the vertex reconstruction, the ring counting, and the particle identification in SK-II are almost the same as in SK-I.

The zenith angle distributions for the sub- and multi-GeV samples are shown in Fig. 1. The $\mu$-like data from SK exhibit a strong up-down asymmetry in zenith angle ($\Theta$) while no significant asymmetry was observed in the $e$-like data. The data were compared with the Monte Carlo expectation without neutrino oscillations and the best-fit expectation for $\nu_\mu \leftrightarrow \nu_\tau$ oscillations. The oscillated Monte Carlo reproduced the zenith angle distributions of the data well. Some fraction of the multi-ring events is also subdivided into $e$-like and $\mu$-like events using the event pattern of the most energetic Cherenkov ring in each event. Fig. 2 shows the zenith angle distribution of multi-ring events which also agrees well with the expectation from neutrino oscillations.

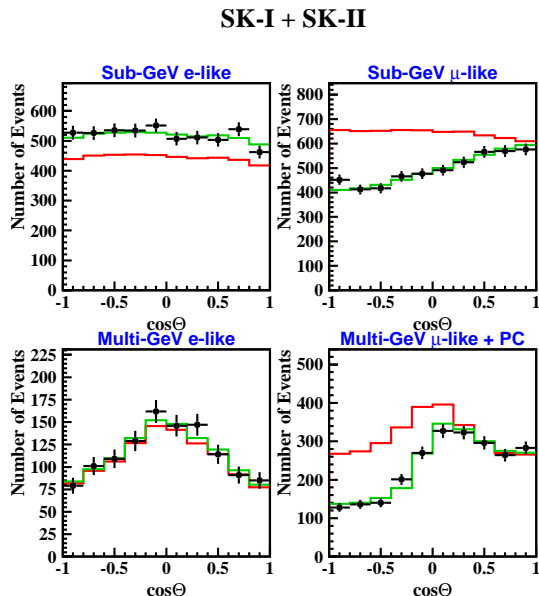Energetic atmospheric $\nu_\mu$'s passing through the Earth in-

## SK-I + SK-II



Fig. 1. The zenith angle distributions for sub-GeV $e$-like, sub-GeV $\mu$-like, multi-GeV $e$-like and multi-GeV (FC+PC) $\mu$-like events. cos$\Theta$ =1 means down-going particles. The red histograms show the MC prediction without neutrino oscillation. The green histograms show the Monte Carlo prediction for $\nu_\mu \leftrightarrow \nu_\tau$ oscillations with $\sin^2 2\theta = 1.0$ and $\Delta m^2 = 2.5 \times 10^{-3}$eV$^2$.
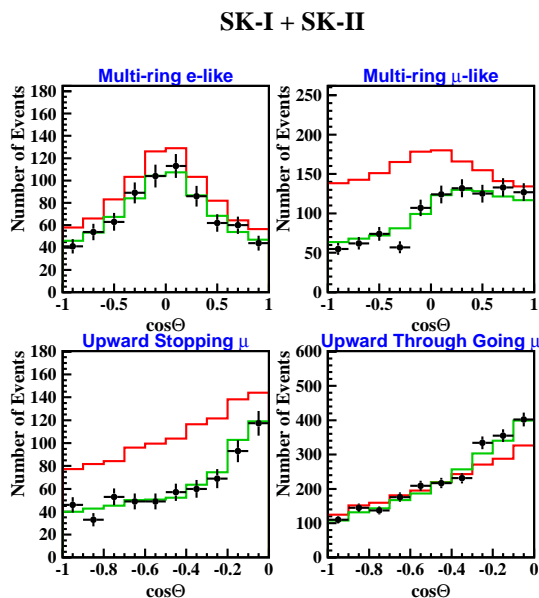
## SK-I + SK-II



Fig. 2. The zenith angle distributions for multi-ring sub-GeV $\mu$-like (upper left) and multi-ring multi-GeV $\mu$-like (lower left) samples. The zenith angle distributions of upward stopping muons (upper right) and upward through-going muons (lower right). The red histograms show the MC expectation without neutrino oscillations. The green histograms show the expected flux for the $\nu_\mu \leftrightarrow \nu_\tau$ oscillation with $\sin^2 2\theta = 1.0$ and $\Delta m^2 = 2.5 \times 10^{-3}$eV$^2$.

teract with rock surrounding the detector and produce muons via charged current interactions. These neutrino events are observed as upward going muons. Upward going muons are classified into two types. One is "upward through-going muons" which have passed through the detector, and the other is "upward stopping muons" which come into and stop inside the detector. The mean neutrino energy of upward through-going muons and upward stopping muons is $\sim$100 GeV and $\sim$10 GeV, respectively. SK-I observed 1856 upward through-going muons and 458 upward stopping muons during 1646 day livetime exposure and SK-II observed 889 and 228 events during 828 days, respectively. Fig. 2 shows the zenithangle distributions of those upward muons. They agree with the MC expectation assuming neutrino oscillations.

We carried out a neutrino oscillation analysis using the entire SK-I and II atmospheric neutrino data set. Fig. 3 shows the allowed neutrino oscillation paramteer regions for $\nu_\mu \leftrightarrow \nu_\tau$ oscillations. The best fit oscillation parameters are $\sin^2 2\theta = 1.0$ and $\Delta m^2 = 2.5 \times 10^{-3}$eV$^2$. The allowed oscillation parameter range is $\sin^2 2\theta > 0.93$ and $\Delta m^2 = (1.9 - 3.1) \times 10^{-3}$eV$^2$ at 90 % C.L.
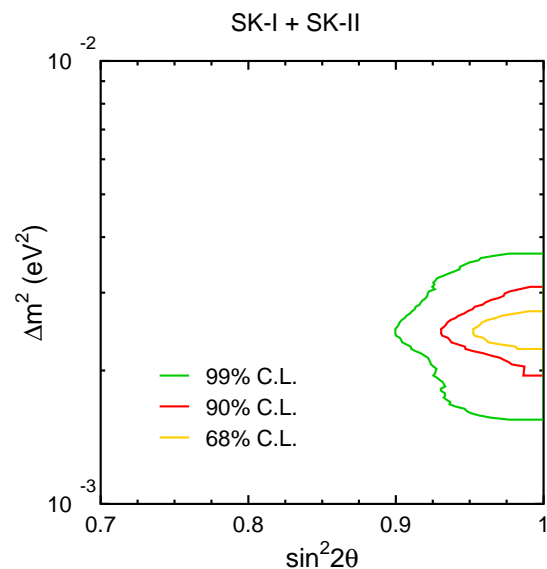


Fig. 3. Allowed region of $\nu_\mu \rightarrow \nu_\tau$ neutrino oscillation parameters obtained by SK using contained atmospheric neutrino events and upward-going muon events.

The atmospheric neutrino data is well described by neutrino oscillations as shown above. In this case, the survival probability of a $\nu_\mu$ is given by a sinusoidal function of $L/E$, where $L$ is the travel distance. $E$ is the neutrino energy. However, the sinusoidal $L/E$ dependence of this survival probability of $\nu_\mu$ has not yet been directly observed. We used a selected sample of these atmospheric neutrino events, those with good resolution in $L/E$, to search for an oscillation maximum in the $L/E$ distribution.

The neutrino energy, $E$, was estimated from the total energy of charged particles observed in the inner detector. The flight length of neutrinos, $L$, which ranges from approximately 15 km to 13,000 km depending on the neutrino zenith angle, was estimated from the reconstructed neutrino direction. The

neutrino direction was taken to be along the total momentum vector of all observed particles. Since the correlation between the neutrino directions and the directions of observed particles is taken into account in the Monte Carlo simulations, we applied the same analysis techniques to both real events and Monte Carlo events. We applied a cut to reject low energy or horizontal-going events since they have either large scattering angles or large $dL/d\Theta_{zenith}$.

Fig. 4 shows the observed $L/E$ distribution of the ratio of data events to unoscillated MC events. In the figure, a dip which corresponds to the first oscillation maximum, is observed around $L/E = 500\,\mathrm{km/GeV}$. The distribution was fit assuming $\nu_\mu \leftrightarrow \nu_\tau$ oscillations. The best-fit expectation shown in the figure corresponds to $(\sin^2 2\theta, \Delta m^2) = (1.00, 2.3 \times 10^{-3}\mathrm{eV}^2)$. Fig. 5 shows the contour plot of the allowed oscillation parameter regions. This result is consistent with that of the oscillation analysis using zenith angle distributions. The observed $L/E$ distribution gives the first direct evidence that the neutrino survival probability obeys the sinusoidal function predicted by neutrino flavor oscillations.
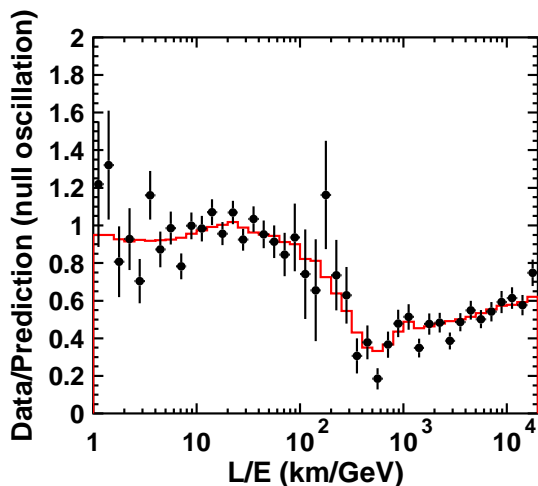


Fig. 5. 68, 90 and 99 % C.L. allowed oscillation parameter regions for 2-flavor $\nu_\mu \leftrightarrow \nu_\tau$ oscillations obtained in the $L/E$ analysis.



Fig. 4. Ratio of the data to the MC events without neutrino oscillation (points) as a function of the reconstructed $L/E$ together with the best-fit expectation for 2-flavor $\nu_\mu \leftrightarrow \nu_\tau$ oscillations (red line). The error bars are statistical only.



Fig. 6. The zenith angle distribution for tau candidate events in the likelihood analysis. The dashed histogram (background neutrinos) and the solid line (excess of $\nu_\tau$) show the best fit for the data.

Another interest is an observation of $\nu_\tau$ in the atmospheric neutrinos since there has not yet been evidence for appearance of $\nu_\tau$ charged current interactions due to $\nu_\mu \leftrightarrow \nu_\tau$ oscillations. We have performed a search for the $\nu_\tau$ appearance by using the SK-I atmospheric neutrino data [4]. The analysis is based on two statistical methods: a likelihood analysis and a neural network. Since $\tau$'s produced in the Super-K detector would immediately decay into many hadrons, the event pattern would be similar to that of high-energy multi-ring $\nu_e$ events. Using the statistical difference in $\tau$-like and background events, we have derived variables to select an enriched sample of $\nu_\tau$ charged current events in the atmospheric neutrino data. The differences appear in the energy spectrum, the number of charged pions in the final state, and in the fraction of lepton energy with respect to neutrino energy. We optimized a combination of the variables and defined a likelihood function so that the signal to noise ratio becomes maximal.
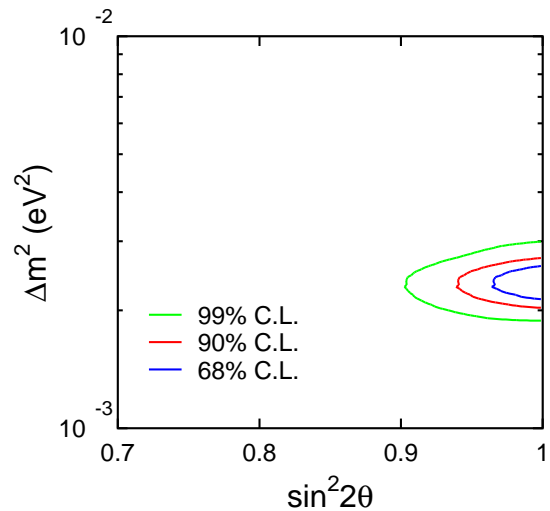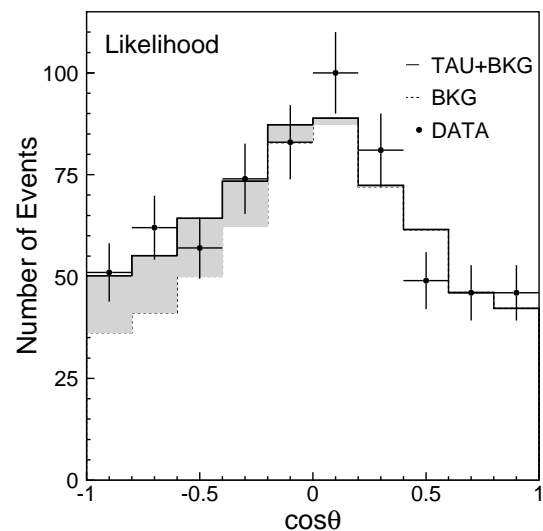
We also use the neural network for the analysis. Before these analyses, we applied pre-selection cuts on: (1) fiducial volume, (2) multi-GeV, and (3) the most energetic ring is $e$-like.

After the pre-selection cuts based on the likelihood and neural network, we fit the zenith angle distribution of the $\nu_\tau$ enriched sample to a combination of the expected $\nu_\tau$ and the atmospheric neutrinos ($\nu_\mu$ and $\nu_e$) including oscillations at $\sin^2 2\theta = 1.0$ and $\Delta m^2 = 2.1 \times 10^{-3}\mathrm{eV}^2$. Fig. 6 shows the fitted zenith angle distribution. Using $\tau$ selection efficiencies estimated by Monte Carlo study, we concluded the number of tau events during the SK-I exposure is $138 \pm 48\,^{+14.8}_{-31.6}$ with the likelihood analysis and $134 \pm 48\,^{+16.0}_{-27.2}$ with the neural network while $78.4 \pm 26$ and $8.4 \pm 27$ are expected for each analysis. Thus the fitted results are found to be consistent with pure $\nu_\mu \leftrightarrow \nu_\tau$ oscillations and $\nu_\tau$ appearance.

Two flavor neutrino oscillations successfully describe the

SK atmospheric neutrino data. However, contributions by electron neutrino oscillations have not been observed yet. We extended our neutrino oscillation analysis in order to treat three neutrino flavors. For the analysis, $\Delta m_{23}^2 \sim \Delta m_{13}^2 \equiv \Delta m^2 >> \Delta m_{12}^2$ was assumed. If the parameter $\theta_{13}$ in the mixing matrix of lepton sector (MNS matrix) is finite, neutrino oscillations among $\nu_\mu \leftrightarrow \nu_e$ may be observed. Moreover, the mixing parameter is affected by potentials caused by matter and oscillations are expected to be resonantly enhanced around 5 GeV. Therefore, we can expect an increase of upward-going Multi-GeV $e$-like events. Fig. 7 shows the result of the three-flavor neutrino oscillation analysis. Though there was no significant excess of electrons, we set an upper limit on $\theta_{13}$. More statistics are needed to improve sensitivity [5].

neutrino. We assume that the mass variation of the neutrinos depends only upon the electron density of the environment, a possible effect from radiative couplings of active neutrinos and electrons. To test for this density dependence, we replace $\Delta m^2$ in the equation for the oscillation probability with an effective mass difference that is proportional to the electron density of the medium, $\Delta m^2 \rightarrow \Delta m^2 \times (\frac{\rho_e}{\rho_0})^n$, where $\rho_e$ is the electron density of the matter, $n$ parameterizes the density dependence and $\rho_0$ is set at $6.02 \times 10^{23} e/cm^3$. Figure 8 shows the relative-$\chi^2$ confidence level contours on the $\Delta m^2$ versus $n$ plane. A minimum $\chi^2$=174.3/178 d.o.f. is obtained at (n,$\Delta m^2$)=(-0.04, $1.95 \times 10^{-3} eV^2$). This result is consistent with the standard 2-flavor oscillation result [6].
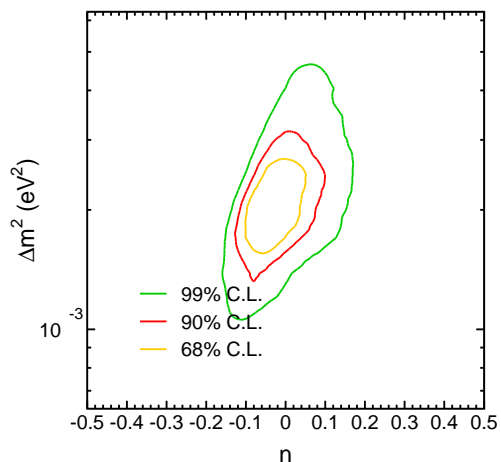


Fig. 8. relative-$\chi^2$ confidence level contours on the $\Delta m^2$ versus $n$ plane.

We performed several studies to search for astrophysical sources of high energy neutrinos using the Super-Kamiokande-I neutrino induced upward-going muon data. The data set consists of 2359 events with a minimum energy 1.6 GeV, of which 1892 are through-going and 467 stop within the detector. No statistically significant evidence for point sources or any diffuse flux from the galactic plane is found. The 90 % C.L. upper limits on upward-going muon flux from astronomical sources which are located in the southern hemisphere and always under the horizon for Super-Kamiokande are $(1 \sim 4) \times 10^{-15} cm^{-2} s^{-1}$[7] [8].

## Solar neutrinos

SK detects solar neutrinos through neutrino-electron scattering, $\nu + e \rightarrow \nu + e$, with which the energy, direction and time of the recoil electron are measured. Due to its large fiducial mass of 22.5 kilotons, SK gives the most precise measurement of the solar neutrino flux with accurate information of the energy spectrum and time variations. For this precision experiment, precise calibrations are performed for the energy scale, energy resolution, angular resolution and the vertex position resolution using a LINAC and $^{16}N$ radioisotope generated by a DT neutron generator.
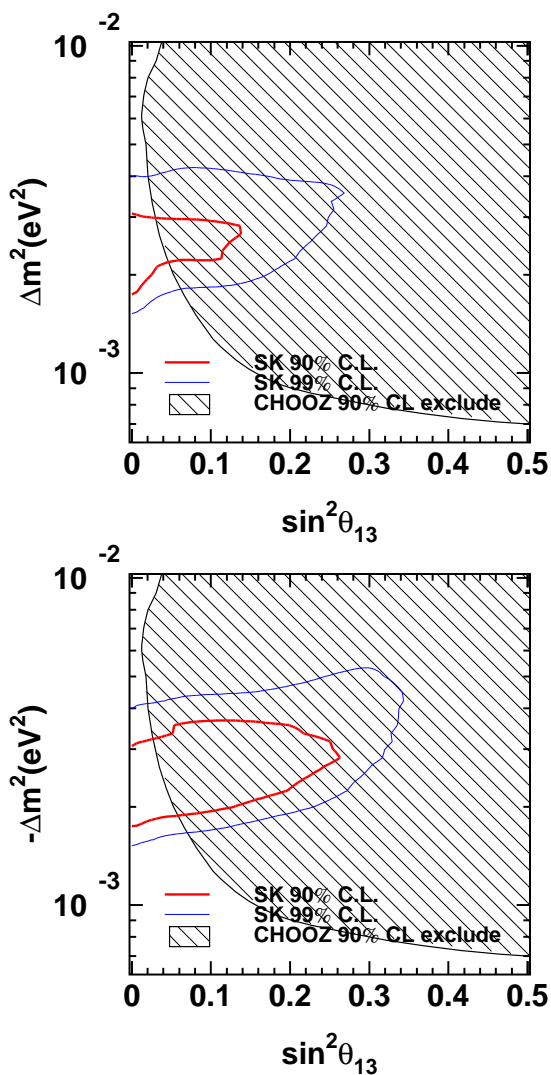


Fig. 7. The allowed region for ($\Delta m^2$, $\sin^2 \theta_{13}$) for the normal (upper figure) and inverted (lower figure) hierarchy. We assumed positive $\Delta m^2$. The red and blue contours correspond to allowed regions obtained by this analysis. The hatched region corresponds to 90% C.L. excluded area by CHOOZ experiment.

We also consider possible consequences of the mass varying neutrino (MaVaN) model. In this model, the neutrino mass can vary depending on the matter density along the path of the
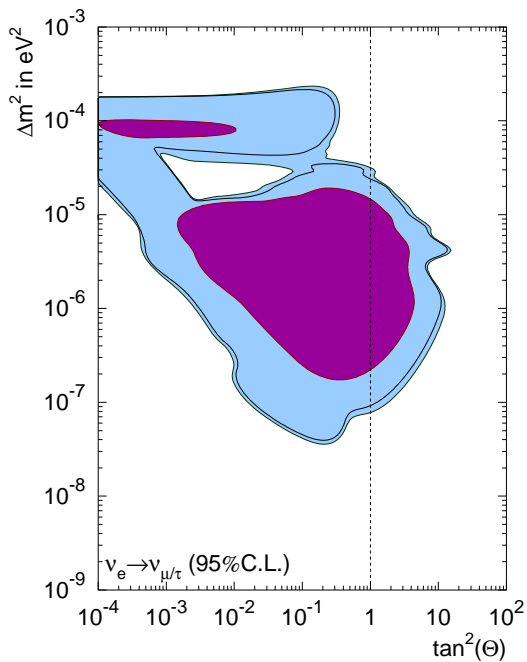
Fig. 9. The excluded areas from SK-I and SK-II. The purple region is SK-II only, and the light blue region is SK-I with SK-II. The black line shows SK-I only. [1]



Fig. 10. The data reduction steps in SK-III in the 22.5 kton fiducial volume. The colored lines are from SK-III, and the black plots are from SK-I.



Fig. 11. The angular distribution in the central region of the SK detector. The red and blue plots correspond to SK-I and SK-III, respectively. The vertical and horizontal lengths are 16m and $R^2 \leq 150\ m^2$, and the fiducial volume is 7.5 kton in these plots.

In this year, we have submitted the final results of the SK-II solar neutrino analysis [1]. The live-time is 791 day between 2002 Dec. 24 and 2006 Oct. 5. The analysis energy threshold for the flux measurement set at 7.0 MeV. The obtained number of signal events is $7212.8^{+152.9}_{-150.9}$(stat.)$^{+483.3}_{-461.6}$(syst.). The corresponding $^8$B solar neutrino flux is $2.38 \pm 0.05$ (stat.)$^{+0.16}_{-0.15}$ (syst.) $\times 10^6\ cm^{-2}\ s^{-1}$. This is consistent with the SK-I result. Figure 9 shows the excluded areas from SK-I and SK-II. The evidence of increased exclusion can be seen with the addition of SK-II data in the plot.

The SK-III solar neutrino observation with a 5 MeV energy threshold was started from Jan. 24, 2007. We have applied preliminary analysis tools, which are basically identical to SK-I, then compared the first SK-III SLE data with SK-I. The data used for this analysis were from January 24 until October 4, 2007. The live time was 110 days for the 5–20 MeV data sat.

Figure 10 shows the low-energy data reduction steps. Most of the additional low-energy background events can be reduced by the pre-ambient BG cut. Then, agreement of SK-III and SK-I in 22.5 kton looks quite good.

However, if we choose the central 7.5 kton region of the SK detector, the observed event rate in SK-III is lower than SK-I. Figure 11 shows the angular distributions of the final data sample in the different energy region in the 7.5 kton center region. The background rates in the lower energy region
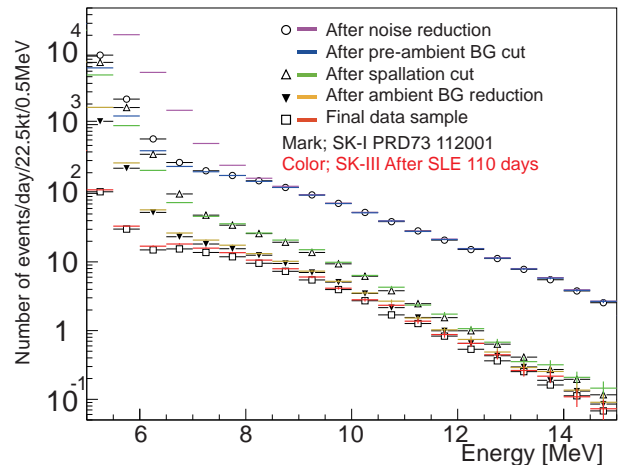
shows improvement in SK-III though the signal rates looks consistent. We think this is due to the water system upgrades and improved analysis tools in SK-III. We are currently accumulating more low-energy data.

## Search for nucleon decay

Proton decays and bound neutron decays (nucleon decays in general) is the most dramatic prediction of Grand Unified Theories in which three fundamental forces of elementary particles are unified into a single force. Super-Kamiokande (SK) is the world largest detector to search for nucleon decays and it has accumulated data of 91.7 kt·yrs (SK-I) and 49.2 kt·yrs (SK-II) resulting in 141 kt·yrs data in total. Various nucleon decay modes have been looked for in SK but we have found no significant signal excess so far.

A proton decay into one positron and one neutral pion ($p \to e^+\pi^0$) is one of the most popular decay modes. This decay mode is mediated by super-heavy gauge bosons and discovery of the signal would give us the information of the mass of the gauge mesons. To discriminate the signal from the atmospheric neutrino background, we reconstruct the number of particles (Cherenkov rings) and reconstruct the total visible energy corresponding to parent proton mass and total momentum corresponding to the proton's Fermi momentum. The signal efficiency and the estimated atmospheric neutrino background for SK-I are 44.9% and 0.20 events in 91.7 kt·yrs. Even with the photo-coverage area about half (19%) in SK-II, we achieved high detection efficiency of signals (43.7%) and low background levels (0.11 events in 49.2 kt·yrs). Because there are no candidate events in SK-I and SK-II data, we obtained a lower limit on the partial lifetime of the proton; $\tau/B_{p\to e^+\pi^0} > 8.2 \times 10^{33}$ years at 90% confidence level.

In addition, we looked for SUSY favored decay modes which include K mesons in final state, $p \to \bar{\nu}K^+$, $n \to \bar{\nu}K^0$, $p \to \mu^+ K^0$, and $p \to e^+ K^0$. In $p \to \bar{\nu}K^+$ search, we looked for 236 MeV/$c$ monochromatic muons from the decay of $K^+$. Figure 12 shows the comparison between data and fitting results of muon momentum distribution for single-ring $\mu$-like events. We observed no excess of signal. In other modes, there are no significant signal excess. Therefore we conclude that there is no evidence of nucleon decays and we calculated partial lifetime limits taking into account systematic uncertainties. Obtained limits are $2.3 \times 10^{33}$, $1.3 \times 10^{32}$, $1.3 \times 10^{33}$ and $1.0 \times 10^{33}$ years at 90% confidence level for $p \to \bar{\nu}K^+$, $n \to \bar{\nu}K^0$, $p \to \mu^+ K^0$, and $p \to e^+ K^0$ modes, respectively.

We also looked for neutron-antineutron oscillation (conversion) in the water that violates Baryon number by 2. The antineutron annihilates with a nearby nucleon (proton or neutron) producing multiple secondary pions and gammas which emit isotropic Cherenkov photons with a visible energy of 1 GeV. In the full SK-I data, the number of observed candidates is 23 events while expected backgrounds is 24. We have set the upper limit on the neutron-antineutron conversion rate to $1.99 \times 10^{32}$ years at 90% confidence level. This limit gives the upper limit on the oscillation time of a free neutron as $2.49 \times 10^8$ sec at 90% confidence level and can be compared with the reactor experiment limit of $0.86 \times 10^8$ sec.
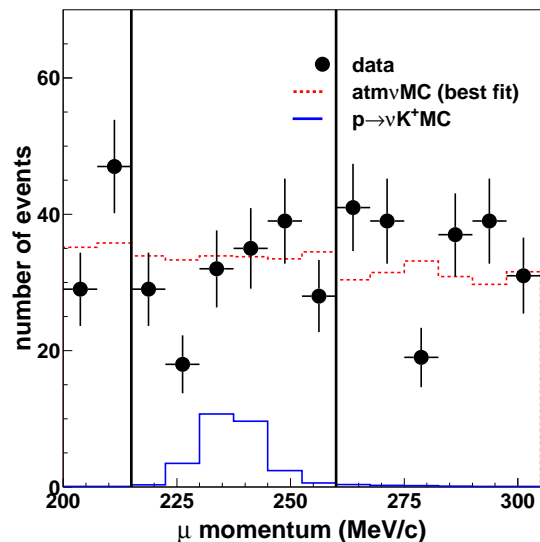


Fig. 12. The comparison between data and fitting results of muon momentum distribution for single-ring $\mu$-like events. The filled circles show data with statistical errors. The solid line shows $p \to \bar{\nu}K^+$ MC. The dashed line shows the best fitted atmospheric neutrino MC with free normalization.

## Supernova neutrinos

Kamiokande and IMB observed the neutrino burst from supernova 1987a. Those observations confirmed that the energy release by neutrinos is about several$\times 10^{53}$erg. Super-Kamiokande is able to detect several thousand neutrino events if it happens near the center of our galaxy. Until now, no clear neutrino burst from a supernova has been observed in Super-Kamiokande. We have performed 3 kinds of neutrino burst searches in SK-I and SK-II and published the results [2].

In this year, we have summarized the preliminary results of the Supernova Relic Neutrino (SRN) search in SK-I and SK-II. The SRN is the diffuse supernova neutrino background from all the supernovae in the past. It is expected that the SRN would become dominant in 18–40 MeV energy region though they haven't been observed yet. So far, SK-I gives the most stringent flux limit for past supernovae.

In SK detector, we have applied special data selections to enhance the SRN candidates. The energy region was 18–82 MeV, and the fiducial volume was 22.5 kton. The live time for this analysis is the same as that for the solar neutrino analysis; that is, 1496 days in SK-I and 791 days in SK-II. The number of events after all data reductions was 218 events in SK-I and 115 events in SK-II. The event rates in the final data samples are consistent between SK-I and II.

The dominant backgrounds are decay electrons from invisible atmospheric $\nu_\mu$ and atmospheric $\nu_e$. In SK-II, the remaining spallation products are also seen around 20 MeV due to worse energy resolution. We have applied a spectrum fit to estimate the possible SRN contributions. Figure 13 shows the energy spectrum of the final data samples and the fitting results in SK-I and SK-II. From this analysis, the best fit was no SRN contribution in both SK-I and II.

We have obtained the preliminary SRN flux limits from the spectrum fits. The updated SRN flux upper limit from only SK-I data is 1.25/cm²/sec at 90% C.L. The same limit
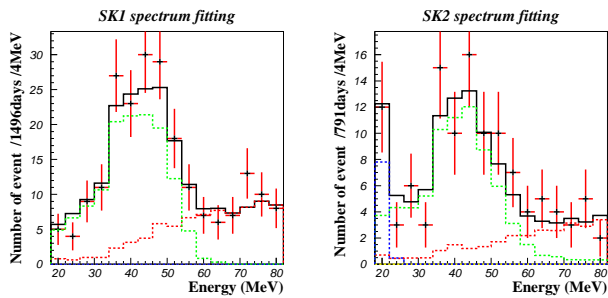
Fig. 13. The preliminary fitting results from the SRN analysis. The left(right) plot shows SK-I(SK-II) result. The solid red points are observed data. The dashed lines are each component of the fitting. The green-dashed, red-dashed, blue-dashed, and yellow–dashed lines correspond to the decay electrons from the invisible muons, atmospheric $\nu_e$, remaining spallation products, and SRN signal, respectively. The black solid line is the sum of the best-fitted components. .

from only SK-II is 3.68/cm$^2$/sec. The combined preliminary SRN flux limit from SK-I and SK-II is 1.08/cm$^2$/sec. We are trying to improve this analysis.

## Bibliography

[1] Super-Kamiokande Collaboration, "Solar Neutrino Measurements in Super–Kamiokande–II", Submitted to Phys. Rev. D, arXiv:0803.4312[hep-ex]. Additional information in http://www-sk.icrr.u-tokyo.ac.jp/sk/lowe/sk2_data/

[2] Super-Kamiokande Collaboration, " Search for Supernova Neutrino Bursts at Super-Kamiokande ", Astrophys J. 669 (2007) 519, arxiv:0706.2283[astro-ph].

[3] Super-Kamiokande Collaboration, "A Measurement of Atmospheric Neutrino Oscillation Parameters by Super-Kamiokande I", Phys. Rev. D 71 (2005) 112005.

[4] Super-Kamiokande Collaboration, "A measurement of atmospheric neutrino flux consistent with tau neutrino appearance", Submitted to Phys. Rev. Lett., hep-ex/0607059.

[5] Super-Kamiokande Collaboration, "Three flavor neutrino oscillation analysis of atmospheric neutrinos in Super-Kamiokande", Phys. Rev. D 774 (2006) 032002.

[6] Super-Kamiokande Collaboration, "Search for Matter-Dependent Atmospheric Neutrino Oscillations in Super-Kamiokande", Phys. Rev. D 77 (2008) 052001.

[7] Super-Kamiokande Collaboration, "High energy neutrino astronomy using upward-going muons in Super-Kamiokande-I" Astrophys. J. 652, (2006) 198.

[8] Super-Kamiokande Collaboration, "Search for Diffuse Astrophysical Neutrino Flux Using Ultrahigh Energy Upward-going Muons in Super-Kamiokande-I." Astrophys. J. 652, (2006) 206.

## K2K Experiment (completed)

The observed neutrino mass difference, $\Delta m^2 \sim 3 \times 10^{-3}$ eV$^2$, means an oscillation length of a few hundred km for one GeV neutrinos. Hence the oscillation can be experimentally tested using an artificial neutrino beam with the detector placed a few hundred km away from the neutrino production point.

The K2K experiment was designed to detect this oscillation effect and to determine the oscillation parameters precisely [1]. The neutrino beam created at KEK with a mean energy of 1.3 GeV was sent to the SK detector, 250 km west of KEK, every 2.2 seconds for a duration of 1.1 $\mu$s. At the KEK site, we prepared a near detector complex which consists of a 1 kt water Cherenkov detector and fine grained detectors, at a distance of 300 m from the target. We have analyzed the data taken from June 1999 to November 2004, which corresponds to $9.2 \times 10^{19}$ protons on target.

There are several beam monitors, proton profile monitors, a muon monitor, and a pion monitor placed along the neutrino beam line to monitor the quality of the beam. The $\pi^\pm$ decay length is about 200 m; therefore the neutrino beams at the near and the far detectors are not scaled exactly by a $1/r^2$ law. The flux ratio of the near to the far detectors was obtained from the beam Monte Carlo (MC) simulation, taking into account the spread and the emittance of the beam at the target, the production of pions, the focusing effect by the horn and the decay of pions to neutrinos. The simulation results were verified by the pion monitor.

The beam flux and the spectrum were measured by the near detectors. The ICRR group had the responsibility for the construction and the analysis of the 1 kt near detector, in addition to providing the data collected at SK. The coverage of PMTs in the 1 kt near detector is 40% of the total inner detector surface, the same as for SK-I. The 1 kt detector provides the information on the absolute neutrino flux. The energy spectrum of the beam is evaluated by using both the 1 kt and the fine grained detectors. The observed spectrum is well reproduced by the MC simulation. With additional constraints from the pion monitor, the neutrino energy spectrum was predicted for the far detector. Systematic errors due to the detector biases and the uncertainties of the neutrino interactions were carefully studied. Also, the data taken at the 1 kt detector enable us to study neutrino interactions in the GeV region. Examples include the neutral current (NC) interactions using single $\pi^0$ events [4], the nuclear de-excitation gamma rays from the NC interaction, and the neutrino interaction backgrounds for the nucleon decay searches.

A GPS system is used for the synchronization of the KEK 12 GeV Proton Synchrotron and the Super-Kamiokande detector. SK identified 112 fully contained events induced by the K2K beam. This number is compared with $158^{+9.4}_{-8.7}$(syst) events that are expected assuming no-oscillation. The deficit in the observed event number is consistent with the $\nu_\mu$ disappearance from the neutrino oscillation.

The neutrino energy spectrum is reconstructed from the observed 58 $\mu$-like single ring events using the energy and the scattering angle of the muons, as shown in Figure 1, where the data are compared with the MC simulation both with and
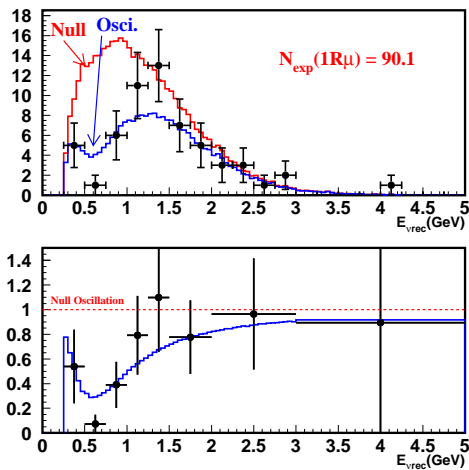
Fig. 1. The upper panel shows the reconstructed $E_\nu$ distribution from single ring fully contained events at SK. The blue line is the best fit spectrum and the red line shows the expected spectrum without oscillation. The lower figure shows the same figure but the vertical axis is normalized by the expected spectrum without oscillation.
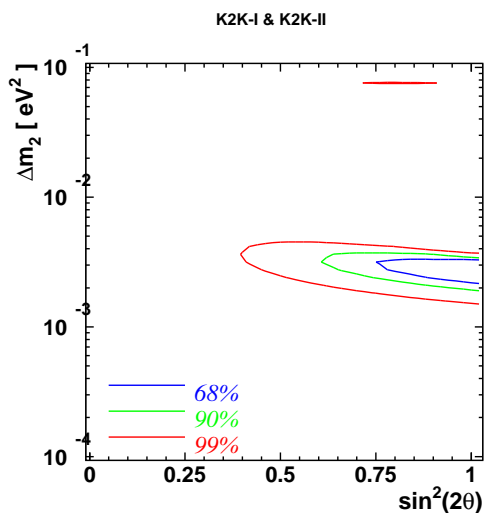


Fig. 2. Allowed regions of $\nu_\mu$-$\nu_\tau$ oscillation parameters. Blue, green and red lines are 68.4%, 90% and 99% C.L. contours, respectively.

without the neutrino oscillation. The observed neutrino spectrum is reproduced well with the oscillation, and the probability for the absence of neutrino oscillation is 0.001% ($4.4\sigma$).

The allowed region for the $\nu_\mu - \nu_\tau$ oscillation parameters, shown in Fig. 2 [5], is consistent with the atmospheric neutrino result.

A $\nu_\mu - \nu_e$ oscillation search is also performed based on the full K2K data, by looking for the $\nu_e$ appearance. We applied a new e/$\pi^0$ separation technique to reduce the $\pi^0$ background from NC $\pi^0$ interactions in the single ring e-like event sample[3].

One candidate event is remained after applying the selection to enrich the $\nu_e$ quasi elastic interaction, while 1.7 events are expected from the MC simulations. Since the number of observed events is consistent with the expected background, we set an upper bound on the $\nu_\mu - \nu_e$ oscil-
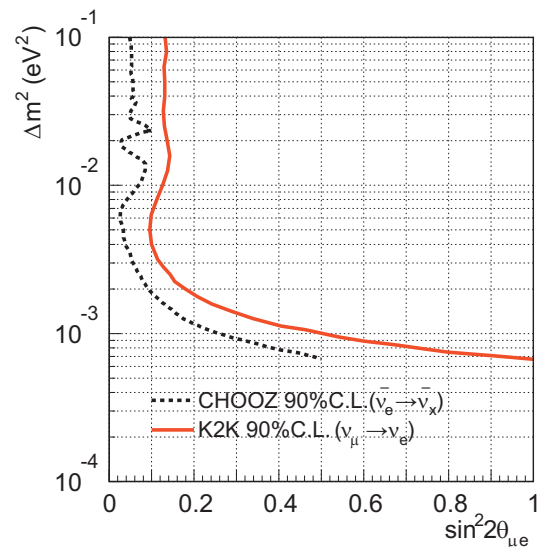


Fig. 3. The upper bound on $\nu_\mu - \nu_e$ oscillation parameters at 90% and 99% C.L. based on $9.2 \times 10^{19}$ protons on target.

lation parameters, which is shown, together with the limit from CHOOZ, in Figure 3 for $\sin^2 2\theta_{23} \sim 1$. The K2K experiment excludes the region $\sin^2 2\theta_{\mu e} > 0.13$ at a 90% C.L. when $\Delta m_{23}^2 = 2.8 \times 10^{-3}$ eV$^2$ [6].

Other than the neutrino oscillation parameter determinations, we have completed and published the results of a study of the atmospheric neutrino background for proton decay searches via $p \rightarrow e^+ \pi^0$ in the ring imaging water Cherenkov detectors[7]. We used the data taken with the 1 kt water Cherenkov detector, which uses the same target material and detection technique as SK. The accumulated numbers of neutrino interactions are equivalent to the atmospheric neutrino exposures of 15.9 and 4.5 Megaton·years (or 700 and 200 years of SK) for the CC and NC background events, respectively. A re-weighting method, using the neutrino fluxes and the detection efficiencies, is used to estimate the background event rate in the search for proton decay in SK. The obtained background rate for $E_\nu < 3$ GeV is $1.63^{+0.42}_{-0.33}$(stat.)$^{+0.45}_{-0.51}$(syst.) events/Megaton·years. Here, about 76% of the background events are expected to be generated in this energy range, $E_\nu < 3$ GeV, according to the study with our Monte-Carlo simulation. This is the first estimation of the background event rate for SK-type water Cherenkov detectors based on the data from an experiment. The obtained results are found to be consistent with the estimation by the full simulation of the SK detector and the neutrino interactions.

## Bibliography

[1] K2K collaboration, Detection of accelerator produced neutrinos at a distance of 250 km, *Phys. Lett. B*, 511, 178–184, 2001.

[2] K2K collaboration, Indication of neutrino oscillation in a 250 km long baseline experiment, *Phys. Rev. Lett.*, 90, 041801, 2003.

[3] K2K collaboration, Search for Electron Neutrino Appearance in a 250 km Long-baseline Experiment, *Phys.*

*Rev. Lett.*, 93, 051801, 2004.

[4] K2K collaboration, Measurement of single pi0 production in neutral current neutrino interactions with water by a 1.3 GeV wide band muon neutrino beam, *Phys. Lett. B*, 617, 255, 2005.

[5] K2K collaboration, Evidence for muon neutrino oscillation in an accelerator-based experiment *Phys. Rev. Lett.*, 94, 081802, 2005.

[6] K2K collaboration, An Improved search for $\nu_\mu \rightarrow \nu_e$ oscillation in a long-baseline accelerator experiment, *Phys. Rev. Lett.*, 96, 1811801, 2006.

[7] K2K Collaboration, Experimental study of the atmospheric neutrino backgrounds for proton decay to positron and neutral pion searches in water Cherenkov detectors, *Phys. Rev. D.*, 77, 032003, 2008.

# T2K Experiment (under construction)

[Spokesperson : K. Nishikawa]

High Energy Accelerator Research Organization, Japan, Tsukuba 305-0801

In collaboration with the members of:
ICRR, University of Tokyo, Japan; Kyoto University, Japan; KEK, High Energy Accelerator Research Organization, Japan; Kobe University, Japan; Osaka City University, Japan; Hiroshima University, Japan; Tohoku University, Japan; University of Tokyo, Japan; Miyagi Edu. University, Japan; Chonnam National University, Korea; Seoul National University, Korea; Dongshin University, Korea; Gyeongsang National University, Korea; Kyungpook National University, Korea; Sejong University, Korea; Sungkyunkwan University, Korea; Boston University, USA; Brookhaven National Lab, USA; Colorado State University, USA; Duke University, USA; Louisiana State University, USA; Stony Brook University, USA; University of California at Irvine, USA; University of Colorado, USA; University of Pittsburgh, USA; University of Rochester, USA; University of Washington, Seattle, USA; TRIUMF, Canada; University of Alberta, Canada; University of British Columbia, Canada; University of Regina, Canada; University of Toronto, Canada; University of Victoria, Canada; York University, Canada; University of Oxford, UK; Imperial College London, UK; Lancaster University, UK; Queen Mary, University of London, UK; Sheffield University, UK; STFC/Rutherford Appleton Laboratory/Daresbury Laboratory, UK; The University of Liverpool, UK; University of Warwick, UK; Universitat Autonoma de Barcelona IFAE, Spain; IFIC University of Valencia, Spain; INRM, Russia; CEA/DAPNIA Saclay, France; IPN Lyon (IN2P3), France; LLR Ecole polytechnique (IN2P3), France; LPNHE-Paris, France; RWTH Aachen University, Germany; INFN Sezione di Roma, Italy; Napoli University, Italy; Padova University, Italy; Rome University, Italy; ETHZ, Swiss; University of Geneva, Swiss; University of Warsaw, Poland; A. Soltan Institute for Nuclear Studies, Poland; H.Niewodniczanski Institute of Nuclear Physics, Poland; Technical University, Poland; University of Silesia, Poland; Wroclaw University, Poland; Institute for Nuclear Research, Russia;

The K2K experiment successfully confirmed the neutrino oscillation phenomena and established the method of the accelerator-based long baseline neutrino oscillation experiment. Meanwhile, precise measurements of accelerator, atmospheric, solar and reactor neutrinos have been done and 2 out of 3 neutrino mixing angles and 2 mass differences have been measured. However, the remaining mixing angle, $\theta_{13}$, has not been measured and has only been found to be small. If there is a much more intense neutrino beam, it will be possible to measure $\theta_{13}$. Furthermore, if $\theta_{13}$ is large enough, there is a possibility to search for CP violation in the lepton sector and to measure the CP phase, $\delta$, which is one of the last parameters of the neutrino oscillation. Therefore, next generation experiments, which utilize much intense beams, was planned for the further investigation of the neutrino oscillations, have been proposed. Among of them, the Tokai to Kamioka long baseline neutrino oscillation experiment (T2K) is under construction and expected to start in 2009. The intense neutrino beam will be produced by a new high intensity proton synchrotron accelerator being constructed at the J-PARC site in Tokai village. T2K utilizes Super-Kamiokande as a far detector, located at 295 km from the beam production point.

The T2K neutrino beam is about 50 times more intense than the K2K beam. The neutrino beam line of T2K utilizes the so-called off-axis technique [1] in order to have a tunability of the peak energy and a narrow energy spread of the neutrino beam. The peak position of the neutrino beam energy will be adjusted to $\sim 650$ MeV by setting the off-axis angle to $\sim 2.5°$. With this configuration, it is possible to maximize the neutrino oscillation effects at a distance of 295 km when the mass squared difference is about $\Delta m^2 = 2.8 \times 10^{-3}$eV$^2$. The beam primarily consists of $\nu_\mu$ with a contamination of $\sim 0.4\%$ $\nu_e$ at the flux peak.

As described, one of the motivations of this experiment is to measure the neutrino oscillation parameter $\theta_{13}$, which is only known to be small ($\sin^2 \theta_{13} < 0.04$) by reactor experiments. It is of great interest to know the value of a nonzero $\theta_{13}$ or how close to zero $\theta_{13}$ is; a new underlying symmetry may be required to explain this. In the case of nonzero $\theta_{13}$, T2K may observe the appearance of electron neutrinos for the first time. Also, there is a possibility to observe the neutrino oscillation signature with an appearing experiment for the first time.

Figure 1 shows T2K's expected sensitivity to $\theta_{\mu e}$ as a function of $\Delta m^2_{23}$. Note that $\sin^2(2\theta_{\mu e}) = \frac{1}{2}\sin^2 2\theta_{13}$.

If the measured $\theta_{13}$ is large enough, it will be possible to investigate CP violation in the lepton sector with further extension of this experiment.

The other purposes are precise measurements of $\theta_{23}$ and $\Delta m^2_{23}$. Owing to the high statistics, these parameters will be measured almost one order of magnitude more precisely than before. Figure 2 shows the expected accuracy of the measurement of $\sin^2 2\theta_{23}$ and $\Delta m^2_{23}$ [1]. So far, $\theta_{23}$ mixing is known to be very large and consistent with unity from the
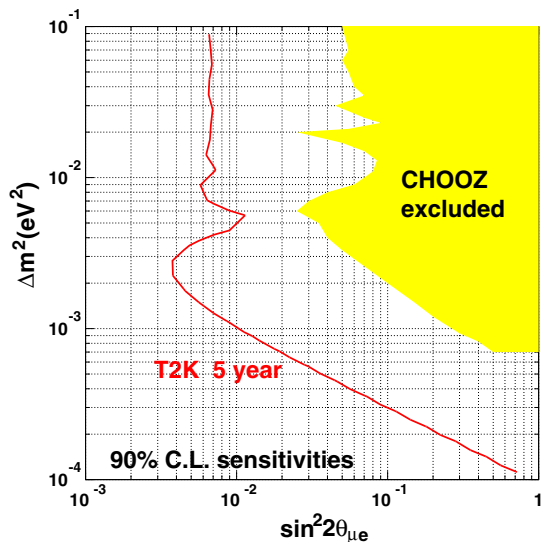
Fig. 1. Expected sensitivity to $\theta_{\mu e}$ by T2K as a function of $\Delta m_{23}^2$ compared with current best limit by the CHOOZ reactor experiment. Note that $\sin^2(2\theta_{\mu e}) = \frac{1}{2}\sin^2 2\theta_{13}$.

Super-Kamiokande, K2K and the MINOS experiments. If $\sin^2 2\theta_{23} = 1$, it may suggest an underlying new symmetry.

To achieve these precise measurements, the Super-Kamiokande detector has several to-do items in the near future: (1) detector upgrade, (2) precise detector calibration, and (3) software upgrade. Details of these items are described below.

## Detector Upgrade

The reconstruction work of Super-Kamiokande was completed in 2006 and all the PMTs were installed just as in SK-I. It will help the T2K experiment in a search for electron neutrino appearance, to distinguish single $\pi^0$ production backgrounds from the $\nu_e$ signal more effectively.

In 2008, the electronics and DAQ systems are planned to be replaced. Newly-developed ADC/TDC modules called QBEEs will be installed. The new QBEE boards consist of a custom analog ASIC and multi-hit TDC chips. The new system will allow us to observe T2K neutrino events with good stability and accuracy.

## Precise Detector Calibration

The response of the far detector must be well understood in order to maximize the sensitivities to oscillation parameters such as $\theta_{13}$, $\theta_{23}$, and $\Delta m_{23}^2$. In the electron appearance search, single $\pi^0$ production backgrounds can fake single-ring electron signals when one of the two $\gamma$ rings is not identified. Even a small portion of muon events mis-identified as electrons could also be a serious background. Therefore, we will study the ring identification and the particle identification capabilities of the detector very carefully. It will also be important to reduce the uncertainty in the absolute energy scale measurement (2.5%) in order to achieve a $\Delta m_{23}^2$ measurement with $\sim 1\%$ accuracy. Moreover, further calibration of the fundamental properties such as the charge and timing responses
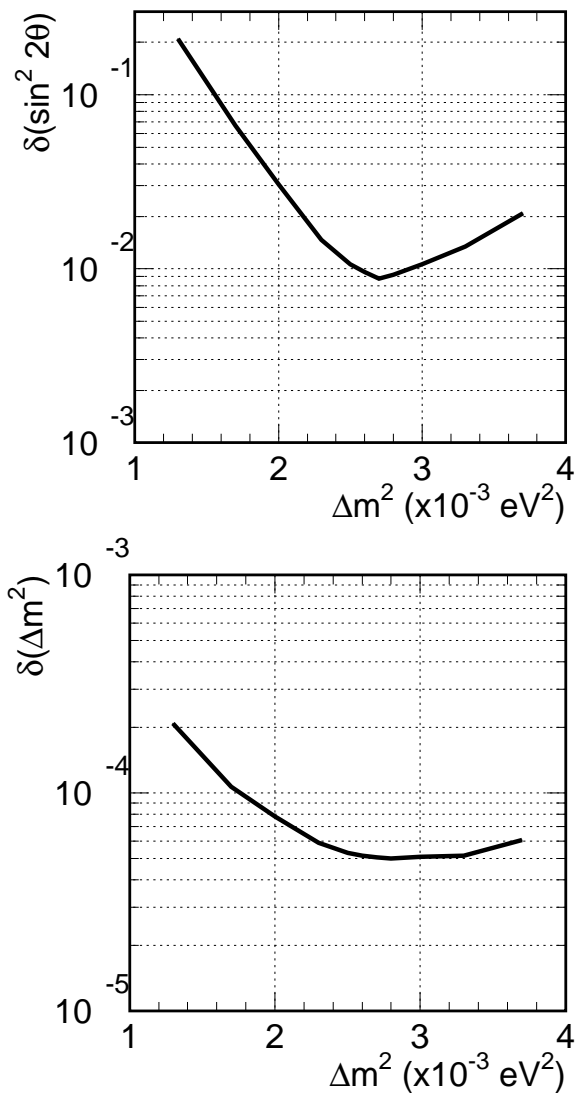


Fig. 2. T2K's expected accuracy of the measurement of $\sin^2 2\theta_{23}$ and $\Delta m_{23}^2$ as a function of $\Delta m_{23}^2$ [1].

of each PMT, the light attenuation and scattering in water, and the light reflection by the detector materials are indispensable.

## Software Upgrade

All measurements of the physical quantities of an event, such as the vertex position, the number of Cherenkov rings, the momentum, the particle type and the number of the decay electrons, are automatically performed based on the reconstruction algorithms. Improvements and re-tuning of these algorithms to meet the physics goals of T2K are underway.

## Bibliography

[1] Y. Itow *et al.*, The JHF-Kamioka neutrino project, (2001), hep-ex/0106019.

## XMASS experiment

XMASS is a multi-purpose experiment using liquid xenon that aims at the detection of cold dark matter, search for neutrinoless double beta decay, and detection of low energy solar neutrinos. Construction of a one-ton liquid xenon detector

(100 kg fiducial volume) was approved in 2007. This detector is expected to search for dark matter with a sensitivity that is improved by a factor of 100 over that in existing experiments.

## Liquid xenon detectors

There are three motivations for developing liquid xenon detectors.

1. Astronomical observations suggest that there is dark matter (non-luminous particles with mass) in the universe. One of the most likely candidates for dark matter is a weakly interacting massive particle (WIMP), such as the lightest supersymmetric particle. The recoil of a xenon nucleus due to an interaction with dark matter will produce scintillation light in liquid xenon.

2. The Super-Kamiokande experiment shows that neutrinos have mass. However, we do not yet know their absolute mass or whether they are Majorana or Dirac type. The Xenon nuclei with mass number 136 is the double beta nuclei best suited for this research.

3. The energy spectrum of solar neutrinos has been measured only above 5 MeV by SK and SNO and that of low-energy solar neutrinos (pp, $^7$Be neutrinos, etc.) has not yet been measured. A 10-ton liquid xenon detector will be able to detect pp neutrinos and $^7$Be neutrinos by detecting $\nu$+e scattering, at a rate of 10 and 5 eevents/day, respectively.

For all these purposes, background caused by gamma rays outside the liquid xenon must be suppressed. The key idea in reducing background is that gamma rays can be absorbed by liquid xenon itself (self-shielding). A sphere of liquid xenon absorbs low energy gamma rays from the outside within the outer 10-20 cm thick layer and realizes a low background radiation in the central volume. WIMPs and neutrinos, however, interact throughout the detector. Therefore, if the vertices of the events can be reconstructed, WIMPs and neutrinos can be observed in a low background environment by extracting only events observed deep inside the detector. The event reconstruction can be accomplished by observing photons with many photo multipliers mounted outside the fiducial volume. Liquid xenon has the following advantages to realize this idea:

- With the high atomic number of xenon ($Z = 54$) and the high density of liquid xenon ($\sim 3\,\mathrm{g/cm}^3$), external gamma-rays can be absorbed within a short distance from the detector wall (self-shielding).
- A large light yield of 42,000 photons/MeV, which is as good as a NaI(Tl) scintillator, enables good event reconstruction as well as detection of small energy signals such as dark matter recoil.
- The 175-nm-wavelength scintillation light of liquid xenon can be detected by a photomultiplier tube (PMT) comprising a bi-alkaline photocathode with a quartz window.
- Purification is easier than with other materials (e.g. distillation is possible).
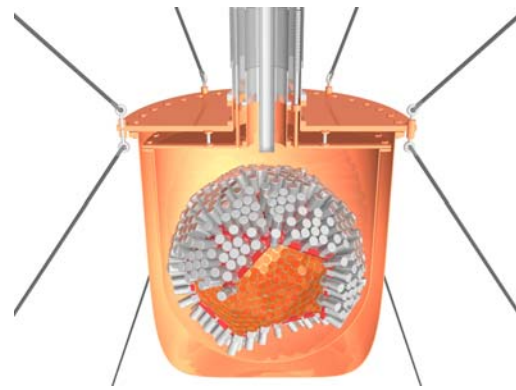


Fig. 1. The central part of the proposed one-ton liquid xenon detector intended for dark matter search. The detector has a sensitivity of $10^{-45} \sim 10^{-44}\mathrm{cm}^2$ in cross section, which is two orders of magnitude better than the current best limit in the world.

- Isotope separation is possible. It is possible to enrich $^{136}$Xe for double beta decay or deplete $^{136}$Xe for solar neutrino measurements.

We have been studying liquid xenon detectors since 2000. A 3 kg fiducial volume liquid xenon detector has been developed for R&D study and test data obtained. Event reconstruction, self-shielding and low internal activity have been confirmed. The description of the one-ton liquid xenon detector in the following sections represents the first phase of this project. The detector aims to detect cold dark matter particles with improved sensitivity by a factor of 100. The second phase of the XMASS project requires a larger detector with more than 10-tons of liquid xenon. The detector is intended for a detailed study of dark matter, and detection of low energy solar neutrinos. The search for neutrinoless double beta decay with the 10-ton detector needs additional efforts in the reduction of background activity in a few MeV energy regions.

## One-ton detector

We plan to make the one-ton detector to search for dark matter down to $10^{-45} \sim 10^{-44}\mathrm{cm}^2$ in cross section which is two orders of magnitude better than the current best limit in the world. Figure 1 shows the central part of the detector. Its background and sensitivity were evaluated by Monte Carlo simulations which were validated by the current experimental results. The advantages of our detector design are as follows:

1. Extension of the detector is straightforward because the target substance is liquid.
2. The energy threshold is as low as 5 keV since the photo electron yield is high.
3. Purification of the target substance is easy because xenon is naturally in a gas phase.
4. It is possible to use pulse shape analysis to select nuclear recoil events.

The expected sensitivity for particle dark matter is better than the current experimental limits by two orders of magnitude. Figure 2 shows the expected sensitivity of the one-ton detector.
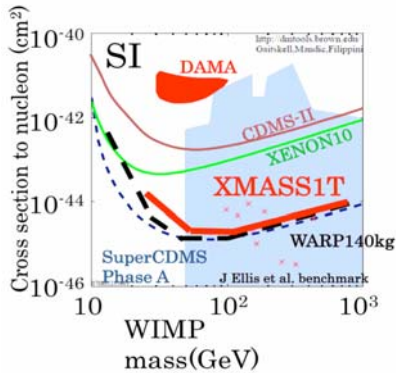
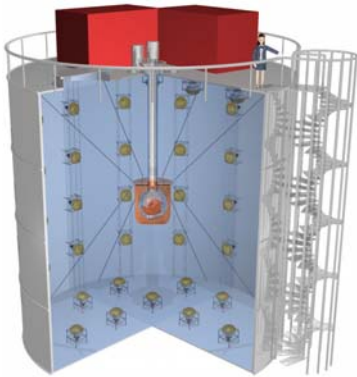Fig. 2. Expected sensitivity of the proposed 800kg liquid xenon detector. See http://dmtools.berkeley.edu/



Fig. 3. A water tank for shielding from gamma ray and neutrons. The liquid xenon detector is located at the center of the tank.

## Construction of the one-ton detector

The construction of the one-ton detector started in 2007 and is expected to be completed by 2009. Important progress related to the construction has been made.

### Excavation of experimental halls

As a part of an extension program of the Kamioka observatory, two experimental halls were excavated. Installation of the one-ton xmass detector in one of the halls was approved by the observatory. The hall is 15 m wide, 21 m deep and 15 m high. The excavation was finished in early 2008, and basic outfitting is planned to be finished by the end of 2008.

### Design of a radiation shield

Ambient gamma rays and neutrons are serious sources of background, and pure water is one of the best materials for reducing it. We designed a liquid xenon detector immersed in the cylindrical water tank shown in Fig. 3. The tank is 10 m in diameter and 11 m high. The tank has been designed and we are ready to accept bids for the construction.

### Circulation system for liquid xenon

We may need to purify liquid xenon before or during detector operation to reduce possible contamination. For example, water vapor in liquid xenon absorbs scintillation lights; thus, it needs to be removed to maintain transparency. Another example is radon gas which is emanated from detector components. If the radon produces more background than expected,

we need to reduce it by circulating liquid xenon. Therefore we have constructed a circulation system for the one-ton detector and plan to test it with a smaller detector in 2008.

### Development of PMTs

The central part of this detector is shown in Fig. 1. The PMTs (shown as many cylinders) are one of the main components of this part. The PMTs consists of a hexagonal photo cathode to maximize the photo sensitive area of the detector. They are specially developed and designed for this experiment since the scintillation wavelength is very short (175 nm) and the operating temperature is low (-100 °C). In addition, the PMT materials are carefully selected and evaluated with a low background germanium detector. The PMTs have been tested in liquid xenon and are now ready for production.

**References**

1. Y. Suzuki et al., "Low energy solar neutrino detection by using liquid xenon", Aug. 2000, hep-ph/0008296.

2. S. Moriyama, "XMASS EXPERIMENT I", Proceedings of the International Workshop on Technique and Application of Xenon Detectors, Kashiwa, Japan, 3-4 Dec. 2001.

3. K. Abe, "XMASS, status of 800kg detector design", presentation at the Joint Meeting of Pacific Region Particle Physics Communities (DPF2006), Honolulu, Hawaii, USA, 29 October - 3 November 2006.

4. M. Nakahata, "Status of XMASS experiment", presentation at the sixth international Heidelberg conference on dark matter in astro and particle physics (dark2007), Sydney, Australia 24-28 September 2007.

# HIGH ENERGY COSMIC RAY DIVISION

## Overview

Three major research activities of the High Energy Cosmic Ray division are the study of very high energy gamma-rays by the CANGAROO group, extremely high energy cosmic rays by the Telescope Array (TA) group, and very high energy cosmic rays and gamma-rays by the Tibet AS$\gamma$ Collaboration. Remarkably, TA has been completed and started this fiscal year. Other activities, such as experiments utilizing the Akeno observatory, the Norikura observatory, the Mt. Chacaltaya observatory (jointly operated with Bolivia), and the emulsion-pouring facilities are closely related to inter-university joint research programs. Also an all-sky high resolution air-shower detector (Ashra) has been installed on the Hawaii island.

The CANGAROO project (Collaboration of Australia and Nippon for a GAmma-Ray Observatory in the Outback) is a set of large imaging Cherenkov telescopes to make a precise observation of high-energy air showers originated by TeV gamma-rays. It started as a single telescope with a relatively small mirror (3.8 m in diameter) in 1992. In 1999 a new telescope with a 7-m reflector has been built, and now it has a 10-m reflector with a fine pixel camera. The main purpose of this project is to explore the violent, non-thermal universe and to reveal the origin of cosmic-rays. An array of four 10-m telescopes has been completed in March 2004 so that more sensitive observation of gamma-rays is realized with its stereoscopic imaging capability of Cherenkov light. Several gamma-ray sources have been detected in the southern sky and detailed study of these sources are now ongoing.

At the Akeno observatory, a series of air shower arrays of increasing geometrical sizes were constructed and operated to observe extremely high energy cosmic rays (EHECRs). The Akeno Giant Air Shower Array (AGASA) was operated from 1991 to January 2004 and covered the ground area of 100 km$^2$ as the world largest air shower array. In 13 years of operation, AGASA observed a handful of cosmic rays exceeding the theoretical energy end point of the extra-galactic cosmic rays (GZK cutoff) at $10^{20}$ eV. The Telescope Array (TA), a large plastic scintillator array with air fluorescence telescopes has just been constructed in Utah, USA, which will succeed AGASA and measure the EHECRs with an order of magnitude larger aperture than that of AGASA to unveil the origin of super-GZK cosmic rays discovered by AGASA. It has been completed and just started taking data as the largest array viewing the northern sky.

An air shower experiment aiming to search for celestial gamma-ray point sources started in 1990 with Chinese physicists at Yangbajing (Tibet, 4,300 m a.s.l.) and has been successful. This international collaboration is called the Tibet AS$\gamma$ Collaboration. An extension of the air shower array was completed in 1995 and an emulsion chamber has been combined with this air shower array since 1996 to study the primary cosmic rays around the knee energy region. After successive extensions carried out in 1999, 2002 and 2003, the total area of the air shower array amounts to 37,000 m$^2$. The sun's shadow in cosmic rays affected by the solar magnetic was observed for the first time in 1992, utilizing its good angular resolution at multi-TeV energy region. From this experiment with better statistics, we expect new information to be obtained on the large-scale structure of the solar and interplanetary magnetic field and its time variation due to the 11-year-period solar activities.

A new type of detector, called Ashra (all-sky survey high resolution air-shower detector), has been developed and the first-phase stations have been installed near the Mauna Loa summit in the Hawaii Island. It will monitor optical and particle radiation from high-energy transient objects with a wide field-of-view. The optical system is under tuning and real observation will start soon.

## CANGAROO-III Project

[Spokespersons : R.W. Clay, M. Mori, and T. Tanimori]

Collaboration list:
Institute for Cosmic Ray Research, University of Tokyo, Chiba, Japan; School of Chemistry and Physics, University of Adelaide, Australia; Mt Stromlo and Siding Spring Observatories, Australian National University, Australia; Dept. of Radiological Sciences, Ibaraki Prefectural University of Health Sciences, Ibaraki, Japan; Faculty of Science, Ibaraki University, Ibaraki, Japan; Institute of Space and Astronautical Science, Japan Aerospace Exploration Agency, Kanagawa, Japan; School of Allied Health Sciences, Kitasato University, Kanagawa, Japan; Department of Physics, Konan University, Hyogo, Japan; Department of Physics, Kyoto University, Kyoto, Japan; Solar-Terrestrial Environment Laboratory, Nagoya University, Aichi, Japan; National Astronomical Observatory of Japan, National Institutes of Natural Sciences, Tokyo, Japan; Faculty of Engineering, Shinshu University, Nagano, Japan; Department of Physics, Tokai University, Kanagawa, Japan; Department of Physics, Yamagata University, Yamagata, Japan; Faculty of Management Information, Yamanashi Gakuin University, Yamanashi, Japan [1].

## Status of the Project

CANGAROO is an acronym for the Collaboration of Australia and Nippon (Japan) for a GAmma Ray Observatory in the Outback. As its third-generation experimental setup, the CANGAROO-III stereoscopic Cherenkov telescope system has been in operation since March 2004 with four imaging Cherenkov telescopes of 10 m diameter in the desert area near Woomera, South Australia (136°47′E, 31°06′S, 160m a.s.l.). Stereoscopic observations of atmospheric Cherenkov light images produced by particle showers caused by high-energy particles bombarding the earth allow effective discrimination of

gamma-rays from charged cosmic-rays which are the over-whelming backgrounds. Three of the four telescopes (called T2, T3 and T4 in the order of construction) are currently used in observations as the first telescope, completed in 2000 and having been used as CANGAROO-II, has degraded and is equipped a different electronics system from the others. A stereoscopic triggering system was installed at the beginning of 2005 and has been working properly, rejecting most single muon events, which are the major background component at low energies. We are continuing observations of various candidates of celestial gamma-ray emitters on moonless, clear nights.

## CANGAROO-III results

### Radio galaxy Cen A/globular cluster $\omega$ Cen [2]

We have observed the giant radio galaxy Centaurus A and the globular cluster $\omega$ Centauri in the TeV energy region. The observations were carried out in March and April 2004. In total, approximately 10 hours data were obtained for each target. No statistically significant gamma-ray signal has been found above 420 GeV over a wide angular region (a one-degree radius from the pointing center) and we derive flux upper limits using all of the field of view. Implications for the total energy of cosmic rays and the density (see Fig. 1) of the cold dark matter are considered.
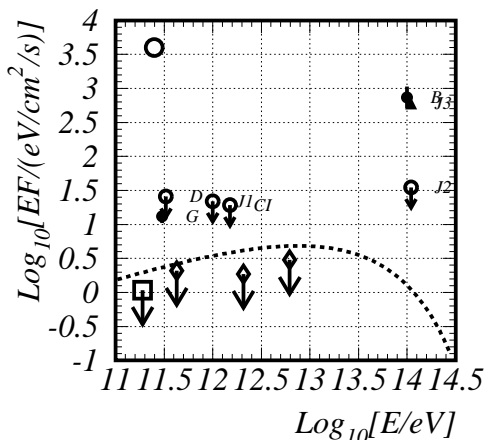


Fig. 1. SED for the jet region of Cen A. The open circle is the prediction. The black square with the arrow is the H.E.S.S. upper limit. The open diamonds are our upper limits. The expected gamma-ray yield with a total electron energy of $10^{54}$ erg with a 100 TeV cutoff energy is shown by the dashed curve.

### Supernova Remnant 1987A [3]

Optical images of SN 1987A show a triple ring structure. The inner (dust) ring has recently increased in brightness and in the number of hot spots suggesting that the supernova shock wave has collided with the dense pre-existing circumstellar medium, a scenario supported by radio and X-ray observations. Such a shocked environment is widely expected to result in the acceleration of charged particles, and the accompanying emission of very high energy gamma-rays. Here, we re-

port the results of observations made in 2004 and 2006 which yield upper limits on the TeV gamma-ray flux, which are compared with a theoretical prediction (see Fig. 2). In addition, we set upper limits on the TeV flux for four high energy objects which are located within the same field of view of the observation: the super-bubble 30 Dor C, the Crab-like pulsar PSR B0540$-$69, the X-ray binary LMC X-1, and the supernova remnant N157B.
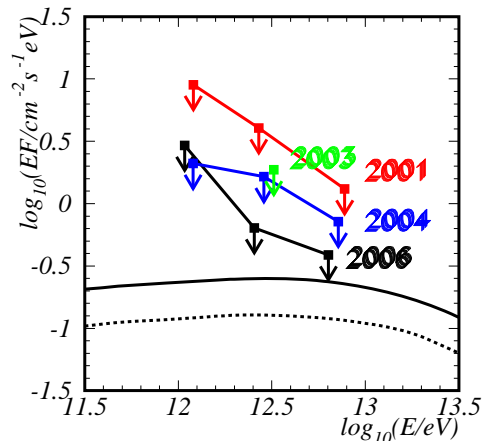


Spectral energy distribution. The blue points and line are obtained from the 2004 data and the black from the 2006 data. The red points are the CANGAROO-II upper limits from 2001 data. The green points are the H.E.S.S. data from 2003. The lines are obtained from the theoretical prediction. The solid and dashed curves are the predictions of the gamma-ray flux 8249 and 7300 days after the supernova, respectively.

Fig. 2.

### Blazar PKS 2155-304 [4]

We have observed the high-frequency-peaked BL Lacertae (HBL) object PKS 2155$-$304 between 2006 July 28 (MJD 53944) and August 2, triggered by the H.E.S.S. report that the source was in a high state of TeV gamma-ray emission. A signal was detected at the 4.8 $\sigma$ level in an effective live time of 25.1 hours during the outburst period. The flux of Very High Energy gamma-rays from the CANGAROO-III observations shows the variability on the time scale of less than a few hours (see Fig. 3). The averaged integral flux above 660 GeV is $(1.6 \pm 0.3_{stat} \pm 0.5_{syst}) \times 10^{-11} \, \text{cm}^{-2} \, \text{sec}^{-1}$ which corresponds to $\sim 45\%$ of the flux observed from the Crab nebula. Follow-up observations between August 17 (MJD 53964) and 25 indicate the source activity had decreased.

### Pulsar Wind Nebula? MSH 15-52 [5]

We have observed the supernova remnant MSH 15$-$52 (G320.4$-$1.2), which contains the gamma-ray pulsar PSR B1509$-$58, from April to June in 2006. We detected gamma rays above 810 GeV at the 7 sigma level during a total effective exposure of 48.4 hours. We obtained a differential gamma-ray flux at 2.35 TeV of $(7.9 \pm 1.5_{\text{stat}} \pm 1.7_{\text{sys}}) \times 10^{-13} \, \text{cm}^{-2} \, \text{s}^{-1} \, \text{TeV}^{-1}$ with a photon index of $2.21 \pm 0.39_{\text{stat}} \pm 0.40_{\text{sys}}$, which is compatible with that of the
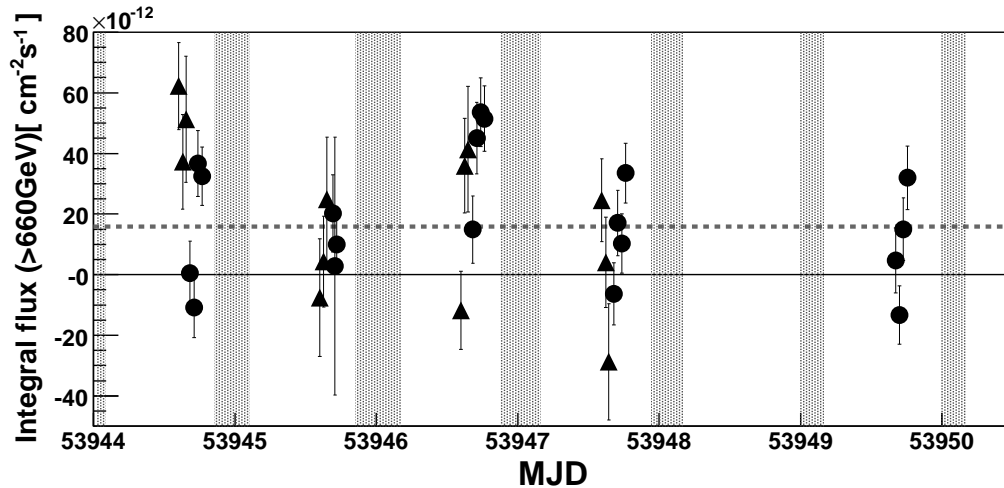
Fig. 3. Light curve of PKS 2155−304 using all the data at zenith angle less than $30\,^\circ$ between 2006 July 28 and August 2, expressed by the integral flux above 660 GeV. Closed triangles and closed circles indicate the results from $2fold$–$SZ$ and $3fold$–$SZ$ datasets, respectively. Dashed line indicates an average integral flux during this observation period. The bin width is 40 minutes. The shaded areas indicate the H.E.S.S. observation periods.

H.E.S.S. observation in 2004. The morphology shows extended emission compared to our Point Spread Function (see Fig. 4). We consider the plausible origin of the high energy emission based on a multi-wavelength spectral analysis and energetics arguments.
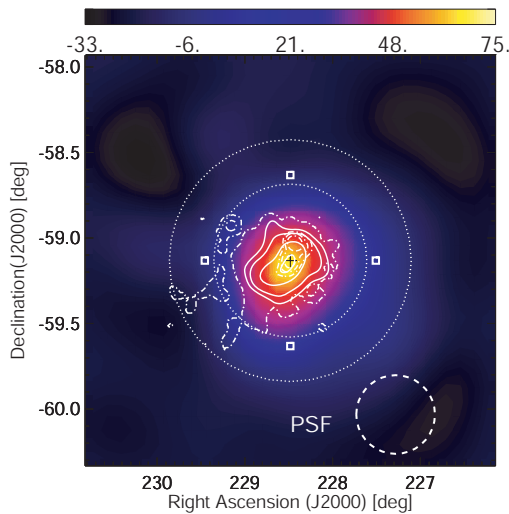


Fig. 4. Morphology of gamma-ray like events, smoothed with a Gaussian of $\sigma = 0.23°$. Our PSF is also shown by a dashed circle(68% containment radius). The squares and the cross represent tracking positions and the pulsar position, respectively. Solid contours show VHE gamma-ray emission as seen by H.E.S.S. and dotted contours by *ROSAT* 0.6-2.1 keV. The region between thin dotted circles are used for the background study.

## Unidentified HESS source HESS1804-216 [6]

We observed the unidentified TeV gamma-ray source HESS J1804−216 with the CANGAROO-III atmospheric Cerenkov telescopes from May to July in 2006. We detected very high energy gamma rays above 600 GeV at the $10\sigma$ level in an effective exposure of 76 hr (see Fig. 5). We obtained a differential flux of $(5.0 \pm 1.5_{\rm stat} \pm 1.6_{\rm sys}) \times 10^{-12}\,({\rm E}/1\,{\rm TeV})^{-\alpha}$

$\mathrm{cm}^{-2}\mathrm{s}^{-1}\mathrm{TeV}^{-1}$ with a photon index $\alpha$ of $2.69 \pm 0.30_{\rm stat} \pm 0.34_{\rm sys}$, which is consistent with that of the H.E.S.S. observation in 2004. We also confirm the extended morphology of the source. By combining our result with multi-wavelength observations, we discuss the possible counterparts of HESS J1804−216 and the radiation mechanism based on leptonic and hadronic processes for a supernova remnant and a pulsar wind nebula.
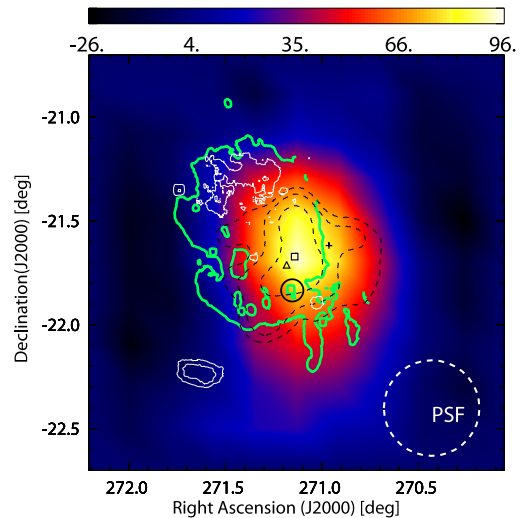


Fig. 5. Smoothed morphology of gamma-ray–like events with our PSF of 0.23° radius. Dashed contours show the VHE gamma-ray emission seen by H.E.S.S. . The thick solid contours (green) show the 20 cm radio emission from G8.7−0.1 recorded by the VLA. The thin solid contours (white) show the X-ray emission detected by the *ROSAT* satellite. The solid circle indicates the position of G8.31−0.09. The cross indicates the PSR B1800−21 position. The triangle and the square indicate the position of Suzaku Src1 and Suzaku Src2, respectively.

## Supernova Remnant Kepler [7]

Kepler's supernova, discovered in October 1604, produced a remnant that has been well studied observationally in the radio, infrared, optical, and X-ray bands, and theoretically. Some models have predicted a TeV gamma-ray flux that is detectable with current Imaging Cherenkov Atmospheric Telescopes.

We report on observations carried out in 2005 April with the CANGAROO-III telescope. No statistically significant excess was observed, and limitations on the allowed parameter range in the model are discussed as shown in Fig. 6.



Fig. 6. The allowed region in the plane of the distance ($d$) versus ambient density ($n_{\rm H}$), based on the neutral pion decay $\gamma$-ray emission model where we assume that the total number spectrum of protons is proportional to a power law with an exponential cutoff and the value of the conversion efficiency from the explosion energy to the cosmic-ray energy is 10%. The solid, dashed, and dotted lines indicate the upper limits obtained from the observed $2\sigma$ upper limits, compared with the integral fluxes o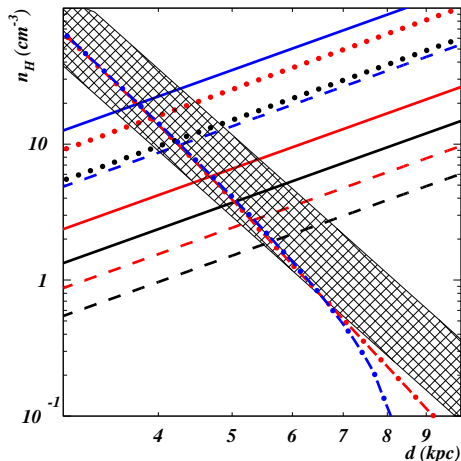f the models for the power-law indices 2.1, 1.9, and 2.3, respectively. The colors of the lines represent the cutoff energy of protons; the black, red, and blue ones are obtained with the values $10^{15}$, $10^{14}$, and $10^{13}$ eV, respectively. The allowed regions lie under these upper-limit lines. The hatched region indicates the region which satisfies the Sedov-Taylor solution of the apparent radius of the Kepler's SNR, 100" at 400 yr with the explosion energy $0.5 \sim 2 \times 10^{51}$ erg. The dot–dashed lines are obtained from the approximate analytic blast-wave positions of the radius 100". The red and blue ones are obtained assuming the ejecta power-law index $n = 6$ and $n = 14$, respectively, with ejecta mass of $1.4 M_\odot$ with the explosion energy $10^{51}$ erg.

## Galactic Plane [8]

In 2004, we searched for very high energy (VHE) gamma-ray emission from the Galactic Plane using the CANGAROO-III stereoscopic observation system. Two different longitude regions ($\ell = -19°.5$ and $\ell = +13°.0$) on the Galactic Plane were observed during July and August 2004. We analyzed events that triggered three telescopes aiming to measure the diffuse emission component. No significant signal associated with the Galactic Plane was found from either of the regions. Assuming that the gamma-ray spectrum is described by a single power law for energies ranging between a few GeV and

TeV, lower limits of the power-law spectral indices were found to be 2.2 for both of the regions with a 99.9% confidence level (see Fig. 7). This result is consistent with the other VHE measurements and constrains a hypothesis in which a very hard ($\sim 2.0$) cosmic ray electron spectrum was introduced to explain the EGRET GeV anomaly.
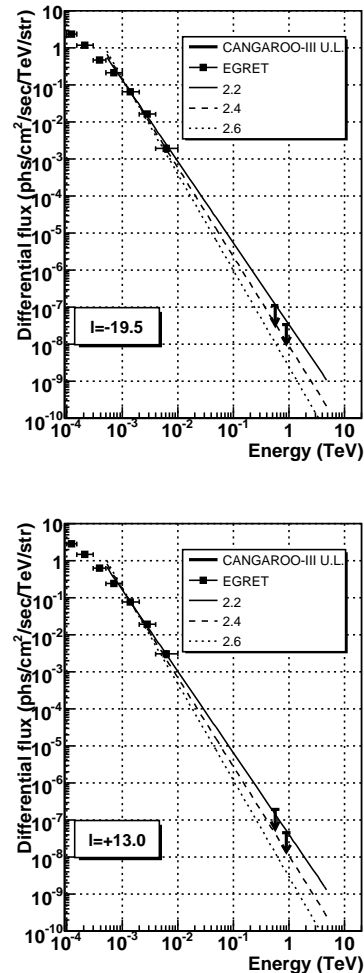


Fig. 7. Relation between the upper limit values of the flux obtained by the CANGAROO-III and the extrapolation of the EGRET data. The arrows show the CANGAROO-III flux upper limit The lines show the extrapolation of the EGRET 1-2 GeV data point, with some sets for different spectral index value.

## Cluster of galaxies [9]

As accretion and merger shocks in clusters of galaxies may accelerate particles to high energies, clusters are candidate sites for the origin of ultra-high-energy (UHE) cosmic-rays. Recently, a prediction was presented for gamma-ray emission from a cluster of galaxies at a detectable level with modern imaging atmospheric Cherenkov telescopes. The gamma-ray emission was produced via inverse Compton upscattering of cosmic microwave background (CMB) photons by electron-positron pairs generated by collisions of UHE cosmic rays in the cluster. We have observed two clusters of galaxies, Abell 3667 and Abell 4038, searching for very-high-energy gamma-ray emission in 2006. The analysis showed no

significant excess around these clusters, yielding upper limits on the gamma-ray emission. By comparing the upper limit for the north-west radio relic region of Abell 3667 with the model prediction, we can derive a lower limit for the magnetic field of the region of $\sim 0.1\mu G$ (see Fig. 8). This shows the potential of gamma-ray observations in studies of the cluster environment. We also discuss the flux upper limit from cluster center regions with a model of gamma-ray emission from neutral pions produced in hadronic collisions of cosmic-ray protons with the intra-cluster medium (ICM). The derived upper limit of the cosmic-ray energy density within this framework was 1 order higher than that of our Galaxy.



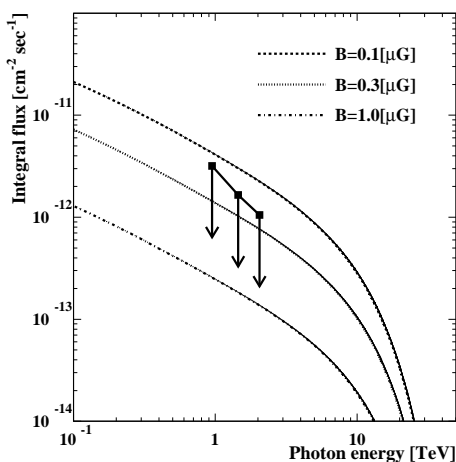Fig. 8. Derived gamma-ray flux upper limits from *NW Relic* region of Abell 3667 (filled squares) with the predicted gamma-ray fluxes. The model was scaled with the mass and the distance of Abell 3667 to that of Coma-like cluster, and is shown in the case of magnetic field of $0.1\mu G$, $0.3\mu G$, and $1.0\mu G$.

## Summary

We have been carrying out stereo observations of sub-TeV gamma-rays with CANGAROO-III since March 2004. There has been a significant progress in the analysis of the stereoscopic observations. On the HESS sources MSH 15-52 and J1804-216, our new results are consistent with the recent H.E.S.S. results. Upper limits were given for the nearby radio galaxy, Cen A, the globular cluster, $\omega$ Cen, supernova remnants, SN 1987A, Kepler's SNR, Galactic Plane, and clusters of galaxies. For the flaring activity of PKS 2155-304 in July/August 2006, we detected time-varying gamma-ray flux from this source. Observations and analyses of other sources are in progress and results will be reported soon.

## Bibliography

[1] Collaboration website: http://icrhp9.icrr.u-tokyo.ac.jp.

[2] S. Kabuki et al., *Astrophys. J.*, **668**, 968 (2007).

[3] R. Enomoto et al., *Astrophys. J.* **671**, 1939 (2007).

[4] Y. Sakamoto et al., *Astrophys. J.* **676**, 113 (2006).

[5] T. Nakamori et al., *Astron. Astrophys.* **677**, 297 (2008).

[6] Y. Higashi et al., *Astrophys. J.*, in press (2008).

[7] R. Enomoto et al., *Astrophys. J.*, in press (2008).

[8] M. Ohishi et al., *Astropart. Phys.*, in press (2008).

[9] R. Kiuchi et al., submitted for publication (2008).

# TA: Telescope Array Experiment

Spokespersons:

M. Fukushima / ICRR, University of Tokyo
P. Sokolsky / Dept. of Physics, University of Utah

Collaborating Institutions:

Chiba Univ., Chiba, Japan; Chungnam Nat. Univ., Daejeon, Korea; Ehime Univ., Matsuyama, Japan; Ewha W. Univ., Seoul, Korea; Hiroshima City Univ., Hiroshima, Japan; Hanyang Univ., Seoul, Korea; ICRR, Univ. of Tokyo, Kashiwa, Japan; INR, Moscow, Russia; Kanagawa Univ., Yokohama, Japan; KEK/IPNS, Tsukuba, Japan; Kinki Univ., Higashi-Osaka, Japan; Kochi Univ., Kochi, Japan; Los Alamos Nat. Lab., Los Alamos, NM, USA; Musashi Inst. of Tech., Tokyo, Japan; Nat. Inst. of Rad. Sci., Chiba, Japan; Osaka City Univ., Osaka, Japan; Pusan Nat. Univ., Pusan, Korea; Rutgers Univ., Piscataway, NJ, USA; Saitama Univ., Saitama, Japan; Tokyo Inst. of Tech., Tokyo, Japan; Tokyo Univ. of Science, Noda, Japan; Univ. of Denver, Denver, CO, USA; Univ. of New Mexico, Albuquerque, NM, USA; Univ. of Utah, Salt Lake City, UT, USA; Utah State Univ., Logan, UT, USA; Waseda Univ., Tokyo, Japan; Yamanashi Univ., Kofu, Japan; Yonsei Univ., Seoul, Korea

## Super-GZK Cosmic Rays

The AGASA air shower ground array observed 11 extremely-high energy cosmic rays (EHECRs) exceeding the energy of $10^{20}$ eV in 13 years of operation. The rate of such events is consistent with a continued spectrum with a power law of $E^{-2.7}$ and the expected GZK-cutoff structure due to the interaction of EHE protons with the cosmic microwave background [1] was not observed. The Fly's Eye air fluorescence telescope also reported an event with $3 \times 10^{20}$ eV in 1994 [2].

High energy astronomical objects such as the active galactic nuclei and radio galaxies were searched as a possible origin of such EHECRs, but none were found in the arrival direction of these events within 100 Mpc of our galaxy [3]. More distant origins may be considered, but only if a special mechanism to allow a longer propagation of EHECRs to take place, for example the violation of special relativity [4] or the EHE neutrinos as the carrier of such energy [5].

It was therefore conceived that super-GZK ($E > 10^{20}$ eV) cosmic rays may be generated by the decay of super-heavy particles in the nearby universe. Energies beyond $10^{20}$ eV are easily attained if the mass of the particle is at the Grand Unification scale. A concentration of the particles in the galactic hallo makes the non-observation of GZK-cutoff viable. Such super-heavy particles may be surviving as a relic particle of
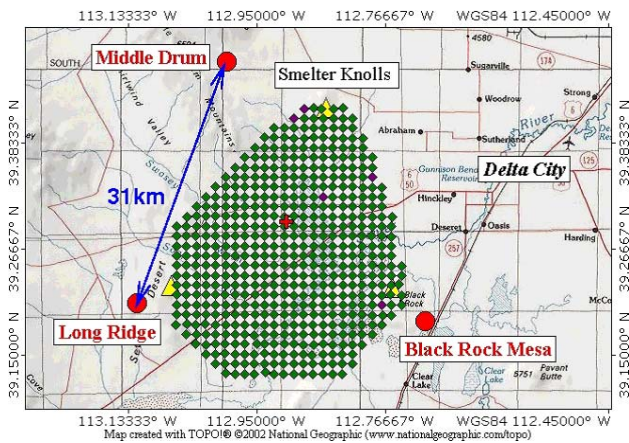
Fig. 1. Detector Arrangement of ph-1 TA. The locations of the 507 surface detectors are indicated by filled green boxes for the deployed ones and filled purple boxes for the four undeployed ones and the one to be moved. The three fluorescence telescope stations are marked by filled red circles. The three communication towers are marked by filled yellow triangles. The central laser facility is marked by a red cross.

the Big Bang or presently generated by the decay of topological defects [6]. An abundant generation of EHE gamma rays and neutrinos, in place of protons and nuclei, is expected in the decay of such particles.

## Overview of TA

The Telescope Array (TA) project was proposed in 2000 [7] to investigate the origin of super-GZK cosmic rays by employing a large array of fluorescence telescopes with $\sim$100 times larger acceptance than AGASA. The HiRes experiment, however, presented an energy spectrum indicating the GZK-cutoff in the 27th ICRC in Hamburg and the result was later published in 2003 [8]. It was a monocular spectrum obtained by the single telescope.

With contradictory results on the existence of GZK cutoff appearing, it became urgent to understand the experimental bias in the energy and the acceptance determination of super-GZK cosmic rays. The construction of full TA is thus deferred, and we initiated constructing a composite detector with AGASA-like ground array and TA fluorescence telescopes [9] instead. We call it as phase-1 TA (ph-1 TA). We expect simultaneous measurement of the same EXECRs by the detectors of two different types will sort out the systematics of two methods. It will guide us to a reliable determination of the primary energy and the acceptance of EHECRs.

The phase-1 TA consists of a large plastic scintillator array and three stations of air fluorescence telescopes overlooking the array from periphery as shown in Fig.1. The ground array will give an aperture of $\sim$1900 km$^2$ sr for zenith angles below 60°, which is approximately an order of magnitude larger than that of AGASA. The fluorescence telescope will have a stereoscopic aperture of $\sim$860 km$^2$ sr with 10% duty factor at $10^{20}$ eV. The telescope will also supply information on the primary particle species by measuring the longitudinal shower profile. It is located in the West Desert of Utah, 140 miles south of Salt Lake City (lat. 39.3°N, long. 112.9°W, alt. $\sim$1400 m). The construction was completed in 2007, and TA is fully operating from March 2008.

## Ground Array of ph-1 TA

The ground detector array consists of 507 plastic scintillators on a grid of 1.2 km spacing. It covers the ground area of $\sim$700 km$^2$. Approximately 80% of them are on the Federal land, $\sim$10% on the state trust land and the rest on privately owned land. The detection (trigger) efficiency is $\sim$100% for cosmic rays with energies more than $10^{19}$ eV with zenith angle less than 45°.

The counter is composed of two layers of plastic scintillator overlaid on top of each other. The scintillator (CIMS-G2; CI Kogyo Ltd.) is 1.2 cm thick, 3 m$^2$ large and is read out by 104 wave length shifter fibers installed in grooves on the surface (see Fig.2). The fiber (Y-11(200)M; Kuraray Co., Ltd.) has a diameter of 1 mm and a length of 5 m. Both ends of the fiber are bundled and optically connected to the photomultiplier (9124SA; Electron Tubes Ltd.). A passage of cosmic ray muon gives $\sim$25 photo-electrons in average. Two layers are used for the coincidence measurement for the muon calibration trigger. There is a possibility for extending the dynamic range by setting different PMT gains for two counters in the future.

The signal from each PMT is continuously digitized with a 12-bit flash ADC with 50 MHz sampling. When both of the PMTs record more than 1/3 of the muon signal, wave forms of 2.56$\mu$s duration are stored with a time stamp supplied by the GPS (M12+ Timing Oncore Receiver; Motorola,Inc.). This rate of local buffering is less than 1 kHz. The relative timing between remotely separated counters will be better than $\pm$20 ns by the GPS, which is sufficient to supply good resolution for the determination of the arrival direction.

When one of the PMT signals exceeds a trigger threshold of three muons, the timing is recorded in a local trigger list. The content of the list is transmitted to a branch DAQ board by the wireless LAN at 1 Hz. The list contains less than 100 events for normal counters. To cover communication in the whole surface detector array, the array is divided into three regions. The branch DAQ board is installed on a communication tower built at the periphery of the array for each region. Each surface detector is assigned to one of the three branch DAQ boards on the tower. A colinear antenna which is indirectional in azimuth is connected to each branch DAQ board. Three communication towers about 12 m high were built in September 2006. An air shower event is identified by the branch DAQ firmware by requiring clustered hits (at least three adjacent counters) with a good coincidence timing (within 8$\mu$sec). The trigger rate of air shower events taken at each tower is around 0.003 Hz.

When an air shower trigger is generated in a branch DAQ board, a command is sent to all counters, and relevant counters storing the event with good coincidence timing ($\pm$32$\mu$sec) respond by transmitting the wave form data to the branch DAQ board. We employ a commercially produced wireless transmitter with the maximum speed of 11 Mbps using 2.4 GHz spread spectrum technology, and we use the speed of 2 Mbps. The dead-time-less DAQ operation is aimed with the high transmission speed together with a large buffering memory at each counter. The data in a branch DAQ board on the tower are transmitted to an industrial PC board inside a cabinet at the tower site. The data taken in the PC board at the tower
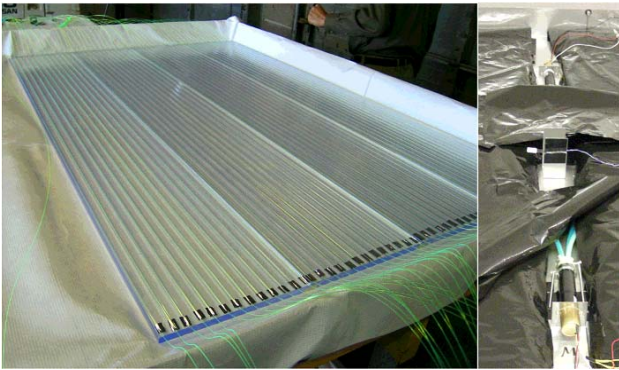
Fig. 2. Scintillation Detector of TA. (left) scintillator plates with fibers on the surface. (right) PMTs with fiber bundles.



Fig. 3. Deployed Surface Detector.



Fig. 4. Air Shower Event Observed with Surface Detectors. (a) an array of surface detectors which observed more than 1/3 of a muon signal. The numbers near the circles indicate the numbers of particles that passed the detectors. The radius of the circle is proportional to logarithm of the number of particles. (b) wave form distributions from the detectors. The numbers show the detector locations.

sites are then transmitted via wireless long-distance communication network and stored in a mass storage at the Cosmic Ray Center in DELTA. Fig.4 shows an air shower event taken with surface detectors.

The total electrical power consumed by the PMT, ADC, GPS and LAN is approximately 6 W and is locally generated by the solar panel of ∼120 W capacity (KC-120J; Kyocera Co., see Fig.3). Behind the panel is a heat-insulated enclosure containing the backup battery (DCS100-L; 12V, ∼100 Ah and deep cycle) and all the electronics. A communication antenna is fixed to a mast 3.3 m tall. The planar-type antenna is used for most of the surface detectors while the parabolic antenna with higher gain is used for the detectors far from the tower. The total weight of the counter is about half tons, such that it can be easily deployed by helicopter without disturbing the wilderness environment.

We started the assembly of scintillator detectors in ICRR in the spring of 2005 and completed the assembly in the autumn of 2006. We exported them to the Cosmic Ray Center in Delta of Utah, USA, where we finally assembled scintillator detectors on the platforms together with other components. We started major deployment of the counters in October 2006. We deployed 485 counters by the end of Februay,
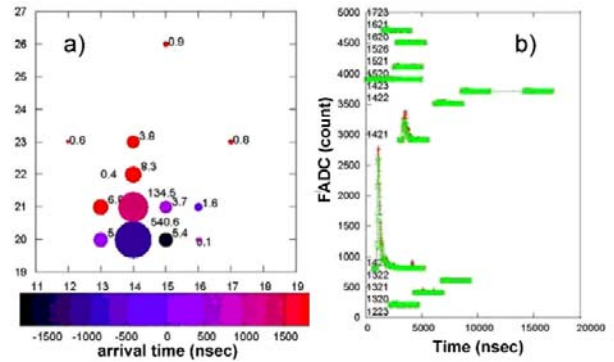
2007. We chose about 50 clustered detectors as a subarray in each branch to check on the stability of communication between the branch DAQ board and the detectors to establish DAQ system. We adjusted the height of the antennas of all the detectors in the three subarrays to minimize the effect of radio wave reflected on the ground upon direct wave between the detectors and a communication tower. Based on the debugging with these subarrays, we tuned all the remaining detectors in October 2007. We have 503 surface detectors in the field after we deployed remaining counters in December 2007. We have been taking data for the whole ground array from March 2008. We plan to deploy remaining four counters in the autumn of 2008.

## Fluorescence Telescope

The ph-1 TA has three fluorescence stations. The fluorescence station in the southeast is called the Black Rock Mesa (BRM) site. The southwestern station is called Long Ridge (LR) site and the station in the north is called Middle Drum (MD) site.

Twelve reflecting telescopes are installed at each of the BRM and LR stations (see Fig.5) and cover the sky of $3° - 34°$ in elevation and $108°$ in azimuth looking toward the center of the ground array.

The field of view of each telescope (see Fig.6) is $18.0°$ in azimuth and $15.5°$ in elevation. A spherical dish of 6.8 m$^2$ is composed of 18 hexagonal mirrors with a radius of curvature of 6067 mm. The direction of each mirror was individually adjusted and a spot size of less than 20 mm in diameter was achieved at the focal plane (2960 mm). The mirror is made by 10.5 mm thick high thermal resistivity glass (Schott Borofloat) and is aluminum coated by vacuum deposition. The surface of the aluminum is protected by producing a ∼50 nm thick anodization layer.

The air shower image is detected by a mosaic PMT camera on the focal plane (see Fig.7). A set of $16 \times 16$ PMTs (Hamamatsu 6234) with a hexagonal window is used for one camera. Each PMT covers $1.1° \times 1.0°$ patch of the sky. A UV transmitting glass filter (Schott BG3, 4 mm thick) is attached in front of each PMT for blocking the night sky background in the vis-

Fig. 5. Fluorescence Telescope Station at Black Rock Mesa.



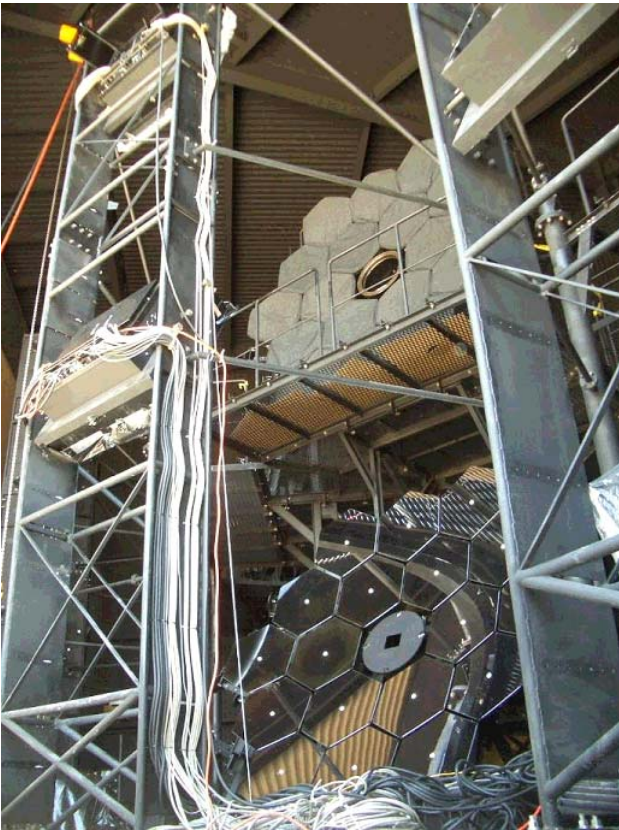Fig. 7. PMT Camera of TA fluorescence Telescope.



Fig. 6. Fluorescence Telescopes of TA.

ible light range. The whole camera is assembled in a chassis with a window made by a UV transparent plexiglass.

Negative high voltage is applied to the PMT by a bleeder circuit using zener diodes to ensure a stable operation under high night sky background. The high voltage was individually adjusted for all PMTs. With a PMT gain of $\sim 10^5$, a linearity of up to 32 k photoelectrons in 100 ns was achieved.

A signal from the PMT is amplified by a factor of 50 by the pre-amplifier and is sent to a Signal Digitizer and Finder (SDF) with a twisted pair cable about 25 m long. The SDF module receives the signal with a shaping filter and digitizes it with a 12-bit, 40 MHz FADC. Consecutive four samplings are added by the following FPGA. A trace of fluorescence

signal is searched in pipeline at the FPGA employing a sliding sum algorithm for every 25.6 $\mu$s of the time window. The dc component from the night sky background is estimated every 1 ms and is subtracted. The SDF is a 9U VME module and 16 channels are mounted in one module. There are 16 SDF modules in one VME crate for one camera.

The result of the "hit" search by the SDF is reported to a Track Finder (TF) in the same VME crate and an air shower track is searched in one camera. A track is found when five or more adjacent PMTs are fired. A looser track definition is applied to a camera-crossing event. The results of all TF modules are concentrated to a Central Trigger Decision (CTD) module and the decision of data acquisition is made. The wave form data stored in the SDF memory are read out to "a camera PC" in parallel. Data are transferred from the camera PCs and collected to a storage PC by Ethernet during the daytime.

Fig.8 shows an air shower event observed by the fluorescence telescope.

The calibration of the telescope sensitivity is important for the measurement of energy. Characterizing parameters of each component such as the mirror reflectivity, filter transmission, PMT quantum efficiency and the electronics gain were measured piece by piece at the production or in situ. The relative gain of all PMTs were adjusted in situ by the Xenon Flasher installed at the center of the mirror. The light from the flasher is diffused and filtered by BG3. The Xenon Flasher supplies a light pulse of good uniformity ($<$3%) to all PMTs in a camera.

There are three "standard" PMTs installed in a camera. The efficiency and the gain of the standard PMT are calibrated before installing to a camera and their values are transmitted to other PMTs by the Xenon Flasher calibration. A tiny YAP (YAlO$_3$:Ce) scintillator with 50 Bq $^{241}$Am source is embedded in the BG3 filter of the standard PMT. The YAP generates a short light pulse of $\sim$3000 photons around 370 nm and has an excellent temperature stability. The calibration of the standard PMT will be maintained by the YAP pulser.

For the calibration of the standard PMT, we developed a light source using a Rayleigh scattering of nitrogen laser (337 nm) in the nitrogen atmosphere. The power of laser is measured pulse by pulse to an accuracy of 5% and the known
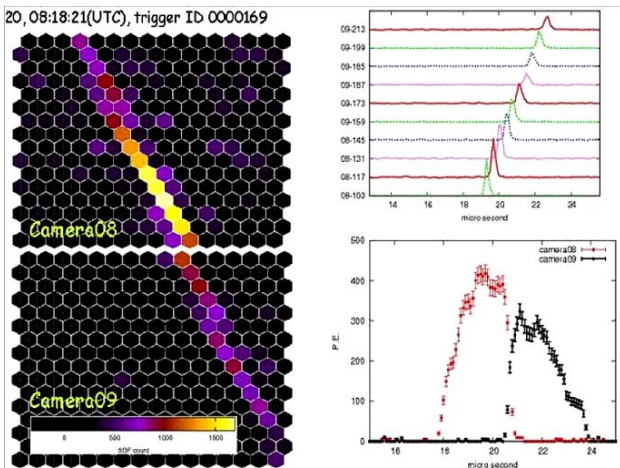
Fig. 8. Air Shower Event Observed by the Fluorescence Telescope. (left) PMTs with signals are shown in the two-dimensional configuration of the camera. (right top) wave forms of PMTs. (right bottom) time evolution of the sum of light output is shown for two cameras. Red data correspond to those from the camera 8 and black data correspond to the camera 9.



Fig. 9. TA Lidar at Black Rock Mesa.

cross section of Rayleigh scattering is applied to calculate the intensity of the scattered light.

The UV fluorescence light generated by the air shower is scattered and lost along the path of transmission to the telescope. The responsible processes are Rayleigh scattering by the air molecule and Mie scattering by the aerosol. The Rayleigh scattering can be calculated with an accuracy of ∼5% from the known density and temperature distribution of the atmosphere. The amount of Mie scattering differs from place to place and changes with time reflecting the aerosol distribution in the air. It has to be continuously monitored on site.

A lidar system located at the Black Rock Mesa station is used for the atmospheric monitoring. It consists of a pulsed Nd:YAG laser (the third harmonic, 355 nm) and a telescope attached to an alto-azimuth mount and sharing the same optical axis as shown in Fig.9. The laser can be shot to any direction and the back-scattered light is received by the telescope to analyze the extinction coefficient along the path of the laser. We had shown in Akeno that the change of the three-dimensional distribution of extinction coefficient can be monitored within 10 km from each station [10].

We are also building a laser shooting facility in the middle of the array. The site is chosen such that a vertical shot of the laser from this station is equidistant to all fluorescence stations. The intensity of the laser shot is monitored to 5%
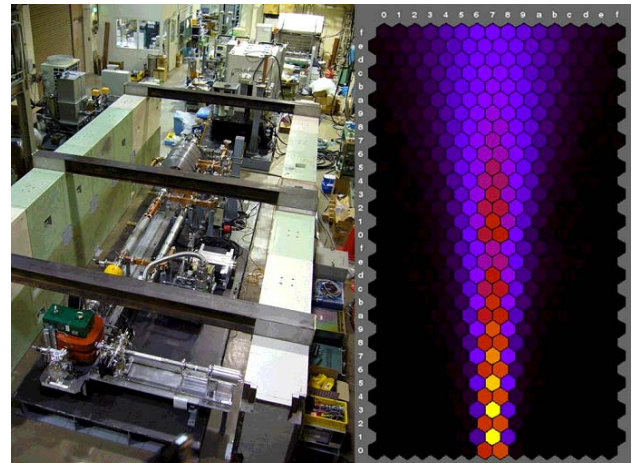


Fig. 10. Electron Linac. (left) the linac which was assembled in KEK. (right) electron linac beam seen by the Fluorescence telescopes (simulation by GEANT).

accuracy and the Rayleigh scattering at high altitude can be considered as a "standard candle" observable at all stations. The comparison of the received light gives a reliable information for the difference and the change of atmospheric conditions. For monitoring the cloud in the night sky, we installed an infra-red CCD camera at the Black Rock Mesa station, and take data of the night sky every hour during FD observation.

In order to confirm the absolute energy scale of the fluorescence detector in situ, we plan to deploy a compact electron linear accelerator ∼ 100 m away from the fluorescence station and inject an electron beam vertically up into the atmosphere. The simulation of observed fluorescence signal by 40 MeV electron beams is shown in Fig.10. A beam of $10^9$ electrons with a duration of 1 $\mu$s well simulates a shower energy deposition of ∼$4 \times 10^{16}$ eV 100 m away from the station, which corresponds to a shower of ∼$4 \times 10^{20}$ eV 10 km away. The calibration is obtained by comparing the observed fluorescence signal with the expected energy deposition calculated by the GEANT simulation. The accelerator was designed with a collaboration of KEK accelerator physicists and was assembled in KEK. We have been testing the basic performance of the accelerator in KEK from February 2007. The main accelerator part will be installed in a 40-feet commercial container, and we will be able to transport the accelerator system to Utah in JFY 2008.

In March 2007, the telescope system at the BRM station was nearly completed. In November, the telescope system both at the BRM and LR stations started regular operation.

The HiRes observatory was shut down in April 2006. The Middle Drum fluorescence station has been constructed using refurbished equipment from the old HiRes-I observatory at Dugway in Utah. Leveling of the site started in November 2006, and construction of the building was completed in March 2007. The Middle Drum Observatory consists of seven bays each about the size of a two car garage as shown in Fig. 11. We started moving HiRes mirrors and installed to a new building in May as shown in Fig. 12 . MD Observatory was partially operated in July 2007, and started regular observation with all the 14 telescopes from the beginning of

Fig. 11. The Middle Drum Observatory Building.



Fig. 12. Mirrors with cameras at the Middle Drum Observatory.

November 2007. HiRes mirrors are 20% smaller in area than the mirrors in the BRM and LR stations. The MD fluorescence detector will also observe at eleveation angles from 3 to 31 degrees.

Three fluorescence stations are fully operated from November of 2007.

## Prospects

The construction of the ph-1 TA was completed in 2007 by the collaboration of Japanese, Korean, and American physicists. We started taking data and the ph-1 Ta is fully operated. The group consists of physicists who have been working in AGASA, HiRes and other HEP experiments in US, Korea, and Japan. The Japanese fund for ph-1 TA was approved in 2003 by the Grants-in-Aid for Scientific Research (Kakenhi) of Priority Areas. The US group has submitted a matching proposal to NSF in 2005. The US proposal includes a construction of TALE, a Low Energy extension of TA down to $10^{17}$ eV, to investigate the modulation of CR composition and spectrum expected by the galactic to extra-galactic transition of CR origins. The infrastructure of TA and TALE in Utah is also the responsibility of US group. The US fund is supported by the US National Science Foundation (NSF) through awards PHY-0307098 and PHY-0601915 (University of Utah)

and PHY-0305516 (Rutgers University).

The Pierre Auger group is constructing a large hybrid experiment in Argentina with 1600 water tank detectors and four fluorescence telescope stations. All the fluorescence telescopes are operated. The Auger group calibrated the ground array energy estimator $\rho(1000)$, the muon density 1000 m away from the shower center, by the measurement of shower energy from the fluorescence telescope. The extrapolation of the calibration from the lower energy, where most of the hybrid events were collected, caused the major part of the systematic error.

Recently the Auger group and the HiRes group published the results of energy spectrum, which are consistent with GZK cutoff [11, 12], although their energy scales are determined only by the method of fluorescence telescope. For the anisotropy, the Auger group claimed there is a correlation between the arrival directions of the highest energy cosmic rays and the positions of AGN [13] while the HiRes group reported that no correlations, other than ramdom correlations, have been found [14].

The acceptance of Auger ground array is $\sim$4.5 times larger than that of ph-1 TA assuming the same zenithal acceptance. The scintillator of TA counts the number of penetrating charged particles and it is dominated by the electrons which outnumber the muons by an order of magnitude. The water tank of Auger on the other hand is more sensitive to the penetrating high energy muons rather than the soft electrons which stop near the surface of the water tank and do not generate as many Cherenkov photons.

The energy measurement of ph-1 TA therefore is less sensitive to the unknown composition of the primary cosmic rays and the details of hadronic interactions at EHE, whereas its sensitivity to the composition determination using the muon content is severely limited particularly for the EHE gamma rays and neutrinos. It is our belief that the characteristic features of ph-1 TA, the sampling of electromagnetic shower energy, the unique calibration of fluorescence generation, usage of HiRes-I telescopes in TA site, and the measurement in the Northern Hemisphere, will make an essential contribution to the understanding of the intricate problem of GZK cutoff.

## Bibliography

[1] K.Greisen, Phys. Rev. Lett. **16**, 748 (1966); T.Zatsepin and V.A.Kuzmin, JETP Lett. **4**, 178 (1966).

[2] D.J.Bird et al., Astrophys. J., **424**, 491 (1994).

[3] Y.Uchihori et al., Astropart. Phys. **13**, 151 (2000); G.Sigl et al., Phys. Rev. **D63**, 081302 (2001).

[4] H.Sato and T.Tati, Prog. Theo. Phys. **47**, 1788 (1972); S.Coleman and S.L.Glashow, Phys.Rev. **D59**, 116008 (1999).

[5] T.J.Weiler, Astropart.Phys. **3**, 303 (1999).

[6] V.Kuzmin and I.Tkachev, JETP Lett. **68**, 271 (1998); V.Berezinsky, P.Blasi and A.Vilenkin, Phys.Rev. **D58**, 103515 (1998); K.Hamaguchi, I.Izawa, Y.Nomura and T.Yanagida , Phys.Rev. **D60**, 125009 (1999); V.Berezinsky, Nucl. Phys. Proc. Suppl. **81**, 311 (2001).

[7] The Telescope Array Project: Design Report, July, 2000.

[8] T.Abu-Zayyad et al., Phys. Rev. Lett. **92**, 151101 (2004); T.Abu-Zayyad et al., Astropart. Phys. **23**, 157 (2005).

[9] M.Fukushima et al., Proc. of 28th ICRC, Tsukuba, **2**, 1025 (2003); S.Kawakami et al., Proc. of 28th ICRC, Tsukuba, **2**, 1033 (2003); F.Kakimoto et al., Proc. of 28th ICRC, Tsukuba, **2**, 1029 (2003); M.Fukushima, Proc. of APPI2003 workshop, KEK Proceedings 2003-6.

[10] T.Yamamoto et al., Nucl. Instr. and Methods **A488**, 191 (2002).

[11] R.U. Abbasi *et al.* (HiRes Collaboration), Phys. Rev. Lett. **100**, 101101 (2008).

[12] J. Abraham *et al.* (Pierre Auger Collaboration), Phys. Rev. Lett. **101**, 061101 (2008).

[13] J. Abraham *et al.* (Pierre Auger Collaboration), Astropart. Phys. **29** (2008); J. Abraham *et al.* (Pierre Auger Collaboration), Science **318**, 939 (2007);

[14] R.U. Abbasi *et al.* (HiRes Collaboration), astro-ph/0804.0382.

# Tibet AS$\gamma$ Project

## Experiment

The Tibet air shower experiment has been successfully operated at Yangbajing (90°31' E, 30°06' N; 4300 m above sea level) in Tibet, China since 1990. It has continuously made a wide field-of-view (approximately 2 steradian) observation of cosmic rays and gamma rays in the northen sky.

The Tibet I array was constructed in 1990 and it was gradually upgraded to the Tibet II by 1994 which consisted of 185 fast-timing (FT) scintillation counters placed on a 15 m square grid covering 36,900 m$^2$, and 36 density (D) counters around the FT-counter array. Each counter has a plastic scintillator plate of 0.5 m$^2$ in area and 3 cm in thickness. All the FT counters are equipped with a fast-timing 2-inch-diameter photomultiplier tube (FT-PMT), and 52 out of 185 FT counters are also equipped with a wide dynamic range 1.5-inch-diameter PMT (D-PMT) by which we measure up to 500 particles which saturates FT-PMT output, and all the D-counters have a D-PMT. A 0.5 cm thick lead plate is put on the top of each counter in order to increase the counter sensitivity by converting gamma rays into electron-positron pairs in an electromagnetic shower. The mode energy of the triggered events in Tibet II is 10 TeV.

In 1996, we added 77 FT counters with a 7.5 m lattice interval to a 5,200 m$^2$ area inside the northern part of the Tibet II array. We called this high-density array Tibet HD. The mode energy of the triggered events in Tibet HD is a few TeV.

In the late fall of 1999, the array was further upgraded by adding 235 FT-counters so as to enlarge the high-density area from 5,200 m$^2$ to 22,050 m$^2$, and we call this array and further upgraded one Tibet III. In 2002, all of the 36,900 m$^2$ area was
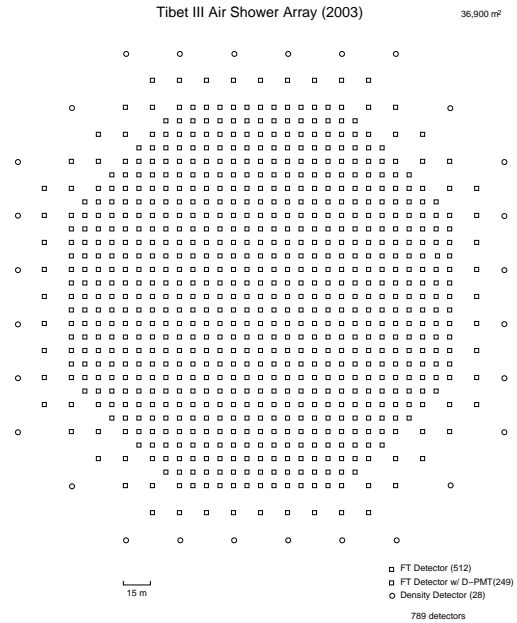


Fig. 1. Schematic view of the Tibet III array.

covered by the high-density array by adding 200 FT-counters more. Finally we set up 56 FT-counters around the 36,900 m$^2$ high density array and equipped 8 D-counters with FT-PMT in 2003. At present, the Tibet air shower array consists of 761 FT-counters (249 of which have a D-PMT) and 28 D-counters as in Fig. 1.

The performance of the Tibet air shower array has been well examined by observing the Moon's shadow (approximately 0.5 degree in diameter) in cosmic rays. The deficit map of cosmic rays around the Moon demonstrates the angular resolution to be around 0.9° at a few TeV for the Tibet III array. The pointing error is estimated to be better than ~0.01°, by displacement of the shadow's center from the apparent center in the north-south direction, as the east-west component of the geomagnetic field is very small at the experimental site. On the other hand, the shadow center displacement in the east-west direction due to the geomagnetic field enables us to spectroscopically estimate the energy scale uncertainty at ±10 % level.

Thanks to high statistics, the Tibet air shower experiment introduces a new method for energy scale calibration other than the conventional estimation by the difference between the measured cosmic-ray flux by an air shower experiment and the higher-energy extrapolation of cosmic-ray flux measured by direct measurements by balloon-borne or satellite experiments.

## Physics Results

Our current research theme is classified into 4 categories:

(1) TeV celestial gamma-ray point/diffuse sources,

(2) Chemical composition and energy spectrum of primary cosmic rays in the knee energy region,

(3) Cosmic-ray anisotropy in the multi-TeV region with high precision,

(4) Global 3-dimensional structure of the solar and inter-planetary magnetic fields by observing the Sun's shadow in cosmic rays.



Fig. 2. From [1]. The observed and reproduced sidereal anisotropy of GCR intensity. The intensity in 5x 5 pixel is represented in a color-coded format as a function of the right ascension on the horizontal axis and the declination on the vertical axis, (a): observed anisotropy, (b): reproduced anisotropy, (c): significance map of the residual anisotropy. The dotted line in each panel shows the celestial equator, while the white curve represents the Galactic equator in the celestial coordinate. The star symbol in each panel indicates the heliospheric nose direction (the upstream direction of the interstellar wind). The black pixels containing strong TeV gamma ray sources indicated in (c) are excluded from the present best-fit analysis,. For more detail, see [1].

We will introduce a part of the results obtained in this fiscal year.

It is demonstrated[1] that the large-scale anisotropy of approximately 5 TeV galactic cosmic ray (GCR) intensity observed by Tibet Air Shower experiment can be reproduced by the superposition of a bi-directional and uni-directional flows (UDF and BDF) of GCRs. The heliosphere is located inside the local interstellar cloud (LIC) very close to the inner edge of the LIC. If the GCR population is lower inside the LIC than outside, the BDF flow is expected from the parallel diffusion of GCRs into LIC along the local interstellar magnetic field (LISMF) connecting the heliosphere with the region outside the LIC, where the GCR population is higher. A type of the UDF, on the other hand, is expected from the $B \times \nabla n$ drift flux driven by a gradient of GCR density (n) in the LISMF (B). The LISMF orientation deduced from the best-fit direction of the BDF is almost parallel to the galactic plane and more consistent with the suggestion of Frisch (1996) than that of Lallement et al. (2005). We note that the model, if holds, yields the LISMF polarity together with its orientation.

We observed the shadowing of galactic cosmic rays in the direction of the Moon, what we call the Moon's shadow, by the Tibet air shower array (Tibet-III) in operation at Yangbajing (4300 m a.s.l.) in Tibet, China since 1999. As almost all the cosmic rays are positively charged, they are bent by the geomagnetic field, thereby shifting the Moon's shadow westward. Cosmic rays will also produce a shadow additionally in the eastward direction of the Moon, if they contain negatively charged particles, such as antiprotons, according to their fraction. We selected $1.5 \times 10^{10}$ air shower events with energy beyond 3 TeV approximately from the dataset accumulated by the Tibet air shower array. With the dataset, we detected the Moon's shadow at $\sim 40\sigma$ level. The center of the Moon was in the direction away from its apparent center of the Moon by $0.23°$ to the west. Comparison between the Moon's shadow data and a full Monte Carlo simulation enables us to search for the existence of the shadow produced by antiprotons at multi-TeV energies. We found no evidence for the existence of antiprotons in this energy region. As is shown in Fig. 3, we set an upper limit of 7 % on the flux ratio of antiprotons to protons at the 90 % confidence level in the multi-TeV energy region.[3]
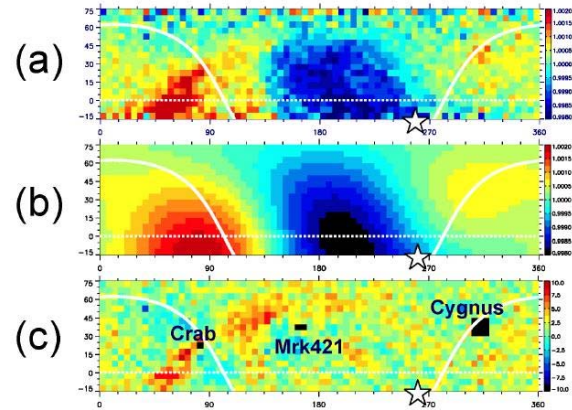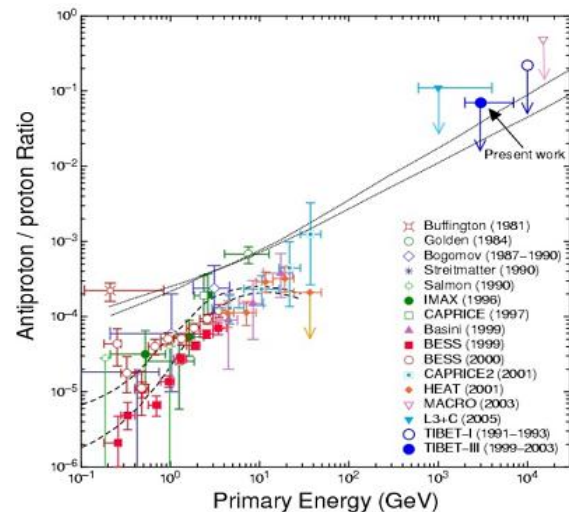


Fig. 3. From [3]. The antiproton/proton ratio at the atmosphere. For more detail, see [3].
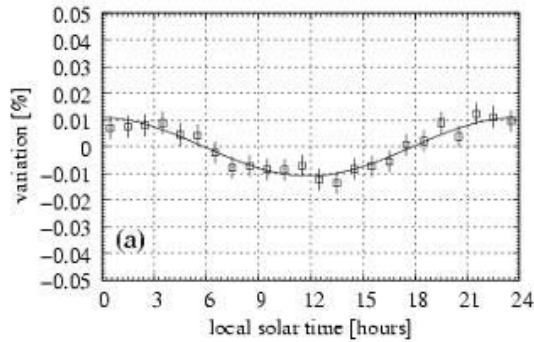
Fig. 4. From [4]. The differential variation of relative CR intensity in the local solar time. The solid lines are the sinusoidal curves best fitted to the data. The error bars are statistical only. For more detail, see [4].
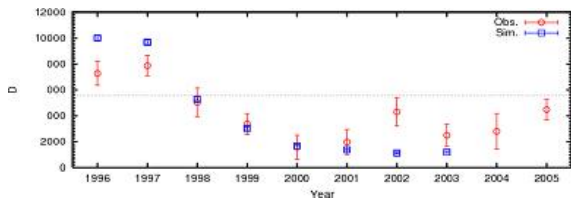


Fig. 5. Observed yearly variation of the Sun's shadow depth compared with our simulation assuming a Radial Field model.

We show[4] that the amplitude of the Compton-Getting (CG) anisotropy contains the power-law index of the cosmic-ray energy spectrum. Based on this relation and with the Tibet air-shower array data, we measure the cosmic-ray spectral index to be $-3.03 \pm 0.55_{stat} \pm < 0.62_{syst}$ between 6 TeV and 40 TeV, consistent with $-2.7$ from direct energy spectrum measurements, as is shown in Fig. 4. Potentially, this CG anisotropy analysis can be utilized to confirm the astrophysical origin of the "knee" against models for non-standard hadronic interactions in the atmosphere.

The solar activity in Cycle 23 gradually changes to final minimum phase. The Sun's shadow generated by multi-TeV cosmic-ray particles has been continuously observed with the Tibet-II and Tibet-III air shower array in 1996 through 2006 during almost whole period of the Solar Cycle 23. We have shown that the Sun's shadow is strongly affected by the solar and interplanetary magnetic fields changing with the solar activity. We present yearly variation of the Sun's shadow in association with the Solar Cycle 23. Additionally, we made a comparison between observation and Monte Carlo simulation of the Sun's shadow depth using a Radial Field model, which is in agreement with the observation, as is shown in Fig. 5

## Other Activities

This group has developed and completed several automatic measuring systems that are powerful for analyzing cosmic ray tracks or air shower spots, that is, automatic microdensitometers, precise coordinate-measuring systems and image scanners controlled by a computer. Enormous data recorded on nuclear emulsion plates or X-ray films are rapidly and precisely measured by the use of these measuring systems.

The emulsion-pouring facilities can meet the demands for making any kind of nuclear emulsion plates which are used for cosmic ray or accelerator experiments. The thermostatic emulsion-processing facilities are operated in order to develop nuclear emulsion plates or X-ray films. Using these facilities, it is also possible to make and develop emulsion pellicles in 600 $\mu$m thickness each. In this way, these facilities are open to all the qualified scientists who want to carry out joint research program successfully.

## Future Plans

### (1) Gamma-ray astronomy in the 100 TeV region

We have a plan to construct a large ($\sim 10,000$ m$^2 \times 1.5$m deep) underground ($\sim 2.5$ m soil+concrete overburden) water Cherenkov muon detector array (Tibet MD) around an extended version (Tibet AS, $\sim 83,000$ m$^2$) of Tibet III. By Tibet AS + MD, we aim at background-free detection of celestial point-source gamma rays in the 100 TeV region (10 TeV – 1000 TeV) with world-best sensitivity and at locating the origins of cosmic rays accelerated up to the knee energy region in the northern sky. The measurement of cut off energies in the energy spectra of such gamma rays in the 100 TeV region may contribute significantly to understanding of the cosmic-ray acceleration limit at SNRs. Search for extremely diffuse gamma-ray sources by Tibet AS + MD, for example, from the galactic plane or from the Cygnus region may be very intriguing as well. Above 100 TeV, the angular resolution of Tibet AS with 2-steradian wide field of view is 0.2° and the hadron rejection power of Tibet MD is 1/10000. The proposed Tibet AS + MD, demonstrated in Fig. 6, has the world-best sensitivity in the 100 TeV region, superior to HESS above 10-20 TeV and to CTA above 30-40 TeV.

Then, how many unknown/known sources do we expect to detect by Tibet AS + MD, assuming the energy spectra of the gamma-ray sources extend up to the 100 TeV region? Eleven of the HESS new 14 sources discovered by the galactic plane survey in the southern sky would be detected by Tibet AS + MD, if it were located at the HESS site. As no extensive search has been done by an appratus with sensitivity comparable to HESS (1 % in unit of RX J1713.7-3946/50-hour observation) in the northern sky, we expect to discover some 10 new gamma-ray sources in the northern sky. In addition to unknown point-like sources, we expect to detect established sources in the 100 TeV region: TeV J2032+4130, HESS J1837-069, Crab, some new Milagro sources, Mrk421, Mrk501 are sufficiently detectable and Cas A, HESS J1834-087,LS I+63 303, IC443 and M87 are marginal.

Furthermore, our integral flux sensitivity to diffuse gamma rays will be the world-best as well. The diffuse gamma rays from the Cygnus region reported by the Milagro group and also diffuse gamma-rays from the galactic plane will be clearly detected. Diffuse gamma-rays of extragalacitic origin may be an interesting target as well.

In fall, 2007, a prototype underground muon detector, composed of two 52m$^2$ water pools, was successfully constructed in Tibet to demonstrate the technical feasibility, cost
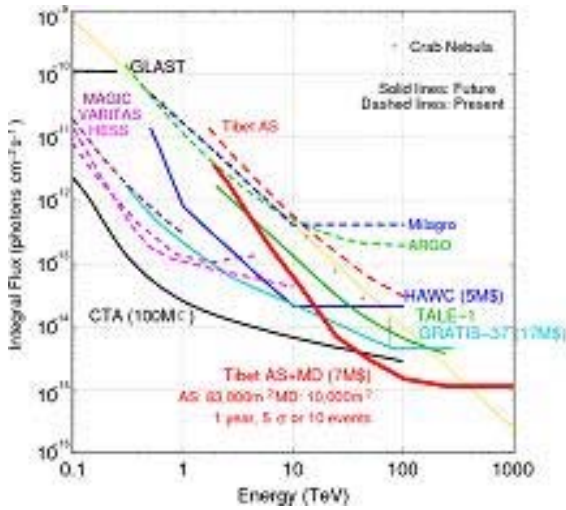
Fig. 6. Tibet AS + MD (red curve) integral flux sensitivity ($5\sigma$ or 10 events/1yr) for a point source.



Fig. 7. Prototype muon detector viewed from outside, just before being covered with soil.

estimate, validity of our Monte Carlo simulation, as is shown in Figs. 7 and 8.



Fig. 8. Prototype muon detector viewed from inside.
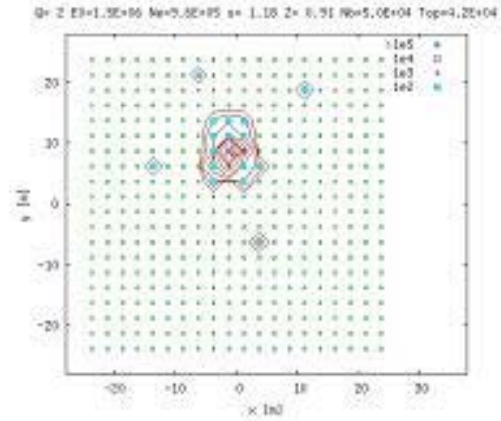


Fig. 9. Illustration of YAC array.
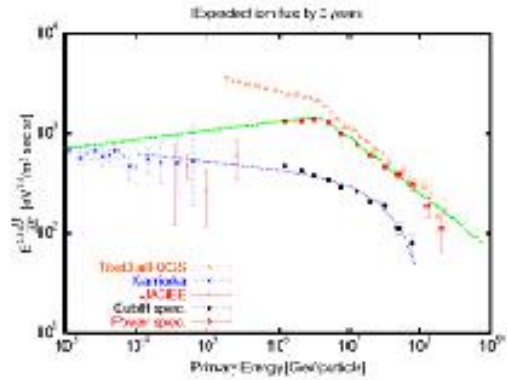


Fig. 10. Expected cosmic-ray iron energy spectra with Tibet AS + YAC.

## (2) Chemical composition of primary cosmic rays making the knee in the all-particel energy spectrum

We have measured the energy spectra of primary cosmic-ray protons, heliums, all particles around the knee energy region. The main component responsible for making the knee structure in the all particle energy spectrum is heavier nulei than helium. The next step is to identify the chemical component making the knee in the all particle energy spectrum. We have a plan to install an air shower core detector array (1000 to 5000 $m^2$ in area) around the center of Tibet III, as is illustrated in Fig. 9 to distinguish the heavy component making the knee by measuring the difference in lateral distribution of energetic air shower cores.

This will be the first experiment to selectively measure the energy spectrum of the heavy component in the knee energy region and will demonstrate that the knee of the all particle energy spectrum is really composed of heavy nuclei. Figure 10 shows the expected energy spectra of cosmic-ray iron nuclei depending on theoretical models. Tibet AS + YAC has a strong model discrimination power.

## Tibet ASγ collaboration

ICRR, Univ. of Tokyo, Kashiwa, Chiba 277-8582

In collaboration with the members of:
Hirosaki Univ., Hirosaki, Japan; Saitama Univ., Urawa, Japan; IHEP, Beijing, China; Yokohama National Univ., Yokohama, Japan; Hebei Normal Univ., Shijiazhuang, China; Tibet Univ., Lhasa, China; Shandong Univ., Jinan, China; South West Jiaotong Univ. Chengdu, China; Yunnan Univ., Kunming, China; Kanagawa Univ., Yokohama, Japan; Faculty of Education, Utsunomiya Univ., Utsunomiya, Japan; ICRR, Univ. of Tokyo, Kashiwa, Japan; Konan Univ., Kobe, Japan; Shibaura Inst. of Technology, Saitama, Japan; Department of Physics, Shinshu Univ., Matsumoto, Japan; Center of Space Science and Application Research, Beijing, China; Tsinghua Univ., Beijing, China; Waseda Univ., Tokyo, Japan; NII, Tokyo, Japan; Tochigi Study Center, Univ. of the Air, Utsunomiya, Japan; AMNC, Utsunomiya Univ., Utsunomiya, Japan; Tokyo Metropolitan Coll. of Aeronautical Eng., Tokyo, Japan; Shonan Inst. of Technology, Fujisawa, Japan; RIKEN, Wako, Japan; School of General Education, Shinshu Univ. Matsumoto, Japan.

## Bibliography

### Papers in refereed journals

[1] "Implication of the sidereal anisotropy of 5TeV cosmic ray intensity observed with the Tibet III air shower array", M. Amenomori *et al.*, Proceedings in AIP Conf. **932** 283–289, (2007).

[2] "Underground water Cherenkov muon detector array with the Tibet air shower array for gamma-ray astronomy in the 100 TeV region", M. Amenomori *et al.*, Astrophysics and Space Science **309** 435–439, (2007).

[3] "Moon Shadow by Cosmic Rays under the Influence of Geomagnetic Field and Search for Antiprotons at Multi-TeV Energies", M. Amenomori *et al.*, Astroparticle Physics **28** 137–142, (2007).

[4] "New Estimation of the Spectral Index of High-Energy Cosmic Rays as Determined by the Compton-Getting Anisotropy", M. Amenomori *et al.*, ApJ **672** L53–L56, (2008).

### Papers in conference proceedings

[5] "Cosmic ray data and their interpretation: about the Tibet Air Shower Array - Chemical Composition of Cosmic Rays at the Knee Viewed from the Tibet Air Shower Experiment -", M. Shibata for the Tibet ASγ experiment, Nuclear Physics B (Proc. Suppl.) **175-176**, 267–272, (2008).

[6] "The cosmic-ray energy spectrum around the knee measured by the Tibet-III air-shower array", M. Amenomori *et al.*, Nuclear Physics B (Proc. Suppl.) **175-176**, 318–321, (2008).

[7] "Spectral index of high-energy cosmic rays by the Compton-Getting effect at solar time frame with the Tibet air shower array", M. Amenomori *et al.*, Nuclear Physics B (Proc. Suppl.) **175-176**, 427–430, (2008).

[8] "Northern Sky Survey for Gamma-ray Point Sources in 100 TeV Region with the Tibet Air Shower Array", M. Amenomori *et al.*, Nuclear Physics B (Proc. Suppl.) **175-176**, 431–434, (2008).

[9] "A large underground water Cherenkov muon detector array with the Tibet air shower array for the Gamma-ray astronomy in the 100 TeV region: Overview and physics goal", M. Amenomori *et al.*, Nuclear Physics B (Proc. Suppl.) **175-176**, 476–479, (2008).

[10] "A large underground water Cherenkov muon detector array with the Tibet air shower array for the Gamma-ray astronomy in the 100 TeV region: detector design and simulation", M. Amenomori *et al.*, Nuclear Physics B (Proc. Suppl.) **175-176**, 480–483, (2008).

## The Ashra Project

### Overview

Ashra (*All-sky Survey High Resolution Air-shower detector*) [1, 2, 3] is a project to build an unconventional optical telescope complex that images very wide field of view, covering 80% of the sky, yet with the angle resolution of a few arcmin, sensitive to the blue to UV light with the use of image intensifier and CMOS technology. The project primarily aims to observe Cherenkov and fluorescence lights from the lateral and longitudinal developments of very-high energy cosmic rays in the atmosphere. It can also be used to monitor optical transients in the wide field of sky.

### Project

The observatory will firstly consist of one main station having 12 detector units and two sub-stations having 8 and 4 detector units. One detector unit has a few light collecting systems with segmented mirrors. The features of the system were studied with a prototype detector unit located on Haleakala. The main station was constructed on Mauna Loa (3,300 m) in 2007.

The key technical feature of the Ashra detector rests on the use of electrostatic lenses to generate convergent beams rather than optical lens systems. This enables us to realize a high resolution over a wide field of view. This electron optics requires:

- *image pipeline;* the image transportation from imaging tube (image intensifier) to a trigger device and image sensors of fine pixels (CCD+CMOS), with high gain and resolution, and

- *parallel self-trigger:* the systems that trigger separately for atmospheric Cherenkov and fluorescence lights.

| Opt. Transients | TeV-$\gamma$ | Mountain-$\nu$ | Earth-skimming-$\nu$ | EeV-CR |
|---|---|---|---|---|
| B-UV | Cherenkov | Cherenkov | Fluorescence | Fluorescence |
| $\lambda$=300$\sim$420nm | 2 TeV | 100 TeV | 10 PeV | 100 PeV |
| 15 mag./4s @3$\sigma$ | 5% Crab/1yr@5$\sigma$ | 5 WB-limit/1yr | 2 WB-limit/1yr | 1600/1yr $>$10 EeV |
| 2 arcmin | 6 arcmin | unknown | 3 arcmin @ 100 PeV | 1 arcmin @ 10 EeV |

Table 1. Summary of performance with the full configuration (Ashra-2) of three Ashra sites. Detected light, energy threshold, sensitivity limit, and angular resolution are listed from top down for each objective. For EeV-CRs, trigger requirement is two or more stations. Waxman and Bahcall have calculated a neutrino flux upper limit from astrophysical transparent source, here referred to as the WB-limit. For the observation time for objectives other than optical transients, the realistic detection efficiency is taken into account.

## Observational Objectives

*optical transients;* Ashra will acquire optical image every 6 s after 4-s exposure. This enables us to explore optical transients, possibly associated with gamma ray bursts (GRBs), flares of soft gamma-ray repeaters (SGRs), supernovae explosion, and so on, in so far as they are brighter than $B \simeq 15$ mag, for which we expect 3-$\sigma$ signals (Fig. 1). The unique advantage is the on-time detection of the events without resorting to usual satellite alerts. 10$\sim$20 events per year are expected in coincidence with the Swift gamma-ray events. The field of view that is wider than satellite instruments allows to detect more optical transients, including an interesting possibility for an optical flash, not visible with gamma rays.
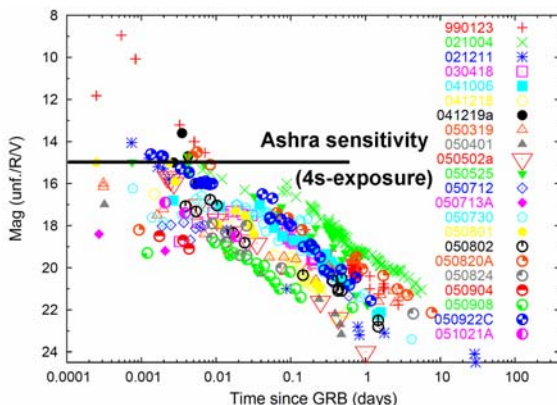


Fig. 1. Early light curves (unfiltered, R and V ) for a set of GRBs with detections within minutes of the gamma-ray event. All the measurements shown have been taken from GCN circulars (Guidorzi et al. astro-ph/0511032). The limiting magnitude ($\simeq$B) expected with Ashra (4s-exposure) is shown as a horizontal line. There are no observations within 10 s after the GRB events.

*TeV gamma rays;* Atmospheric Cherenkov radiation will be imaged by Ashra. Requiring the signal-to-noise ratio (SNR) $>$5, the system will allow to explore VHE gamma-ray sources with the energy threshold of 2 TeV at the limiting flux sensitivity of 5% Crab for 1-year observation.

*EeV cosmic rays;* For fluorescence lights from VHE cosmic rays the effective light gathering efficiency is comparable with that of the High Resolution Fly's Eye detector (HiRes). The arcmin pixel resolution of Ashra provides finer images of longitudinal development profiles of EeV cosmic ray (EeV-CR) air showers. The resolution of arrival direction with the stereo

reconstruction is thus significantly improved and it is better than one arcmin for the primary energy of EeV and higher [4]. This is useful to investigate events clustered around the galactic and/or extragalactic sources. This in turn would give us information as to the strength and coherence properties of the magnetic field.

*PeV-EeV neutrinos;* Ashra may detect Cherenkov and/or fluorescence signals generated from tau-particle induced air-showers that is generated from interactions of tau neutrinos with the mountain and/or the earth. This is identified by peculiar geometry of the air-shower axis. The 1-year detection sensitivity with the full configuration of Ashra is 5 and 2 times larger than the Waxman-Bahcall limit for mountain-produced event (Cherenkov) and earth-skimming event (fluorescence), respectively. The most sensitive energy of around 100 PeV is suitable for the GZK neutrino detection.

The expected performance for each observational object is summarized in Table 1.

## Test Observation

We have constructed a 2/3-scale prototype Ashra detector and a 3m-diameter altazimuth Cherenkov telescope on Haleakala to verify the optical and trigger performances. From October 2004 to August 2005 at the observatory, We made good observations for 844 hours out of 1,526 hours of the moonless nighttime. The efficiency is 55% of the moonless nighttime and 11% of entire time. This inefficiency is due primarily to bad weather.

The fine resolution (arc-minutes) in the ultra wide field of view (0.5 sr) has already been demonstrated using a 2/3-scale model. Fig. 2 shows an example of a 50-degree FOV image in which the constellations Taurus and Orion can be clearly identified with the 2/3-scale prototype. The inset, a two-degree square window, shows a close-up view of the Pleiades.

Our wide field observation covered the HETE-2 WXM error box at the time of GRB041211. 2,000 images were taken every 5 s with 4-s exposure from the time 1h7m before GRB041211 to 1h41m after GRB041211. We detected no objects showing time variation in the WXM error box. It indicates the 3-sigma limiting magnitudes of B$\sim$11.5 magnitude [5]. This is compared with other observations in Fig. 3 [6] [7]. We also successfully performed two more observations coincident with Swift: GRB050502b [8] and GRB050504 [9].

A demonstration of air Cherenkov imaging of high-energy gamma/cosmic ray is shown in Fig. 4 which was taken during observing Mkr501. Separately, we have confirmed the
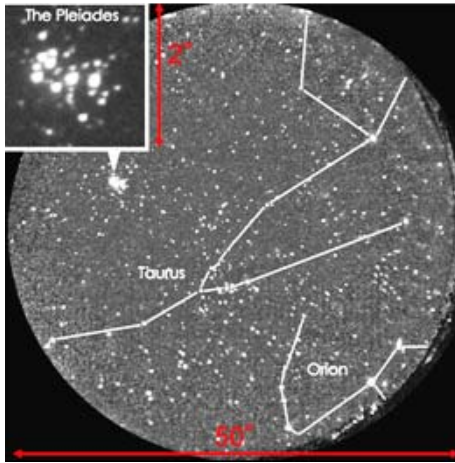
Fig. 2. Example of a 50-degree FOV image taken by the Ashra prototype. The solid lines are drawn to indicate the constellations Taurus and Orion. The inset, a two-degree square window, shows a close-up view of the Pleiades.
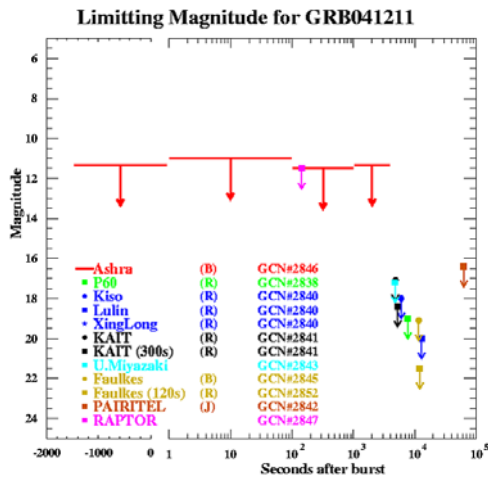


Fig. 3. 3-sigma limiting magnitudes of the test observation with the Ashra prototype and comparison with other observations for GRB041211 as a function of time after GRB. Note that the horizontal axis unavoidably stands for time (s) in logarithmic scale after the burst (positive) and in linear scale before the burst (negative).

alpha-parameter peak of TeV $\gamma$-rays from the Crab nebula to be greater than 5 $\sigma$.

## Site Preparation

After finishing the grading work for the area of 2,419 m$^2$ at the Mauna Loa site at the end of July 2005, installation of electrical power lines and transformers was performed until the beginning of September. We started the construction of the detector in October 2005 after receiving materials from Japan. By the middle of December 2005, the first shelters having motorized rolling doors, acrylic plate windows to maintain air-tightness, and heat-insulating walls and floors have been constructed and positioned on eight construction piers of concrete blocks at the Mauna Loa site. In the shelters, the optical elements of the light collectors have been already installed. The optical performance were checked and adjusted to be op-
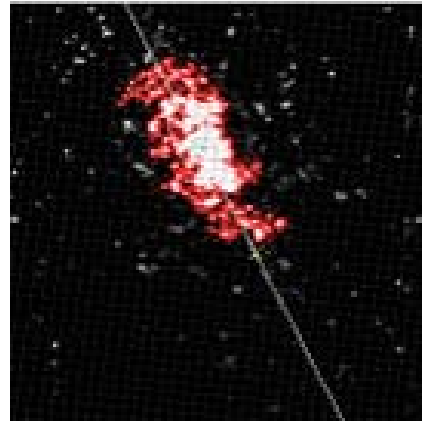


Fig. 4. Self-triggered Cherenkov image of air shower detected by using the Ashra photoelectric image pipeline and a prototype trigger sensor system. This image was taken during tracking Mkr501.

timum with star light images from the pilot observation.

In December 2005, we evaluated the night sky background flux on Mauna Loa using the Ashra light collector installed and aligned in a shelter. The result is fairly consistent with the background in La Palma and Namibia by the HESS group From the star light observations, our understanding of the light correction efficiency to be accurate within 5% level.
The civil engineering construction of light collectors in shelters at the Mauna Loa site was completed in August 2007.

Figure 5 shows a picture of the constructed Mauna Loa stations. In this Ashra-1 experiment, we are performing device installation and specific observation in a step-by-step way to enhance the scientific impacts.



Fig. 5. The Ashra main and sub stations at the Mauna Loa sites.

## Observation

As a first step, we have started the observation of optical transients. During observation, Optical images were constantly collected every 6 s after 4-s exposure. Table 2 summarizes our observation statistics up to now. In the table, maximum observable time is defined by the following condition:

- *Sun condition;* the altitude of the sun must be lower than $-18$ degree.

- *Moon condition;* the altitude of the moon is lower than 0 degree, or the moon fraction is less than 0.1.

| Season | Period | Maximum Observable Time (astronomically allowed) | Observable Time (good weather rate) | Observed Time (operation efficiency) | Number of Images |
|--------|--------|------------|------------|------------|------------|
| S001 | 6/28 –7/16 | 99.5 hr | 93.2 hr (94 %) | 86.1 hr (92 %) | 41000 |
| S002 | 7/21 –8/14 | 123.1 hr | 115.0 hr (93 %) | 113.7 hr (99 %) | 64300 |
| S003 (on going) | 8/19 –9/4 | 99.0 hr | 99.0 hr (100 %) | 98.1 hr (99 %) | 57100 |

Table 2. Summary of Ashra optical transients observation.

Apparently, we have made a good start in terms both of good weather rate and operation efficiency. In particular, good weather rate greater than 90 % is very impressive.

The next step is to start observation of Cherenkov air showers using the light collector towards Mauna Kea. It may detect Cherenkov signals originated from tau neutrinos which interacts with the mountain and/or the earth as described in Section . We have prepared the optical and photoelectric image pipeline system in that light collector as shown in Fig. 6. The installation of trigger and DAQ system is in progress now. Pilot observation to confirm the detection principle of tau neutrino will be carried out soon.



Fig. 6. The light collector towards Mauna Kea equipped with Photo-electric Image Pipeline.

## Perspective

The full Ashra observatory (Ashra-2) will consist of three experimental sites separated by about 30 km on Mauna Loa (3,300 m), Camp Kilohana (2,014 m) on the side of Mauna Kea, and Hualalai (2,320 m) on the island of Hawaii. The full configuration emphasizes the stereoscopic observation Cherenkov and fluorescence lights from air showers with two or three stations at separated sites as well as the effective detection area for air showers. The parallax observation for optical transients with two or more stations is also useful for rejecting local background events.

## Bibliography

[1] http://www.icrr.u-tokyo.ac.jp/~ashra

[2] Sasaki, M., "Very High Energy Particle Astronomy with All-sky Survey High Resolution Air-shower Detector (Ashra)", *Progress of Theoretical Physics Supplement,* vol. 151, pp. 192–200, 2003.

[3] Sasaki, M., et al., 2005. "Status of Ashra project," Proc. 29th Int. Cosmic Ray Conf. Pune 8, 17-200.

[4] Sasaki,M., et al., "Design of UHECR telescope with 1 arcmin resolution and 50° field of view", *Nucl. Instrum. Methods,* vol. A492, pp. 49–56, Oct. 2002.

[5] Sasaki, M., et al., 2004. GCN Circ. 2846.

[6] Sasaki,M., et al., 2005. Proc. 29th Int. Cosmic Ray Conf. Pune 8, 17-200.

[7] Sasaki, M., et al., 2005. "Observation of Optical transients with the Ashra Prototype," Proc. 29th Int. Cosmic Ray Conf. Pune 5, 319-322.

[8] Sasaki, M., et al., 2005. GCN Circ. 3499.

[9] Sasaki, M., Manago, N., Noda, K., Asaoka, Y., 2005. "GRB050502b: Early Observation," GCN Circ. 3421.

# ASTROPHYSICS and GRAVITY DIVISION

## Overview

Astrophysics and Gravity Division consists of Gravitational Wave Group, The Sloan Digital Sky Survey Group and Theory Group. The Gravitational Wave Group conducts R&Ds for LCGT project jointly with researchers of gravitational wave experiment and theory in Japan. The main items of those R&Ds are TAMA project and CLIO project. The Sloan Digital Sky Survey Group continues accumulating data of images and spectroscopic observation of galaxies and publishing papers in collaboration with worldwide researchers. Theory Group conducts both theoretical study of the Universe and astroparticle physics.

## Gravitational Wave Group

### Introduction

A gravitational wave is a physical entity in space-time predicted by Einstein's theory of general relativity. Its existence was proven by the observation of PSR1913+16 by Taylor and Hulse [2], who won the Nobel prize in 1993. However, nobody has succeeded to directly detect gravitational waves. The theory of gravitation can be tested by the detection of gravitational waves. A gravitational wave detector is the last eye of mankind to inspect the universe. In order to directly observe gravitational waves, we aim to construct the Large scale Cryogenic Gravitational wave Telescope (LCGT). For the first step of constructing sensitive laser interferometer, we developed a 300 m baseline interferometric gravitational wave detector, TAMA, at the Mitaka campus of the National Astronomical Observatory of Japan (NAOJ) and several observations had been conducted. TAMA project started in April, 1995, as a five-year project and it was extended by two years after 1999. TAMA is organized by researchers belonging to universities and national laboratories. We achieved nine data-taking runs that span from two to eight weeks, which ended in 2004. Since 2004, we were trying to attain its ultimate sensitivity as reported in the previous Annual reports (2004-2006). About TAMA project, we present its development of Seismic Attenuation System (SAS) newly installed for four main mirrors. In regard with CLIO project, the construction of which was started in 2003 and ended in March, 2007, we have succeeded to operate its sensitive laser interferometry at cryogenic temperature at first in the world. In addition to these R&Ds, we conducted research on optical quality measurement, Resonant Sideband Extraction scheme, practical suspension system by crystal fibers, digital control system and so on.

### Status of TAMA Project

[Spokesperson : Kazuaki Kuroda] ICRR, Univ. of Tokyo, Kashiwa, Chiba 277-8582

In collaboration with the members of: TAMA collaboration

*2   J. H. Taylor and J. M. Weisberg, Astrophysical J., **345** (1989) 434.

NAOJ, Tokyo; KEK, Tsukuba; UEC, Tokyo; Osaka City Univ., Osaka; Kyoto Univ., Kyoto; Osaka Univ., Osaka; Niigata Univ., Niigata

The achieved sensitivity of TAMA at the time of Data Taking Run 9 was reported in the previous Annual report (2005-2006).[1] We recognize that there is still a gap between the achieved sensitivity and the practically attainable one, at low frequencies. However, we could demonstrate that the basic techniques for the interferometer operation was acquired by the fulfillment of the target noise curve at frequencies more than 800 Hz, where the optical system properly worked and the control system was appropriate. The noise spectrum at frequencies lower than 30 Hz was disturbed by non-stationary ground motion and the spectrum in a frequency range from 30 Hz to 300 Hz was determined by the actuator noise to stabilize the mirror alignment mainly due to relatively larger seismic noise at Mitaka campus of NAOJ. In order to identify the noise source governing the spectrum in the frequency range from 300 Hz to 800 Hz, we have finally finished the installation of Seismic Attenuation System (SAS) for four main mirrors and improved the performance of anti-vibration at low frequencies. One set of the new SAS is illustrated in Fig 1.
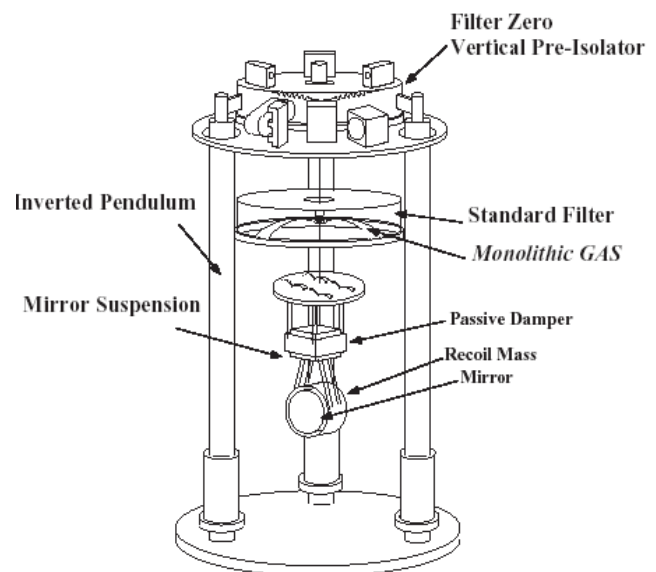


Fig. 1. One set of Seismic Attenuation System (SAS) newly installed to TAMA. The previous mirror suspension system was modified and the system was suspended through the monolithic geometrical anti-spring (Standard Filter) with the vertical pre-isolator (Filter Zero) sit on the plate supported by three inverted pendulums that was electrically controlled to maintain its neutral position.

The previous mirror suspension system had been mounted on an optical table supported by three sets of stack consisting of multilayer sandwiches of sealed rubber and mass plate. The optical table was removed and the mirror sus-
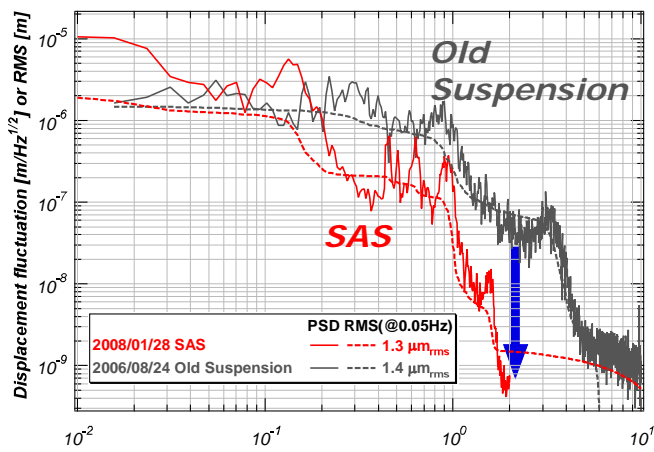
Fig. 2. Improved displacement noise at the test mass by newly installed SAS. Comparing with the old system, the displacement noise is decreased by more than one order at 2 Hz. Improvement of the interferometer sensitivity is ongoing.

pension that was slightly modified was suspended through the monolithic geometrical anti-spring with the vertical pre-isolator sit on the top plate supported by three inverted pendulums electrically controlled to maintain its neutral position. The resonant frequency of the inverted pendulum was set as 30 mHz by a feedback circuit utilizing outputs of accelerometers mounted on the top table. This mechanism serves as the anti-vibration system against low frequency horizontal seismic motion. Vertically, two sets of geometrical anti-spring were installed through the top plate. Each resonances were set 0.5 Hz. The mirror suspension system was designed as the previous one except the recoil mass to hold the parts of actuators. The upper plate suspends four wires suspending the second mass part that behaves as a passive damper. This passive damper suspends both the main mirror and the recoil mass part. [2]

Figure 2 shows the improvement of anti-vibration performance at low frequencies. Comparing with the old system, the displacement noise was decreased by more than one order at 2 Hz. Although the displacement amplitudes at frequencies less than 0.2 Hz were larger than the old system due to widening the working frequency range, RMS amplitude has been improved from $1.4\mu$m to $1.3\mu$m as in Fig.2. Preliminary experiment to achieve the ultimate sensitivity using SAS shows apparent improvement of sensitivity at low frequencies.

In parallel with the improvement by mounting SAS, analog parts of the interferometer control system are being replaced by digital ones.[3] Optimizing filters and lock acquisition procedure are expected to be conducted rather shorter time scale than before, which naturally enhances the speed of commissioning.[4] We expect that noise sources of TAMA interferometer are identified by these improvements. In regard with data analysis, we made reports with LIGO project at the time when the sensitivity of TAMA300 had competitiveness [5, 6]. Without new observation, persistent activity on the development of data analysis was conducted using existing TAMA 300 observation data.[7, 8]

# CLIO Project

[Spokesperson : Masatake Ohashi]

ICRR, Univ. of Tokyo, Kashiwa, Chiba 277-8582
In collaboration with members of: KEK, Tsukuba; Kyoto-U, Kyoto; ERI of UT, Tokyo

CLIO (Cryogenic Laser Interferometer Observatory) is a 100 m-baseline underground cryogenic interferometer at the Kamioka Mine. CLIO forms a bridge connecting the CLIK (7 m prototype cryogenic interferometer at Kashiwa campus) and the planed LCGT (3 km cryogenic interferometer at Kamioka). The site of CLIO, near the Super-Kamiokande neutrino detector, is shown in Fig. 3. The tunnel was dug in 2002, and a strain meter for geophysics was installed in 2003 [3]. The construction of CLIO began in late 2003, and installation of the mode cleaner vacuum system was reported in the annual report (2003–2004). Four sets of cryostats and whole vacuum system were installed (annual report 2004–2005). We started the operation of CLIO in 2006 (annual report 2006).



Fig. 4. Overview of the CLIO interferometer.

One of the aims of CLIO is to demonstrate the thermal noise suppression by cooling the mirrors. The main mirrors are cooled at 20 K by refrigerators. The lowest noise level of CLIO is designed to be $10^{-19}$m/$\sqrt{\text{Hz}}$ around 100 Hz, which would be $10^{-18}$m/$\sqrt{\text{Hz}}$ if cryogenics is not applied [1]. The current best sensitivity at the room temperature was obtained in the end of 2006. The displacement sensitivity arround 300Hz reached at $6 \times 10^{-19}$m/$\sqrt{\text{Hz}}$. Of special note is its high strain sensitivity below 20Hz. It is comparable with LIGO sensitivity in spite of much shorter baseline. Now we are reducing the excess noise to realize the thermal noise limited sensitivity. And we have checked the cooling of mirrors not to harm the sensitivity in 2007.

Once the objective is attained, the CLIO interferometer is used to observe gravitational wave events in parallel with the TAMA interferometer until completion of the construction of LCGT. The merits of the underground site are lower seismic noise and temperature stability. The former characteristic makes interferometer locking easily controlled, and the latter assures long-term stable operation (LISM) [2].

The 57-hours observation data were taken at February 2007 and analyzed for continuous gravitational wave from

Fig. 3. Location of the CLIO interferometer.



Fig. 5. a sapphire mirror and cryogenic suspension system.
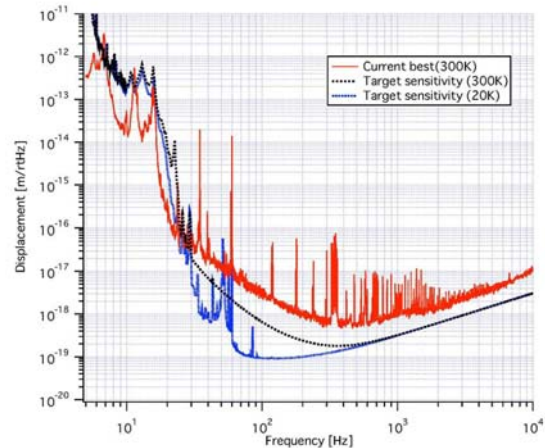


Fig. 6. CLIO displacement noise spectrum: The red curve is the current best sensitivity. The dotted line is the target sensitivity at room temperature.

the pulsar J0835-4510 (Vela pulsar) at twice its rotation frequency ( 22.38 Hz). We use an analysis method based on a matched filtering with a correction of pulsar spin down, a Doppler effect caused by the relative motion between the pulsar and the Earth, and so on. We obtained an upper limit of $h_{0(\text{U.L.})} = 5.3 \times 10^{-20}$ at 99.4 % confidence level. This value corresponds to the upper limit on the ellipticity of the neutron star, $\varepsilon = 29$ [6].

We have started preparing for cooling the mirrors just after the observation. High purity aluminum wires were used

as the mirror suspension wires and heat conductor for cooling the mirrors. We tried two configurations[7]. The first is that only one mirror suspension was modified for the cooling and diameter of 1mm high purity aluminum wires are used for the suspension wires. Figure 7 shows three displacement noise spectrum those are the best sensitivity presented in Fig. 6, before and after cooling one mirror. This is the first demonstration of the noise suppression of cooling. The second is that all the suspension wires for the sapphire mirrors are replaced to the aluminum wires diameter of 0.5mm and we tried the cooling all the mirrors. The mirrors were cooled successfully

at 14K̇ which is satisfied with our design temperature of 20K̇ and the mirrors temperature were maintained for 10 months by refrigerators. Even the mirrors were cooled, operation and control of the interferometer have been done without problem. Figure 8 shows the displacement noise spectrum, when all the mirrors were cooled.



Fig. 7. CLIO displacement noise spectrum: The blue curve shows the case that all the mirrors were the room temperature, but one suspension wires were replaced to thick aluminum wires for cooling. The red curve shows that after one mirror was cooled at 14K̇. The green curve shows the best sensitivity without cooling.



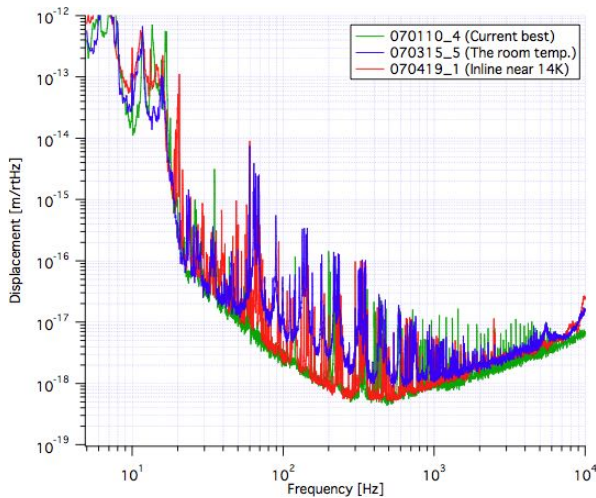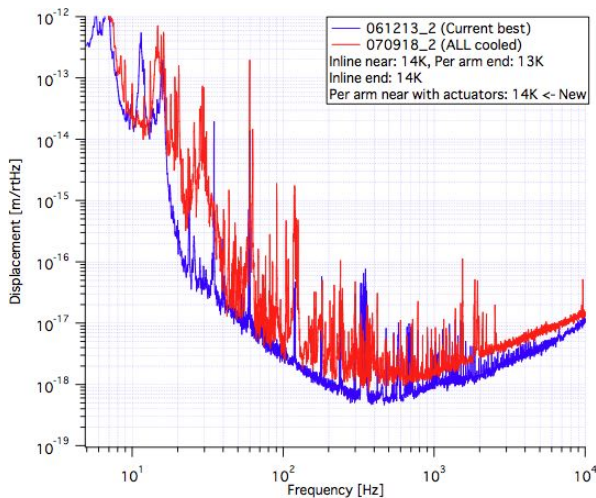Fig. 8. CLIO displacement noise spectrum: The red curve is the sensitivity with cryogenic cooled mirrors.The blue curve is the current best sensitivity.

## Bibliography

[1] M. Ohashi, *et al.*, Class. Quantum Grav. **20** (2003) S599.

[2] S. Sato, *et al.*, Phys. Rev. **D 69** (2004) 102005.

[3] S. Takemoto, *et al.*, Journal of Geodynamics **41** (2006) 23.

[4] S. Miyoki, *et al.*, Class. Quantum Grav. **23** (2006) S231.

[5] T. Uchiyama, *et al.*, Journal of Physics **32** (2006) 259.

[6] T. Akutsu, submitted for publication (2007)

[7] K. Yamamoto, *et al.*, 2008 J. Phys. Conf. Ser. **122** (2008) 012002.

## LCGT Project

[Spokesperson : Kazuaki Kuroda] ICRR, Univ. of Tokyo, Kashiwa, Chiba 277-8582

In collaboration with the members of:
LCGT collaboration; National Astronomical Observatory (Japan), KEK, Physics Department (Univ. of Tokyo), Department of Advanced Material Science (Univ. of Tokyo), Earthquake Research Institute (Univ. of Tokyo), Department of Earth Science and Astronomy (Univ. of Tokyo), Institute for Laser Science (Univ. of Electro-Communications), Department of Physics (Osaka City Univ.), Department of Physics (Osaka Univ.), Physics Department (Kyoto Univ.), Yukawa Institute (Kyoto Univ.), Advanced Research Institute for Sciences and Humanities (Nihon Univ.), Agency of Industrial Science and Technology, National Institute of Information and Communications Technology, Department of Astronomy (Beijing Normal Univ.), Center for Astrophysics (Univ. of Science and Technology, China), Institute for High Energy Physics (Chinese Academy of Science), Inter University Centre for Astronomy & Astrophysics (IUCAA), Physics Department of Physcis (University of Western Australia), Laboratory of Laser Interferometry (Sternberg State Astronomical Institute, Moscow Univ.), Louisiana State University.

## Objective of LCGT

After the discovery of the highly relativistic binary neutron star system [3], a new young binary pulsar has been detected [4]. The former discovery had increased the coalescence rate from $10^{-6}$ to $10^{-5}$ a year in a galaxy as big as our Galaxy [5] and the latter pushes up by another factor of six. Although it is a good news for the detection of gravitational waves, we still need to wait for long time to detect by the presently existing detectors. This is the reason why we have planed LCGT (Large-scale Cryogenic Gravitational wave Telescope). The objective of LCGT is to detect at least one gravitational wave event in a year. There are many other possible gravitational wave sources in the universe other than the coalescence of binary neutron stars. However, the coalescence of binary neutron stars differs completely from other sources in the sense that its wave form is precisely predicted, and its existence has certainly been confirmed.

## Status of LCGT Project

The target sensitivity of LCGT is to observe binary neutron star coalescence events occurring at 180 Mpc with S/N=10 in its optimum configuration. [9, 10] This is ten-times more sensitive than that of the LIGO (I), and by two

*3 M. Burgay, *et al.*, Nature, **426** (2003) 531.
*4 D.R. Lorimer, *et al.*, Astrophysical J. **640**(2006) 428.
*5 C. Kim, V. Kalogera and D. R. Lorimer, Astrophysical J. **584** (2003) 985.

Table 1. LCGT design parameters to detect binary neutron-star coalescence events in 180 Mpc.

| Item | Parameter |
|---|---|
| Baseline Length | 3 km |
| Interferometer | One set |
| | Power recycled Fabry-Perot -Michelson with RSE |
| Optical Power | Laser:150 W; Finesse:1550 |
| | Input power at BS: 825 W |
| | Cavity power 780 kW |
| Beam radius at End | 3 cm |
| Main Mirror | Sapphire 30 kg, 20 K |
| | Diameter 25 cm |
| | Mechanical Q:$10^8$ |
| Suspension | Frequency: 1 Hz; Q:$1 \times 10^8$ |
| pendulum | 10 K |
| Vacuum | $\leq 10^{-7}$ Pa |



Fig. 10. LCGT sensitivity (dotted blue line) compared with those of TAMA (red line), CLIO (a 100m prototype cryogenic interferometer placed underground of Kmioka mine, blue line), LIGO (initial LIGO, green line) and the design of TAMA (red broken line). The horizontal axis is frequency [Hz] and the vertical axis represents sensitivity spectrum for gravitational waves [1/√Hz].

orders more than that of TAMA at their most sensitive frequencies. This will be attained by an interferometers located underground, using a three-kilometer length baseline, cooling mirrors at cryogenic temperature, and a high-power laser source employing 150 W output. The optical configuration is a power recycled Fabry-Perot-Michelson interferometer with the resonant-sideband-extraction (RSE) scheme (in Fig. 9). The detailed design of the control system is being tested for the resonant sideband extraction scheme.[11] Table 1 lists the important parameters of LCGT, which were revised three times from the original design.[12] Ultimate sensitivity of a laser interferometer is determined by seismic noise at low frequencies (10-30 Hz) (which is reduced by improving the vibration isolation system), and it is limited by photon shot noise at higher frequencies (more than 300 Hz), which can be improved only by increasing the light power in the main cavities. The sensitivity of middle frequencies (30-300 Hz) is limited by the photon recoil force noise. This requires that thermal noise is reduced both by decreasing the temperature and by decreasing the internal mechanical loss (*i.e.*, increasing the mechanical Q of vibration modes). The source of thermal noise comes from both mirror internal vibration, mechanical loss of the optical coating and swing noise of the pendulum suspending the mirror. The reduction of thermal noise is attained by cooling both the mirror, itself, and the suspension system that suspends the mirror.

The large change of the design this year was that the number of interferometers was reduced to one in order to consider the non-negligible increase of material prices, reflecting world economy, which means that LCGT gave up some part of original data analysis, such as back ground radiation, early detection independent from other observations and so on. However, this does not mean that we gave up to firstly detect the event but we do our best to keep the attitude of the first detection.

Figure 10 compares the sensitivity curve of LCGT with those of TAMA, CLIO (a 100 m prototype cryogenic interferometer placed underground of Kmioka mine), LIGO (initial

LIGO) and the design of TAMA. The sensitivity at low frequencies of LCGT is attained by SAS, which will be proven by the current SAS in TAMA. That of higher frequencies is attained by higher laser power, which has been basically shown by TAMA. The mid-frequency region is improved by cryogenic mirror and suspension system, which will be proven by the on-going project of CLIO. Although the improvement, especially two orders of magnitude at low frequencies, is adventurous, it is not impossible until the construction period of LCGT that needs four years after the beginning of the construction.

The main effort on the research and development for LCGT has been placed on cryogenic mirrors for the past years. The implementation of cryogenic mirrors is one of the most straight-forward solutions to improve the sensitivity.

The design of the cryogenic mirror system is shown in Fig. 11. The mirror is suspended by two loops of sapphire fibers connected to an auxiliary mirror that is a part of suspension point interferometer. This mirror is also suspended from an alignment control platform that is suspended with an insulator rod connected through the center holes of the radiation shields to an isolation table suspended by a low-frequency vibration isolator, which is placed at room temperature. The auxiliary mirror has a heat link to the platform and another heat link connects the platform and a heat anchor point (4 K) inside the vacuum located just above the platform.

Both the cryogenic system and the vibration isolator are put inside a common high-vacuum chamber.

To realize this concept, the following research subjects were conducted and reported:

1. Removal of heat produced by high-power laser illumination (annual report 1997-1998 and also in references [13])

2. Holding the high Qs of the mirror internal modes and suspension pendulum [14]

3. Reducing the contamination of mirror surfaces (annual report 2000-2001 and also in [15]).
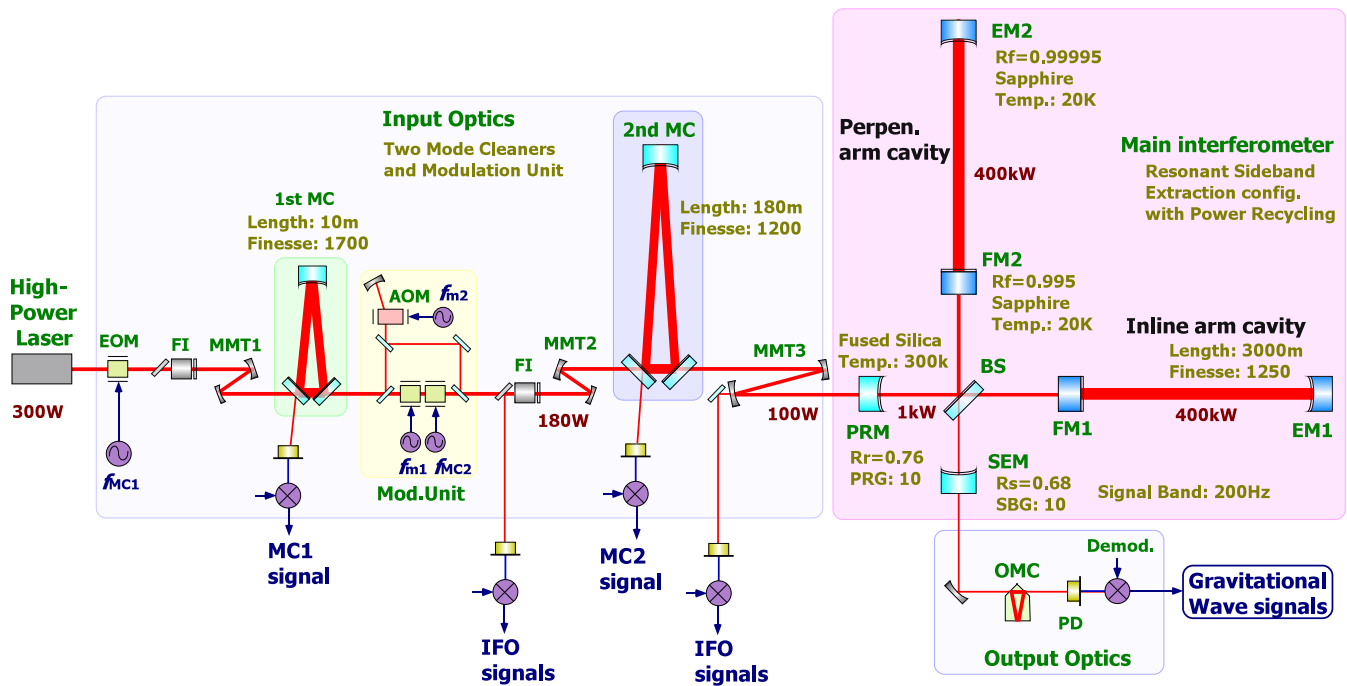
Fig. 9. Optical design of LCGT. The optical configuration is a power recycled Fabry-Perot-Michelson interferometer with the resonant-side-band-extraction (RSE) scheme.
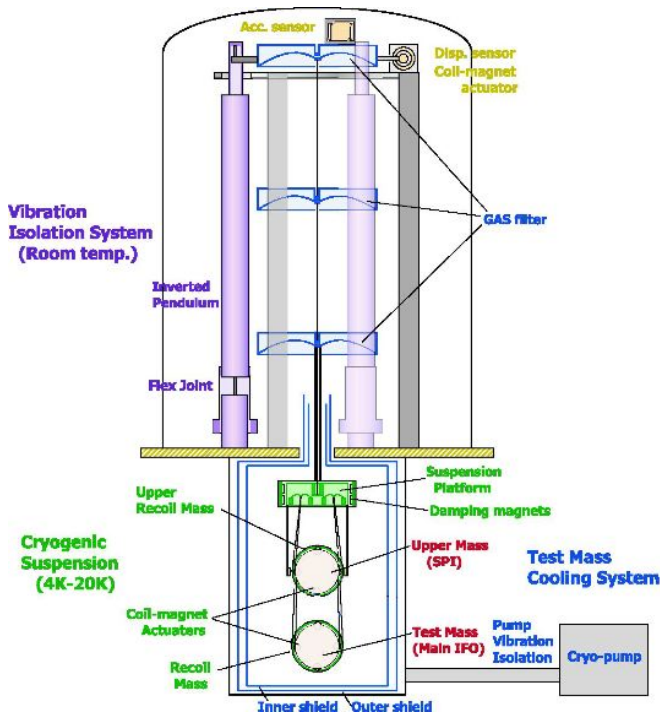


Fig. 11. Schematic design of the cryogenic suspension system. The mirror is suspended by sapphire fibers connected to an auxiliary mirror, which is suspended by metal wires from a platform that has a heat link to a 4 K heat anchor inside the vacuum. The platform is also suspended with an insulator rod connected through the holes of radiation shields to an isolation table suspended by a seismic attenuation system placed at room temperature in the common high vacuum.

4. Estimating heat production by optical loss in the mirror [16].

5. Alignment control of mirrors in a cryogenic environment [17]

6. Low mechanical loss of the optical coating (annual report 2003–2004 and also in reference [18])

As for item 5, we confirmed that a superconducting film could be used for the receptor of the magnetic force in place of permanent bar magnets that are normally used in the existing detectors. The film can be easily sputtered on the mirror surface without harmfully degrading the mechanical Q of the mirror. With respect to the last item, we reported on a measurement of the bulk substrate of the mirror at cryogenic temperature in the annual report (2003–2004). We could correctly estimate the thermal vibration noise of the optical coating while considering the inhomogeneous loss that had been neglected at an early stage of interferometer development. The substrate of the cryogenic mirror was sapphire, which has a large thermo-elastic thermal noise at room temperature. However, since the thermal-expansion ratio of sapphire at cryogenic temperature goes down to nearly 0 and the heat conductivity becomes greater, the thermo-elastic noise drastically reduces at the cryogenic temperature. Thermal noise estimated from the Q of the coating was well below the design sensitivity of LCGT, which means that this coating noise does not limit the sensitivity, whereas, the sensitivity of a room-temperature mirror is limited by this effect. This is the significant merit of the cryogenic mirror system.

The most dangerous problem was pointed by Braginskii. [6] Large power density of Fabry-Perot cavity may cause so-

*6  Braginskii, *et al.*, Physics Lett. A **305** (2002)111.

called parametric instability, which is produced by the coupling between optical cavity modes with elastic vibration modes of the mirror substrate. Since the sapphire has larger elastic wave velocity, the number density of elastic modes is fewer than that of synthesized silica mirror, which is the case of advanced LIGO. And also the coupling constant between optics and mechanics is smaller in LCGT than in advanced LIGO due to the smaller beam size of LCGT. This merit comes from the adoption of cryogenics of LCGT[19].

All of the above R&D confirmed the feasibility of reducing the thermal noise of the interferometer in the middle-frequency region. This research underlines the basis of LCGT. However, for a practical cryogenic detector, many practical R&Ds are needed for the installation of cryogenic mirrors. One of the earliest R&D activities along this line was the Kashiwa cryogenic interferometer system reported in the annual report (2000–2001; 2002–2003; 2003–2004). By this Kashiwa cryogenic interferometer, we learned the necessity of several practical R&D items and began to construct the CLIO interferometer in Kamioka to establish techniques for the cryogenic interferometer.

**Practical R&Ds: Measurement of the optical qualities of sapphire**

LCGT adopts cryogenic mirrors to reduce thermal noise in place of expanding laser beam radius that is planed both in the Advanced LIGO and the Advanced Virgo. $Al_2O_3$ monocrystal is selected as the cryogenic mirror substrate because it has excellent mechanical and thermal properties. However, there are some optical problems to be solved. High optical absorption and in-homogeneity of refractivity are concerned with rather difficult reproducibility of large ingots exceeding 20 cm. While some small-sized $Al_2O_3$ crystal substrates have good absorption quality and better homogeneity enough to satisfy the LCGT requirement (10cm in diameter, 6cm in length), larger samples have less quality [20]. Moreover, we know that the fabrication technology of $Al_2O_3$ crystal to date is not mature enough to consistently produce large substrates of adequate quality. In order to inspect optical homogeneity of large pieces of $Al_2O_3$ crystal for the production of better quality, we developed a scanning technique of birefringence measurement with high sensitivity and reported the determination of the optical axis of the uni-axial crystal and the measurement of the fluctuation of birefringence. This measurement was compared with both the measurement of Rayleigh scattering (University of Western Australia) and the measurement of refractive index (LMA, Laboratoire des Matriaux Avances - Universit Claude Bernard Lyon 1 - IN2P3 / CNRS) as reported in the previous annual report (2004-2005) and confirmed its sensitivity that makes possible to be used for evaluating optical quality required for LCGT specification.

We applied the measuring system to a large sapphire piece, 250mm in diameter, 100mm in length. This was lent by the courtesy of LIGO project, which was used to compare with synthesized silica for the advanced LIGO interferometer. Since it weighs 30 kg, the previous scanning mechanism is not durable to hold with required precision. Without changing measuring procedure of the previous system, optical readout system was mounted on a revised scanning cradle and the
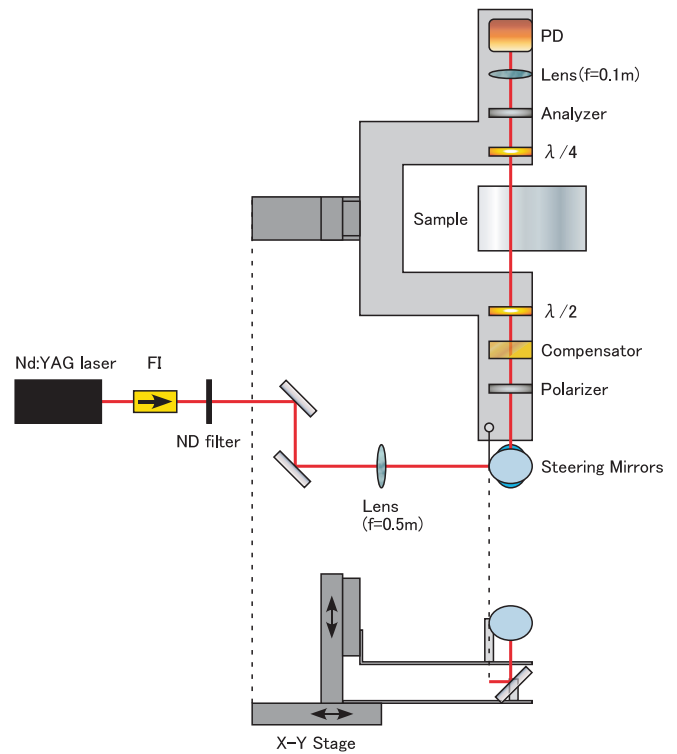


Fig. 12. Birefringence measurement was applied to a large sapphire piece weighing 30 kg, which was fixed on a measurement table and its optical readout system was mounted on the scanning cradle without changing the previous measurement procedure.
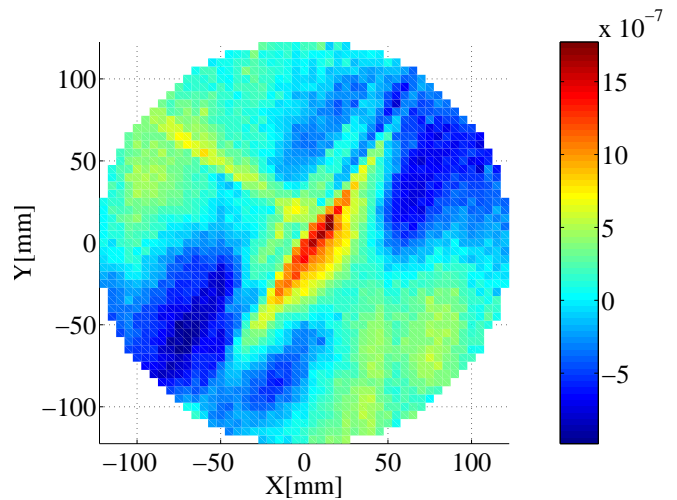


Fig. 13. Result of birefringence measurement of a large sapphire piece lent from LIGO project. The cylindrical axis coincides with m-axis of the crystal.

piece was firmly fixed on the measurement table as shown in Fig. 12.

The result is shown in Fig. 13, which shows un-negligible defect in the center of the piece. Numerically, the standard deviation of the fluctuated birefringence ($\sigma(\delta n)$) represents the grade of homogeneity. The designed beam radius of LCGT at the front mirror is 35 mm and averaged homogeneity of this beam area is $2.5 \times 10^{-7}$, where the worst homogeneity

is $5.0 \times 10^{-7}$, and the best homogeneity is $1.6 \times 10^{-7}$. Even in this small area, the required quality of LCGT is not satisfied. Since homogeneity of even the same grade piece is individually different by nearly three times according to previous measurements, the fact that this large piece does not meet the requirement does not mean that a piece of higher quality cannot be produced. The important point in this R&D is that we establish a tool to distinguish the quality required to pass the specification of LCGT.

Apart from the above R&D issues, a high power laser system that produces more than 100 W is continually being developed by a group in Advanced Material Science, School of New Frontier Science, University of Tokyo. Also, researchers at KEK tested the mechanical strength of suspension fiber of sapphire crystal [22] and the result of heat radiation leaking from room temperature tube to the cryogenic chamber was quantitatively measured as reported in the section of CLIO.[16] We steadily advance towards the realization of LCGT by these R&D activities.

## Bibliography

[1] H. Tagoshi it et al., Phys. Rev. D **63**(2001)062001-1-5.

[2] R. Takahashi *et al.*, Class. Quantum Grav. **25** (2007) 114036.

[3] D. Tatsumi *et al.*, "TAMA 300 interferometer development", TAUP 2007, September 11-15, 2007, Sendai.

[4] K. Arai*et al.*, "Recent Progress of TAMA 300", TAUP 2007, September 11-15, 2007, Sendai; D. Tatsumi *et al* "Current status of Japanese detectors", Class. Quantum Grav. **24**(2007)S399.

[5] B. Abbott *et al.*, Phys. Rev. D **72** (2005) 122004.

[6] B. Abbott *et al.*, gr-qc/0512078 (2005)

[7] H. Tagoshi *et al.*, "Results of Searches for inspiraling compact star binaries from TAMA 300fs observation in 2004-2004", TAUP 2007, September 11-15, 2007, Sendai.

[8] N. Kanda *et al.*,lq'Short gravitational wave signal searches in TAMA 300 data: stellar collapse and black hole", TAUP 2007, September 11-15, 2007, Sendai.

[9] M. Ohashi *et al.* "Status of LCGT and CLIO", TAUP 2007, September 11-15, 2007, Sendai.

[10] K. Kuroda *et.al.*, "Current status of LCGT", Seventh Edoardo Amaldi conference on gravitational waves, Sydney, July 8-14, 2007.

[11] F. Kawazoe *et al.*, presented at Amaldi 7 meeting, Sydney, July 8-14, 2007.

[12] K. Kuroda *et.al.*, Int. J. Mod. Phys. **D 8** (1999) 557; K. Kuroda,*et al.*, Class. Quantum Grav. **19** (2002) 1237; T. Uchiyama, *et al.*, Class. Quantum Grav. **21** (2004) S1161.

[13] T. Uchiyama, *et.al.*, Phys. Lett. **A 242** (1998) 211.

[14] T. Uchiyama, *et.al.*, Phys. Lett. **A 261** (1999) 5;*ibid* **A273**(2000)310.

[15] S. Miyoki, *et al.*, Cryogenics **40** (2000) 61: *ibid* **41** (2001) 415.

[16] T. Tomaru, *et al.*, Phys. Lett. **A 283** (2001) 80.

[17] N. Sato, *et al.*, Cryogenics **43** (2003) 425.

[18] K. Yamamoto, *et al.*, Class. Quantum Grav. **21** (2004) S1075.

[19] K. Yamamoto, *et al.*, presented at Amaldi 7 meeting, Sydney, July 8-14, 2007.

[20] M. Tokunari et al., J. Phys.: Conference Series 32 (2006) 432.

[21] Z. Yan, *et al.*, Applied Optics **40**(2006) 1.

[22] Seventh Edoardo Amaldi conference on gravitational waves, Sydney, July 8-14, 2007.

[23] Seventh Edoardo Amaldi conference on gravitational waves, Sydney, July 8-14, 2007.

# Sloan Digital Sky Survey

[Spokesperson : Masataka Fukugita]

ICRR, University of Tokyo, Kashiwa, Chiba 277-8582

In collaboration with the members of:
University of Tokyo, 7-3-1 Hongo, Bunkyo-ku, Tokyo 113-0033, Japan; Nagoya University, Chikusa, Nagoya 464-8602, Japan; National Astronomical Observatory of Japan, 2-21-1 Osawa, Mitaka, Tokyo 181-8588, Japan; Tohoku University, Aramaki, Aoba, Sendai 980-8578, Japan; Japan Women's University, 2-8-1, Mejirodai, Bunkyo-ku, Tokyo, 112-8681, Japan; The University of Chicago, 5640, South Ellis Ave., Chicago, IL 60637, USA; Fermi National Accelerator Laboratory, P.O. Box 500, Batavia, IL 60510, USA; Institute for Advanced Study, Einstein Drive, Princeton, NJ 08540, USA; Johns Hopkins University, Baltimore, MD 21218, USA; Los Alamos National Laboratory, Los Alamos, NM 87545, USA; Max-Planck-Institute for Astronomy, Königstuhl 17, D-69117 Heidelberg, Germany; Max-Planck-Institute for Astrophysics, Karl Schwarzschildstrasse 1, D-85748 Garching, Germany; New Mexico State University, P.O. Box 30001, Dept 4500, Las Cruces, NM 88003, USA; University of Pittsburgh, 3941 O'Hara St., Pittsburgh, PA 15260, USA; Princeton University, Princeton, NJ 08544, USA; United States Naval Observatory, P.O. Box 1149, Flagstaff, AZ 86002-1149; University of Washington, Box 351580, Seattle, WA 98195, USA

The SDSS completed its originally planned phase of opeations — SDSS-I — on 30 June 2005 after five years of operation. The goal initially set was to cover 10,000 square degrees of sky, but at the time the production survey began, the Five Year Baseline was developed to provide a more realistic metric against which the progress was evaluated. This decreased the target area to 8,387 square degrees (7,642 square degrees in the northern sky and 745 square degrees in the southern sky). The imaging carried out over 5 years has sustained the planned pace. At the end of the survey 97% of the baseline area were observed for the northern-sky baseline and 99% of southern-sky baseline were completed. Spectroscopic surveys, however, are somewhat behind the schedule. Only 74% of the baseline area were observed for the north (100% for the south). This is due to unusually poor weather conditions in the spring of 2003 and in the winter of 2004. The time consuming spectroscopic runs were severely affected. Otherwise, all the operations have been working smoothly (98% is the mean uptime fraction), producing the data as expected. Software has undergone extensive fine tunings and all the data were re-reduced for a number of times, which are now made public as *The Data Release of the Sloan Digital Sky Survey I* to *VI* (DR1-DR6), the last one comprising 8,417 square degrees of imaging and 6,860 square degrees of spectroscopic surveys done to 30 June 2006. This database contains 230 million objects including 1,163,520 objects with spectroscopic information. These numbers include 790,220 galaxies and 102,350 quasars obtained with the uniform selection criteria.

The SDSS has entered a new phase, SDSS-II, continuing through June, 2008. SDSS-II will carry out three distinct surveys — the Sloan Legacy Survey, SEGUE (The Sloan Extension for Galactic Understanding and Exploration), and the Sloan Supernova Survey — to address fundamental questions about the nature of the Universe, the origion of galaxies and quasars, and the formation and evolution of our own Galaxy, the Milky Way.

The Sloan Legacy Survey is the continuation of SDSS-I to complete spectroscopic survey to fill the gap in the Northern Galactic Cap which was not observed during SDSS-I due to poor weather conditions. Constructing the largest possible single contiguous survey volume will improve the following three main results: the determination of the power spectrum, the photometric calibration, and the legacy which SDSS will supply to the astronomical world. The goal is contiguous region of 7,808 square degrees in both imaging and spectroscopy. By the second quater of 2007, 100% of imaging and 91% of spectroscopy have been completed.

SEGUE is mining the stellar content of the Milky Way in order to create a detailed 3-dimensional map of the Galaxy. SEGUE will image 3,320 square degrees mostly at $|b| < 30°$ and obtain spectra of 240,000 stars in the disk and spheroid, revealing the age, composition and phase space distribution of stars within the various Galactic components. These stellar excavations will provide essential clues to the structure, formation, and evolution of our Galaxy. By the second quater of 2007, 97% of imaging and 63% of spectroscopy have been completed.

The Sloan Supernova Survey is a time-domain survey involving repeat imaging of the same region of the sky (the SDSS Southern equatorial stripe; about 2.5 degree wide by ∼120 degree long) every other nights over the course of three 3-month campaigns (Sep-Nov). A primary scientific motivation is to detect and measure multi-band light-curves for ∼200 Type Ia supernovae in the redshift range $z = 0.1 − 0.3$. This sample, with excellent photometric calibration, should provide insights into systematics of SNe Ia as calibrated standard candles. The survey of the three years (2005-2007) have been finished successfully and found 494 spectroscopically confirmed SNe Ia in the redshift range between 0.05 and 0.40. About 85% of SNe Ia are discovered before maximum light. Follow-up spectra were teaken at various telescopes through collabaration including MDM(2.4m), NOT(2.6m), APO(3.5m), NTT(3.6m), KPNO(4m), WHT(4.2m), Subaru(8.2m), HET(9.2m), Keck(10m), and SALT(10m).

The prime scientific goals of the SDSS are focused on extragalactic themes, such as the large-scale structure of galaxies over a very large volume of the Universe, and detailed characterisations of the galaxy properties and those of quasars.

The clustering of galaxies observed in the SDSS, when mapped in three dimensional space, looks very similar to that expected in the model of the Universe dominated by cold dark matter (CDM) with density fluctuations starting from nearly scale-invariant adiabatic perturbations, as predicted in the model of inflation. As a quantitative measure this density field is characterised by the statistic called the power spectrum, the squared amplitude of the Fourier modes of fluctuations, which is written,

$$P(k) = |\delta_k|^2 = \int d^3 r \xi(r) e^{-ik \cdot r} \tag{1}$$

where $\xi(r)$ is the two-point correlation function of galaxies.

The important result is an accurate derivation of this power spectrum from galaxy clustering over the scale from 10 to 200 Mpc, and the demonstration that it joins smoothly the spectrum derived from the temperature field imprinted on the cosmic microwave background measured by *Wilkinson Microwave Anisotropy Probe* (WMAP) (see Fig. 1). Combined with WMAP that explores the Universe at $z \approx 1000$, this lends the most convincing support to the standard model of structure formation in the Universe based on the $\Lambda$CDM model. Moreover, the large-scale structure data of SDSS reduced the parameter degeneracies that exist within the CMB analyses; the combined data of WMAP and SDSS yield the cosmological parameters $\Omega_m = 0.29 \pm 0.04$, $\Omega_\Lambda = 0.71 \pm 0.04$ and $H_0 = 71 \pm 4$ km s$^{-1}$Mpc$^{-1}$ at the year of 2004. Two years later, 3-year WMAP data was released. It includes the new measurement of the low-$l$ polarization power spectrum, which detects the reionization signature and determines the corresponding optical depth. This measurement breaks the severe degeneracy in the 1-year WMAP data and causes the dramatic tightening of the constraints on various important cosmological parameters. Now the value added by other datasets is clearly reduced. However, the information from large scale structure of galaxies give substantial improvements by cutting error bars.

SDSS has applied another selection of galaxies — the selection of luminous red galaxies (LRG). Approximately 10% of SDSS galaxies belong to this category. The advantage of this selection is to allow us to explore much deep sky. The sight increases from $600h^{-1}$ Mpc ($z = 0.2$) to $1200h^{-1}$ Mpc ($z = 0.4$), quadrupling the survey volume compared with the main galaxy sample. The constraints on cosmological parameters obtained by combining 3-year WMAP data and SDSS LRG measurements are $\Omega_m = 0.239 \pm 0.018$, $\Omega_\Lambda = 0.761 \pm 0.018$ and $H_0 = 73 \pm 2$ km s$^{-1}$Mpc$^{-1}$. This set is taken as an authoritative in the astronomy community.

Baryonic acoustic oscillations (BAO) is a reminiscence of the sound wave oscillation in the pre-recombination era, which is most dramatically seen in CMB multipoles. In real space this leads to a peak in the two-point correlation function $\xi(r)$ at about $r_s = 100h^{-1}$ Mpc. In Fourier space this process leads to oscillations in the power spectrum. The wavelength of these oscillations will be $k_s = 2\pi/r_s = 0.06h$ Mpc$^{-1}$. Eisenstein et al. (2005) has detected this acoustic peak in correlation function of SDSS LRG and determine the curvature of the Universe to 1% accuracy, $\Omega_\Lambda + \Omega_m = 1.01 \pm 0.01$, which is comparable to the latest WMAP3+SDSS LRG analysis. The analysis of the main galaxies and LRGs in the SDSS DR5 sample determines $\Omega_m = 0.256 \pm 0.029$ using the dependence of $r_s$ on the matter density $\Omega_m$ (Fig. 2). This value of the matter density is derived from the locations of BAO in the galaxy power spectrum and in the CMB. This is an extermely clean geometrical cosmological measurement, as the physics of the BAO production is well understood. With larger samples and a wider redshift range, the BAO "standard ruler" can be used to constrain the comsmology at high precision through the comoving distance-redshift relation. Forthcoming surveys will be designed to exploit this effect.

Although CDM models seem to be very successful on large scales, one of the most serious challenges facing CDM
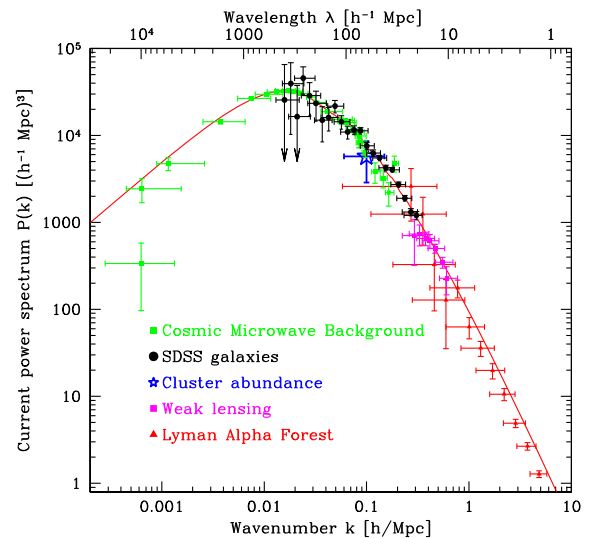


Fig. 1. The power spectrum of galaxy clustering scaled to the present epoch (SDSS galaxies) plotted with four other independent measures, extending four decades on spatial resolution, and demonstrating remarkable consistency. These data provide fundamental constraints on cosmological models. Figure is taken from Tegmark et al. Astrophys. J. **606**, 702 (2004).
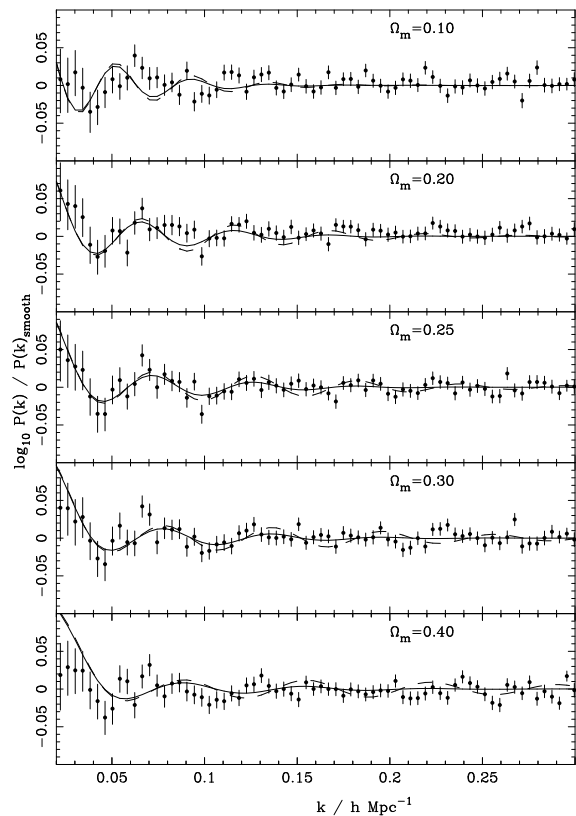


Fig. 2. Ratio of the power spectra calculated from the SDSS to the overall shape of the measured power spectra (filled circles with $1\sigma$ errors). Solid lines represents the BAO predicted by a CDM model with matter densities given in each panel and h = 0.73, and a 17% baryon fraction. As can be seen, the observed oscillations approximately match those predicted for $0.2 \leq \Omega_m \leq 0.3$. Figure is taken from Percival et al. Astrophys. J. **657**, 51 (2007).
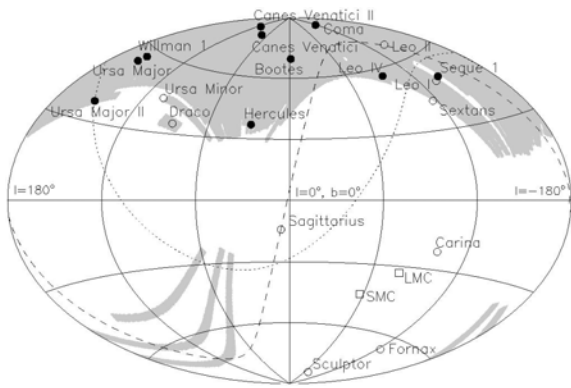
Fig. 3. Locations of Milky Way satellites in Galactic coordinates. Filled circles are satellites discovered by SDSS, and open circles are previously known Milky Way dSphs. Figure is taken from Belokurov et al. Astrophys. J. **654**, 897 (2007).

models is the so-called "missing satellite" problem. CDM models predicts at least 1-2 orders of manitude more low-mass sub-halos at the present epoch compared to the observed abundance of dwarf galaxies surrounding the Milky Way and M31. All-sky photographic surves cover most of the sky, but are limited to surface brightnesses of $\sim 25.5$ mag arcsec$^{-2}$. The selection effects are also difficult to model with accuracy. The SDSS makes it possible to carry out a systematic survey for satellite galaxys, which are detectable through over-density of stars in position-color-magnitude space. A total of 10 new Milky Way satellites with effective surface brightness $\mu_V \geq 28$ mag arcsec$^{-2}$ have been discovered in SDSS data (Fig. 3) in addition to the previously known 9 Milky Way dwarf spheroidals. Some preliminary studies of these indicate that they may be dark matter dominated. We need more investigation to see if these are the "missing satellites".

Gravitational lensing is also a subject to which the SDSS is making a significant contribution in a number of ways. The SDSS is one of the first few that observed a weak effect of gravitational lensing of galaxy images by foreground galaxies. The lensing effect appears as distorted images of galaxies due to the gravitational shear field, but it is only on the order of a few percent, compared with the order of unity effect of randomly oriented galaxies that have intrinsically different shapes. Millions of galaxies are needed to extract this small signal from noise of the order of unity. With the SDSS galaxy sample, this distortion was unambiguously detected, showing that the mass concentration around galaxies behaves as $r^{-0.8}$ as a function of distance $r$, consistently with the famous $r^{-1.8}$ law of the galaxy-galaxy correlation. Another effect of gravitational lensing by foreground galaxies is a magnification of distant sources, *cosmic magnification*. Graviational magnification has two effects. First, the flux received from distant sources is increased, resulting in a relatively deeper apparent magnitude limited survey. Second, the solid angle is stretched, diluting the surface density of source images on the sky. The net result of these competing effects is an induced cross-correlation between physically separated populations that depends on how the loss of sources due to dilution is balanced by the gain of sources due to flux magnification. Us-
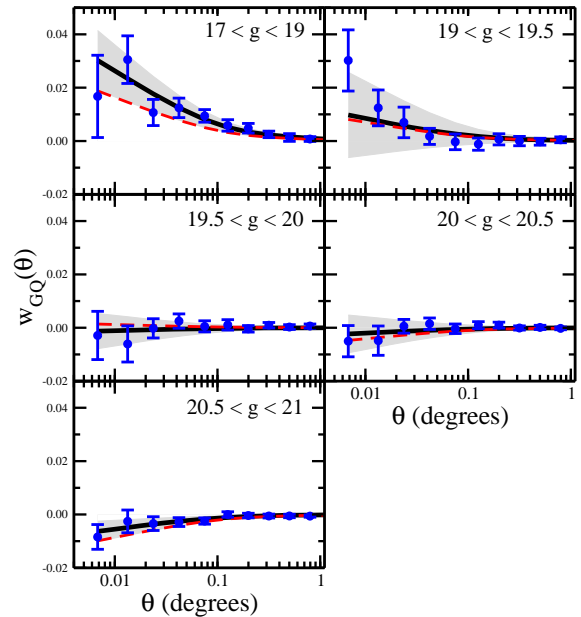


Fig. 4. Measurement of $w_{GQ}(\theta)$, cross-correlation between foreground galaxies and distant quasars, as a function of quasar g-band magnitude. The dark solid curve is the fitting model. Fugure is taken from Scranton et al. Astrophys., J. **633**, 589 (2005).

ing $\sim 200,000$ quasars and 13 million galaxies, cosmic magnification has been detected for the first time at $8\sigma$ level (Fig. 4).

The large quasar sample of the SDSS also provides an excellent platform to search for classical strong gravitational lenses of quasar images, i.e., splitting of images. 16 lenses are found from 46000 quasar images. Among the novel cases that deserve special scientific discussion, we quote the large-separation lensed quasar, SDSS J1004+4112 of four images with their maximum separation being 14.6 arcsec and SDSS J1029+2623 with two images with their separation of 22.5 arcsec (Figure5). These are the case where split lensed images are further enhanced by a cluster of galaxies. A statistical analysis to infer cosmological and mean galaxy parameters from the lens sample yielded $\Omega_m = 0.26 \pm 0.08$, $\Omega_\Lambda = 0.74 \pm 0.17$, consistent with the values dervied from WMAP and SDSS power spectrum analysis.

As it became apparent already at imaging first light, the SDSS project has made unrivalled contributions to our understanding of high redshift quasars from its commissioning phase. By now the project has found 19 quasars with redshift higher than 5.7 (*i*- dropout quasars) from $\sim$6,600 square degrees — Among them 8 are with $z > 6$: there are no $z > 6$ quasars reported from other projects. The highest redshift is 6.42, which means that the light was emitted only 0.84 Gyr after the Big Bang. These high-$z$ quasars, together with a sample for lower-$z$, show the abundance of luminous quasars declining exponentially with redshift from $z \approx 3$ towards early epochs. This is a significant constraint on the model of quasar formation at high redshifts.
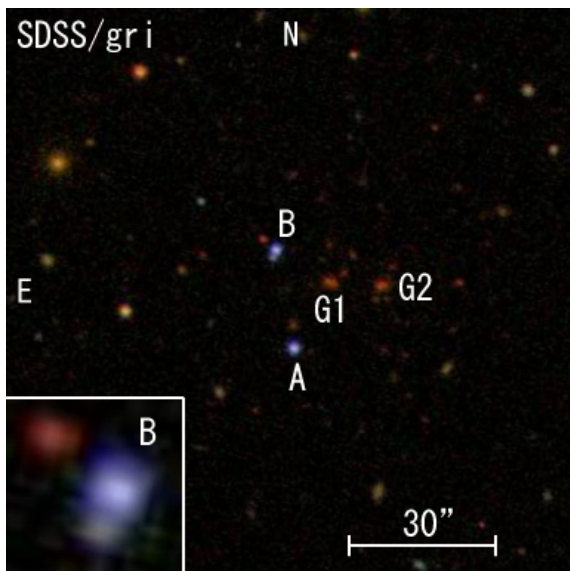
Fig. 5. *gri* composite SDSS image of SDSS J1029+2623. The quasar images (blue stellar objects) are indicated by A and B. G1 and G2 (red extented objects) are likely to be member galaxies of a lensing cluster at $z \sim 0.55$. Figure is taken from Inada et al. Astrophys. J. (Letters) **653**, L97 (2006).



Fig. 6. Evolution of optical depth combined with the Ly$\alpha$, Ly$\beta$, and Ly$\gamma$ results. At $z > 5.5$, the best-fit evolution has $\tau_{GP}^{eff} \approx (1+z)^{>10.9}$, indicating an accelerated evolution. Figure is taken from Fan et al. Astron. J. **132**, 117 (2006).

Also important aspect with high redshift quasars is that they allowed us to observe a change of the ionisation state of the intergalactic medium (IGM) in a high redshift universe. We know that a free electron and a proton recombine to form a neutral hydrogen atom at $z \approx 1000 - 1500$. We also know that IGM was again highly reionised before $z \approx 3$. When and how the reionisation took place is a matter of significant interest from the point of view of galaxy formation. The SDSS quasar spectra show the flux shortwards the Lyman $\alpha$ line rapidly vanishing at $z \geq 6$ (called the Gunn-Peterson trough), indicating the change of state of the IGM at this redshift (Figure 6). Cosmic reionisation is also evident from the WMAP 3-year data and its epoch $z_r = 8 \pm 2$ is consistent with SDSS result if we consider the error of optical depth determined from WMAP data. A problem newly created is the question whether the star formation activity, as inferred from faint galaxy observations, is sufficient to ionise the entire IGM at $z \approx 6$.

Besides high redshift quasars, a large number of quasars are collected and their properties are being studied. We have released four catalogues of quasars, the fourth one containing 77,429 quasars in 5,740 square degrees. The long-awaited quasar luminosity function (the work requires proper understanding of the selection function) was determined for well-defined and homogeneous sample consisting of 15,343 quasars within an effective area of 1622 square degrees. Derived luminosity function has a flatter bright-end slope at high redshift than at low redshift (Fig. 7). This slope change must be accounted for in models of the evolution of accretion onto supermassive black holes.
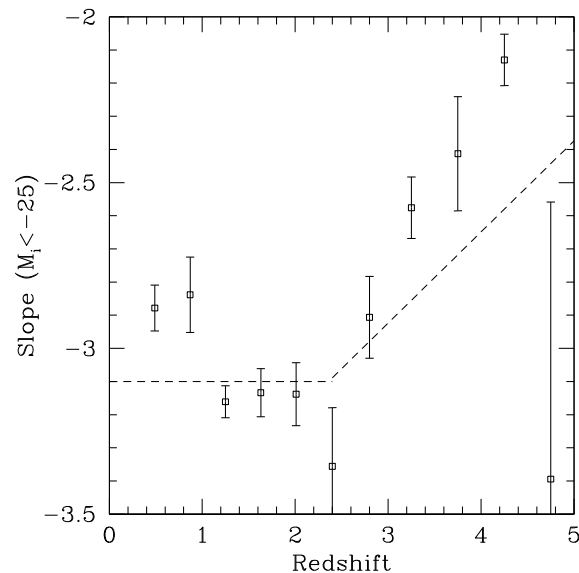


Fig. 7. Bright-end slope of the Quasar Luminosity Function as a function of redshift detemined from a linear least-squares fit to the $M_i(z = 2) < -25$. The slope of the luminosity function significantly flattens with redshift $z > 3$. Figure is taken from Richards et al. Astron. J. **131**, 2766 (2006).

# Theory Group

## Lepton Flavour Violating $\tau$ Decays in the Left-Right Symmetric Model

[Spokesperson : M. Aoki]

ICRR, Univ. of Tokyo, Kashiwa, Chiba 277-8582

In collaboration with the members of KEK and Taiwan, Natl. Cheng Kung U..

The Left-Right symmetric extension of the Standard Model with Higgs isospin triplets can provide neutrino masses via a TeV scale seesaw mechanism. The doubly charged Higgs bosons $H_L^{\pm\pm}$ and $H_R^{\pm\pm}$ induce lepton flavour violating decays $\tau^\pm \to lll$ at tree-level via a coupling which is related to the Maki-Nakagawa-Sakata matrix ($V_{\mathrm{MNS}}$). We study the magnitude and correlation of $\tau^\pm \to lll$ and $\mu \to e\gamma$ with specific assumptions for the origin of the large mixing in $V_{\mathrm{MNS}}$ while respecting the stringent bound for $\mu \to eee$. It is also shown that an angular asymmetry for $\tau^\pm \to lll$ is sensitive to the relative strength of the $H_L^{\pm\pm}$ and $H_R^{\pm\pm}$ mediated contributions and provides a means of distinguishing models with doubly charged Higgs bosons.

## Probing Majorana Phases and Neutrino Mass Spectrum in the Higgs Triplet Model at the LHC.

[Spokesperson : M. Aoki]

ICRR, Univ. of Tokyo, Kashiwa, Chiba 277-8582

In collaboration with the members of KEK, Taiwan, Natl. Cheng Kung U. and SISSA.

Doubly charged Higgs bosons ($H^{++}$) are a distinctive signature of the Higgs Triplet Model of neutrino mass generation. If $H^{++}$ is relatively light ($m_{H^{++}} < 400\,\mathrm{GeV}$) it will be produced copiously at the LHC, which could enable precise measurements of the branching ratios of the decay channels $H^{++} \to l_i l_j$. Such branching ratios are determined solely by the neutrino mass matrix which allows the model to be tested at the LHC. We quantify the dependence of the leptonic branching ratios on the absolute neutrino mass and Majorana phases, and present the permitted values for the channels $ee, e\mu$ and $\mu\mu$. It is shown that precise measurements of these three branching ratios are sufficient to extract information on the neutrino mass spectrum and probe the presence of CP violation from Majorana phases.

## Unitarity bounds in the Higgs model including triplet fields with custodial symmetry

[Spokesperson : M. Aoki]

ICRR, Univ. of Tokyo, Kashiwa, Chiba 277-8582

In collaboration with the members of Toyama U..

We study bounds on Higgs boson masses from perturbative unitarity in the Georgi-Machacek model, whose Higgs sector is composed of a scalar isospin doublet, a real and a complex isospin triplet fields. This model can be compatible with the electroweak precision data without fine tuning because of the imposed global $SU(2)_R$ symmetry in the Higgs potential, by which the electroweak rho parameter is unity at the tree level. All possible two-body elastic-scattering channels are taken into account to evaluate the S-wave amplitude matrix, and then the condition of perturbative unitarity is imposed on the eigenvalues to obtain constraint on the Higgs parameters. Masses of all scalar bosons turn out to be bounded from above, some of which receive more strict upper bounds as compared to that in the standard model (712 GeV). In particular, the upper bound of the lightest scalar boson, whatever it would be, is about 270 GeV.

## Bibliography

[1] A. G. Akeroyd, M. Aoki and Y. Okada, Phys. Rev. D **76** (2007) 013004

[2] A. G. Akeroyd, M. Aoki and H. Sugiyama, Phys. Rev. D **77** (2008) 075010

[3] M. Aoki and S. Kanemura, Phys. Rev. D **77** (2008) 095009

## Neutralino Dark Matter in Light Higgs Boson Scenario

[Spokesperson : M. Senami]

Kyoto Univ., Kyoto 606-8501

In collaboration with the members of KEK, Tohoku Univ., and SISSA.

Phenomenology of neutralino dark matter in the minimal supersymmetric model is discussed for a scenario where the lightest Higgs boson mass is lighter than 114.4 GeV. We show that the scenario is consistent not only with many collider experiments but also with the observed relic abundance of dark matter. The allowed region may be probed by experiments of Bs to $\mu^+\mu^-$ in near future. The scenario predicts a large scattering cross section between the dark matter and ordinary matter and thus it may be tested in present direct detection experiments of dark matter.

## Bibliography

[1] M. Asano, S. Matsumoto, M. Senami and H. Sugiyama, Phys. Lett. B **663** (2008) 330 arXiv:0711.3950 [hep-ph].

## Relic abundance of dark matter in universal extra dimension models with right-handed neutrinos

[Spokesperson : M. Senami]

Kyoto Univ., Kyoto 606-8501

In collaboration with the members of Saitama Univ. and Tohoku Univ..

Relic abundance of dark matter is investigated in the framework of universal extra dimension models with right-handed neutrinos. These models are free from the serious Kaluza-Klein (KK) graviton problem that the original universal extra dimension model has. The first KK particle of the right-handed neutrino is a candidate for dark matter in this

framework, and its relic abundance is determined by three processes, (1) the decay of the KK photon into the first KK right-handed neutrino in the late universe, (2) production of the first KK right-handed neutrino from the thermal bath in the early universe, and (3) the decay of higher KK right-handed neutrinos into the first KK right-handed neutrino in the late universe. When ordinary neutrino masses are large enough such as the degenerate mass spectrum case, the last process contribute to the abundance significantly, even if the reheating temperature is low. The scale of the extra dimension consistent with cosmological observations can be 500 GeV in the minimal setup of universal extra dimension models with right-handed neutrinos.

## Bibliography

[1] S. Matsumoto, J. Sato, M. Senami and M. Yamanaka, Phys. Rev. D **76** (2007) 043528 [arXiv:0705.0934 [hep-ph]].

## Primordial Non-Gaussianity in Multi-Scalar Slow-Roll Inflation.

[Spokesperson : T. Suyama]

ICRR, Univ. of Tokyo, Kashiwa, Chiba 277-8582

In collaboration with the members of Kyoto University

We analyze the non-Gaussianity for primordial curvature perturbations generated in multi-scalar slow-roll inflation model including the model with non-separable potential by making use of $\delta N$ formalism. Many authors have investigated the possibility of large non-Gaussianity for the models with separable potential, and they have found that the non-linear parameter, $f_{NL}$, is suppressed by the slow-roll parameters. We show that for the non-separable models $f_{NL}$ is given by the product of a factor which is suppressed by the slow-roll parameters and a possible enhancement factor which is given by exponentials of quantities of O(1).

## Bibliography

[1] S. Yokoyama, T. Suyama and T. Tanaka, JCAP **07**, 013 (2007) [arXiv:0705.3178 [astro-ph]].

## Non-Gaussianity in the modulated reheating scenario.

[Spokesperson : T. Suyama]

ICRR, Univ. of Tokyo, Kashiwa, Chiba 277-8582

In collaboration with the members of Aoyamagauin University

We investigate the non-Gaussianity of primordial curvature perturbation in the modulated reheating scenario where the primordial perturbation is generated due to the spacial fluctuation of the inflaton decay rate to radiation. We use the $\delta N$ formalism to evaluate the trispectrum of curvature perturbation as well as its bispectrum. We give expressions for three non-linear parameters $f_{NL}, \tau_{NL}$ and $g_{NL}$ in the modulated reheating scenario. If the intrinsic non-Gaussianity of scalar field fluctuations and third derivative of the decay rate

with respect to scalar fields are negligibly small, $g_{NL}$ has at least the same order of magnitude as $f_{NL}$. We also give general inequality between $f_{NL}$ and $\tau_{NL}$ which is true for other inflationary scenarios as long as primordial non-Gaussianity comes from super-horizon evolution.

## Bibliography

[1] T. Suyama and M. Yamaguchi, Phys. Rev. D **77**, 023505 (2008) [arXiv:0709.2545 [astro-ph]].

## Primordial Non-Gaussianity in Multi-Scalar Inflation.

[Spokesperson : T. Suyama]

ICRR, Univ. of Tokyo, Kashiwa, Chiba 277-8582

In collaboration with the members of Kyoto University

We give a concise formula for the non-Gaussianity of the primordial curvature perturbation generated on super-horizon scales in multi-scalar inflation model without assuming slow-roll conditions. This is an extension of our previous work. Using this formula, we study the generation of non-Gaussianity for the double inflation models in which the slow-roll conditions are temporarily violated after horizon exit, and we show that the non-linear parameter $f_{NL}$ for such models is suppressed by the slow-roll parameters evaluated at the time of horizon exit.

## Bibliography

[1] S. Yokoyama, T. Suyama and T. Tanaka, Phys. Rev. D **77**, 083511 (2008) [arXiv:0711.2920 [astro-ph]].

## Non-Gaussianity, Spectral Index and Tensor Modes in Mixed Inflaton and Curvaton Models.

[Spokesperson : T. Suyama]

ICRR, Univ. of Tokyo, Kashiwa, Chiba 277-8582

In collaboration with the members of ICRR, Saga University and Aoyamagakuin University

We study non-Gaussianity, the spectral index of primordial scalar fluctuations and tensor modes in models where fluctuations from the inflaton and the curvaton can both contribute to the present cosmic density fluctuations. Even though simple single-field inflation models generate only tiny non-Gaussianity, if we consider such a mixed scenario, large non-Gaussianity can be produced. Furthermore, we study the inflationary parameters such as the spectral index and the tensor-to-scalar ratio in this kind of models and discuss in what cases models predict the spectral index and tensor modes allowed by the current data while generating large non-Gaussianity, which may have many implications for model-buildings of the inflationary universe.

## Bibliography

[1] K. Ichikawa, T. Suyama, T. Takahashi and M. Yamaguchi, arXiv:0802.4138 [astro-ph].

## "Flavored" Electric Dipole Moments in Supersymmetric Theories

[Spokesperson : M. Nagai]

ICRR, Univ. of Tokyo, Kashiwa, Chiba 277-8582

In collaboration with the members of ICRR and Valencia Univ..

The Standard Model (SM) predictions for the hadronic electric dipole moments (EDMs) are well far from the present experimental resolutions, thus, the EDMs represent very clean probes of New Physics (NP) effects. Especially, within an MSSM framework with flavor-changing (but not necessarily CP violating) soft terms, large and potentially visible effects to the EDMs are typically expected. In this Letter we point out that, beyond-leading-order (BLO) effects, so far neglected in the literature, dominate over the leading-order (LO) effects in large regions of the parameter space, hence, their inclusion in the evaluation of the hadronic EDMs is unavoidable.

### Bibliography

[1] J. Hisano, M. Nagai and P. Paradisi, arXiv:0712.1285 [hep-ph].

## Stability of Metastable Vacua in Gauge Mediated SUSY Breaking Models with Ultra Light Gravitino

[Spokesperson : M. Nagai]

ICRR, Univ. of Tokyo, Kashiwa, Chiba 277-8582

In collaboration with the members of ICRR.

Recently Murayama and Nomura proposed a simple scheme to construct the gauge mediation models, using mextastable supersymmetry breaking vacua. It has a possibility to predict the ultra light gravitino mass with a mass less than 16 eV, while such a light gravitino may destabilize the metastable vacua. We investigate stability of the metastable vacuum of their model. The transition rate from the false vacuum to true ones is evaluated by numerical calculation, including the Coleman-Weinberg potential destabilizing the metastable vacuum. It is found that when the messenger sector is minimal, stability of the metastable vacuum imposes an upperbound on squark mass $M_{sq}$ for the ultra light gravitino as $M_{sq} < 1800$ GeV at most. Squarks with this mass may be found in the LHC experiments.

### Bibliography

[1] J. Hisano, M. Nagai, M. Senami and S. Sugiyama, Phys. Lett. B **659** (2008) 361 [arXiv:0708.3340 [hep-ph]].

## Cosmological constraints on neutrino injection

[Spokesperson : T. Kanzaki

ICRR, Univ. of Tokyo, Kashiwa, Chiba 277-8582

In collaboration with the members of ICRR, Lancaster Univ. and Tohoku Univ..

We derive general constraints on the relic abundances of a long-lived particle which mainly decays into a neutrino (and something else) at cosmological time scales. Such an exotic particle may show up in various particle-physics models based on physics beyond the standard model. The constraints are obtained from big-bang nucleosynthesis, cosmic microwave background and diffuse neutrino and photon fluxes, depending on the lifetime and the electromagnetic and hadronic branching ratios.

### Bibliography

[1] T. Kanzaki, M. Kawasaki, K. Kohri and T. Moroi Phys. Rev. D **76**, 105017 (2007).

## Affleck-Dine leptogenesis via multiscalar evolution in a supersymmetric seesaw model

[Spokesperson : T. Takayama]

ICRR, Univ. of Tokyo, Kashiwa, Chiba 277-8582

In collaboration with the member of Kyoto Univ.

A leptogenesis scenario in a supersymmetric standard model extended with introducing right-handed neutrinos is reconsidered. Lepton asymmetry is produced in the condensate of a right-handed sneutrino via the Affleck-Dine mechanism. The $LH_u$ direction develops large value due to a negative effective mass induced by the right-handed sneutrino condensate through the Yukawa coupling of the right-handed neutrino, even if the minimum during the inflation is fixed at the origin. The lepton asymmetry is nonperturbatively transfered to the $LH_u$ direction by this Yukawa coupling.

### Bibliography

[1] M. Senami and T. Takayama, JCAP **0711** (2007) 015

## Formation of IMBHs as PBHs in the inflationary cosmology with running spectral index

[Spokesperson : T. Takayama]

ICRR, Univ. of Tokyo, Kashiwa, Chiba 277-8582

In collaboration with the members of ICRR, Aoyama Gakuin Univ., RESCEU and IPMU.

Formation of primordial black holes (PBHs) on astrophysical mass scales is a natural consequence of inflationary cosmology if the primordial perturbation spectrum has a large and negative running of the spectral index as observationally suggested today, because double inflation is required to explain it and fluctuations on some astrophysical scales are enhanced in the field oscillation regime in between. It is argued that PBHs thus produced can serve as intermediate-mass black holes (IMBHs) which act as the observed ultraluminous X-ray sources (ULXs) by choosing appropriate values of the model parameters in their natural ranges. Our scenario can be observationally tested in near future because the mass of PBHs is uniquely determined once we specify the values of the amplitude of the curvature perturbation, spectral index and its running on large scales.

Bibliography

[1] T. Kawaguchi, M. Kawasaki, T. Takayama, M. Yamaguchi and J. Yokoyama, arXiv:0711.3886 [astro-ph]

## Increasing effective number of neutrinos by decaying particles

[Spokesperson : K. Nakayama]

ICRR, Univ. of Tokyo, Kashiwa, Chiba 277-8582

In collaboration with the members of ICRR and DESY.

We present models of decaying particles for increasing the effective number of neutrinos $N_\nu$ after big bang nucleosynthesis but before the structure formation begins. We point out that our scenario not only solves the discrepancy between the constraints on $N_\nu$ from these two epochs, but also provides a possible answer to deeper inconsistency in the estimation of the matter power spectrum amplitude at small scales, represented by $\sigma_8$, between the WMAP and some small scale matter power measurements such as the Lyman-alpha forest and weak lensing. We consider (a) saxion decay into two axions; (b) gravitino decay into axino and axion; (c) Dirac right-handed sneutrino decay into gravitino and right-handed neutrino.

Bibliography

[1] K. Ichikawa, M. Kawasaki, K. Nakayama, M. Senami and F. Takahashi, JCAP **0705** (2007) 008 [arXiv:hep-ph/0703034].

## Baryon Asymmetry in Heavy Moduli Scenario

[Spokesperson : K. Nakayama]

ICRR, Univ. of Tokyo, Kashiwa, Chiba 277-8582

In collaboration with the members of ICRR.

In some models of supersymmetry breaking, modulus fields are heavy enough to decay before BBN. But the large entropy produced via moduli decay significantly dilutes the preexisting baryon asymmetry of the universe. We study whether Affleck-Dine mechanism can provide enough baryon asymmetry which survives the dilution, and find several situations in which desirable amount of baryon number remains after the dilution. The possibility of non-thermal dark matter is also discussed. This provides the realistic cosmological scenario with heavy moduli.

Bibliography

[1] M. Kawasaki and K. Nakayama, Phys. Rev. D **76** (2007) 043502 [arXiv:0705.0079 [hep-ph]].

## Nonthermal dark matter in mirage mediation

[Spokesperson : K. Nakayama]

ICRR, Univ. of Tokyo, Kashiwa, Chiba 277-8582

In collaboration with the members of ICRR.

In mirage-mediation models there exists a modulus field whose mass is O(1000) TeV and its late-decay may significantly change the standard thermal relic scenario of the dark matter. We study nonthermal production of the dark matter directly from the modulus decay, and find that for some parameter regions non-thermally produced neutralinos can become the dark matter.

Bibliography

[1] M. Nagai and K. Nakayama, Phys. Rev. D **76** (2007) 123501 [arXiv:0709.3918 [hep-ph]].

## Cosmological implications of supersymmetric axion models

[Spokesperson : K. Nakayama]

ICRR, Univ. of Tokyo, Kashiwa, Chiba 277-8582

In collaboration with the members of ICRR.

We derive general constraints on supersymmetric extension of axion models, in particular paying careful attention to the cosmological effects of saxion. It is found that for every mass range of the saxion from keV to TeV, severe constraints on the energy density of the saxion are imposed. Together with constraints from axino we obtain stringent upper bounds on the reheating temperature. We also find that all the cosmological difficulties, including gravitino, axino overproduction and axionic isocurvature fluctuation, can be avoided if the saxion field has large initial amplitude during inflation and decays before big-bang nucleosynthesis.

Bibliography

[1] M. Kawasaki, K. Nakayama and M. Senami, JCAP **0803** (2008) 009 [arXiv:0711.3083 [hep-ph]].

[2] M. Kawasaki and K. Nakayama, arXiv:0802.2487 [hep-ph], to be published in Phys. Rev. D.

## Space laser interferometers can determine the thermal history of the early Universe

[Spokesperson : K. Nakayama]

ICRR, Univ. of Tokyo, Kashiwa, Chiba 277-8582

In collaboration with the members of ICRR, Univ. of Tokyo and RESCEU.

It is shown that space-based gravitational wave detectors such as DECIGO and/or Big Bang Observer (BBO) will provide us with invaluable information on the cosmic thermal history after inflation and they will be able to determine the reheat temperature $T_R$ provided that it lies in the range preferred by the cosmological gravitino problem, $T_R \sim 10^{5-9}$ GeV. Therefore it is strongly desired that they will be put into practice as soon as possible.

Bibliography

[1] K. Nakayama, S. Saito, Y. Suwa and J. Yokoyama, arXiv:0802.2452 [hep-ph], to be published in Phys. Rev. D.

## Cosmological Constraints on Isocurvature and Tensor Perturbations

[Spokesperson : T. Sekiguchi]

ICRR, Univ. of Tokyo, Kashiwa, Chiba 277-8582

In collaboration with the members of ICRR.

We investigate cosmological constraints on primordial isocurvature and tensor perturbations, using recent observations of the cosmic microwave background and the large scale structure. We find that present observations are consistent with purely adiabatic initial conditions for the structure formation under any priors on correlations of isocurvature modes, and upper limits on the contribution of isocurvature and tensor perturbations are presented. We also apply the obtained constraints to some specific theoretical models, axion isocurvature perturbation models and curvaton models, and give some implications for theoretical models.

## Primordial Helium Abundance from CMB: a constraint from recent observations and a forecast

[Spokesperson : T. Sekiguchi]

ICRR, Univ. of Tokyo, Kashiwa, Chiba 277-8582

In collaboration with the members of ICRR and Saga Univ.

We study a constraint on the primordial helium abundance $Y_p$ from current and future observations of CMB. Using the currently available data from WMAP, ACBAR, CBI and BOOMERANG, we obtained the constraint as $Y_p = 0.25 \pm 0.10$ at $1\sigma$ level. We also provide a forecast for Planck using the Markov Chain Monte Carlo approach. In addition to forecasting the constraint on $Y_p$, we investigate how assumptions for $Y_p$ affect the constraints on the other cosmological parameters.

## Probing the Effective Number of Neutrino Species with Cosmic Microwave Background

[Spokesperson : T. Sekiguchi]

ICRR, Univ. of Tokyo, Kashiwa, Chiba 277-8582

In collaboration with the members of ICRR and Saga Univ.

We discuss how much we can probe the effective number of neutrino species $N_\nu$ with cosmic microwave background alone. Using the data of WMAP, ACBAR, CBI and BOOMERANG experiments, we obtain a constraint on the effective number of neutrino species as $0.23 < N_\nu < 5.54$ at 95% C.L. for a power-law LCDM flat universe model. The limit is improved to be $0.64 < N_\nu < 5.03$ at 95% C.L. if we assume that the baryon density, $N_\nu$ and the helium abundance are related by the big bang nucleosynthesis theory. We also provide a forecast for the PLANCK experiment using a Markov chain Monte Carlo approach. In addition to constraining $N_\nu$, we investigate how the big bang nucleosynthesis relation affects the estimation for these parameters and the other cosmological parameters.

## Bibliography

[1] M. Kawasaki and T. Sekiguchi, arXiv:0705.2853.

[2] K. Ichikawa, T. Sekiguchi and T. Takahashi, arXiv:0712.4327

[3] K. Ichikawa, T. Sekiguchi and T. Takahashi, arXiv:0803.0889.

# OBSERVATORIES and
#         A RESEARCH CENTER

**Location of the Institute and the Observatories in Japan**
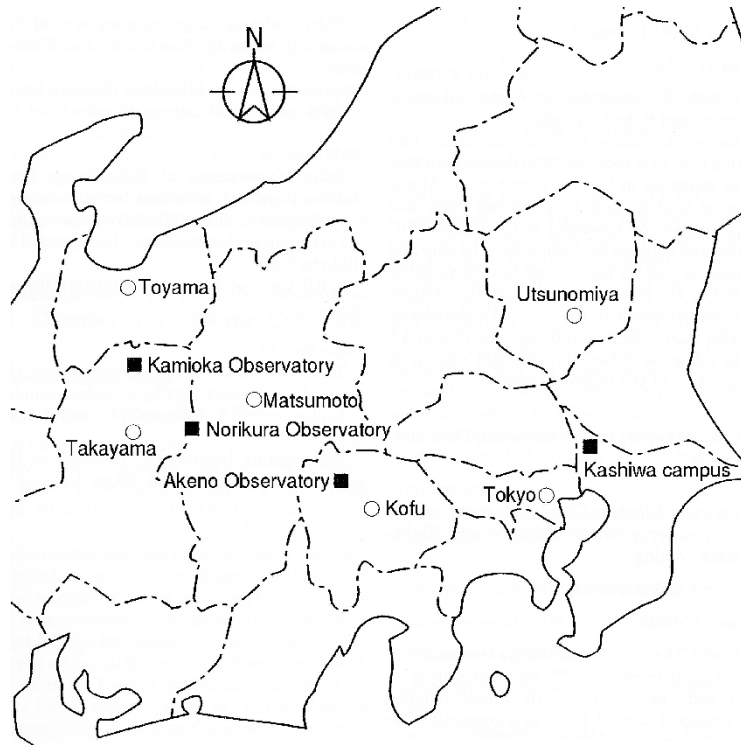


## Norikura Observatory

| | |
|---|---|
| Location: | Nyukawa-mura, Ohno-gun, Gifu Prefecture 506-2100 |
| | N 36°06′, E 137°33′, 2770 m a.s.l. |
| Telephone (Fax): | +263-33-7456 |
| Telephone (satellite): | 090-7721-5674 |
| Telephone (car): | 090-7408-6224 |

## Akeno Observatory

| | |
|---|---|
| Location: | Akeno-mura, Kitakoma-gun, Yamanashi Prefecture 407-0201 |
| | N 35°47′, E 138°30′, 900 m a.s.l. |
| Telephone / Fax: | +551-25-2301 / +551-25-2303 |

## Kamioka Observatory

| | |
|---|---|
| Location: | 456 Higashi-mozumi, Kamioka-cho, Hida-shi, Gifu Prefecture 506-1205 |
| | N 36°25′26″, E 137°19′11″, 357.5 m a.s.l. |
| Telephone / Fax: | +578-85-2116 / +578-85-2121 |

## Research Center for Cosmic Neutrinos

| | |
|---|---|
| Location: | 5-1-5 Kashiwanoha, Kashiwa, Chiba Prefecture 277-8582 |
| Telephone / Fax: | +4-7136-3138 / +4-7136-3115 |

# Norikura Observatory

[Director of Norikura Observatory : Masato Takita]
ICRR, Univ. of Tokyo, Kashiwa, Chiba 277-8582
In collaboration with the members of:

## 1. Introduction

Norikura Observatory (36.10°N and 137.55°E) was founded in 1953 and attached to ICRR in 1976. It is located at 2770 m above sea level, and is the highest altitude manned laboratory in Japan. Experimental facilities of the laboratory are made available to all the qualified scientists in the field of cosmic ray research and associated subjects. The AC electric power is generated by the dynamo and supplied throughout the observatory. In 1996, two dynamos of 70 KVA each were replaced with the new ones. The observatory can be accessed easily by car and public bus in summer (July-September). The 50th anniversary of Norikura Observatory was celebrated in 2003.

The feasibility of the automatic operation of Norikura Observatory during winter period has been tested since winter 2004 in order to study the possiblities to reduce maintenance and labor costs without seriously damaging to the use of researches. A long-distance (~40km) wireless LAN system (11M bps) was set up in 2003. Two new easy-to-handle and easy-to-maintain dynamos of 115 KVA each were installed in 2004 as well. The unmanned operation of Norikura Observatory was successful in the first winter, during which the battery backed-up solar panels and/or wind power generators kept supplying the electricity to the wireless LAN and on-going cosmic-ray experiments.



Fig. 1. Norikura Observatory.

Present major scientific interests of the laboratory is focused on the modulation of high energy cosmic rays in the interplanetary space associated with the solar activity and the generation of energetic particles by the solar flares, both of which require long-term monitoring. This research has been carried out by the group of universities, where ICRR provides them with laboratory facility. A part of the facility has been open for the environmental study at high altitude such as the aerosol removal mechanism in the atmosphere or for the botanical study of the high altitude environment.

## 2. Cosmic Ray Physics

For the modulation study[2], two small experiments have been operated continuously for a long time. One is a neutron monitor operated to study the correlation of solar activity and the cosmic ray flux. The other is a high counting muon telescope consisting of 36 m$^2$ scintillation counters to study the time variation of cosmic rays with energies of 10–100 TeV over 20 years. The neutron monitor data are open to researchers worldwide as a world obsevation network point (WDC). The 5 years from 2000 corresponded to the solar maximum (2000) to a declining phase in the solar cycle 23. The sun spot number in 2004 is approximately one fourth of the those at maximum. Nonetheless, there occurred active cosmic-ray phenomena associated with Coronal Mass Ejection (CME). As regards solar cosmic rays, although many ground level enhancement (GLE) phenomena took place every year, such GLEs were observed only by neutron monitors in Japan, as the maximum cosmic-ray energy was several GeV in the GLEs and the magnetic rigidity cutoff in Japan is approximately 10 GeV for charged particles initiating secondary muons. The sunspot numbers in the solar cycle 23 was smaller than those in the previous cycle 22, indicating less solar activities of cycle 23. Although the GLEs above 10 GeV were not observed in cycle 23, the total number of GLEs were greater in cycle 23 than in cycle 22. This suggests that the charged particle acceleration associated with CME was less frequent in the cycle 23 than in the cycle 23. On the other hand, Forbush decreases in galactic cosmic rays caused by CME in the Sun were observed frequently in cycle 23, though the solar acitivities have been in a declining phase since 2000. The worldwide observation of Forbush decreases may contribute significantly to space weather study.

In addition, space weather observation is actively made by a 25 m$^2$ muon hodoscope at Norikura Observatory[1], [2],[3],[4],[5], [6],[7],[8]. A loss cone anisotropy is observed by a ground-based muon hodoscope in operation at Norikura Observatory in Japan for 7 hours preceding the arrival of an interplanetary shock at Earth on October 28, 2003. Best fitting a model to the observed anisotropy suggests that the loss cone in this event has a rather broad pitch-angle distribution with a half-width about 50° from the interplanetary magnetic field (IMF). According to numerical simulations of high-energy particle transport across the shock, this implies that the shock is a "quasi-parallel" shock in which the angle between the magnetic field and the shock normal is only 6°. It is also suggested that the leadtime of this precursor is almost independent of the rigidity and about 4 hour at both 30 GV for muon detectors and 10 GV for neutron monitors (see paper [7]).

The Sun is the nearest site to the Earth capable of accelerating particles up to high energies. When the Sun becomes active, flares are frequently observed on its surface. The flare accelerates the proton and ion to high energy and they are detected on the Earth soon after the flare. Among the particles generated by the flare, high energy neutrons provide the most direct information about the acceleration mechanism as they come straight from the flare position to the Earth without deflected by the magnetic field.

In 1990, Nagoya group constructed a solar neutron telescope consisting of scintillators and lead plates, which measures the kinetic energy of incoming neutrons up to several hundred MeV. This telescope observed high energy neutrons associated with a large flare occurred on the 4th of June, 1991. The same event was simultaneously detected by the neutron monitor and the high counting muon telescope of Norikura Observatory. This is the most clear observation of solar neutrons at the ground level in almost ten years since the first observation at Jungfraujoch in 1982.

A new type of the large solar neutron telescope (64 m$^2$ sensitive area) was constructed by Nagoya group in 1996. It consists of scintillators, proportional counters and wood absorbers piled up alternately. This takes a pivotal role among a worldwide network of ground based solar neutron telescopes of the same type in Yangbajing in Tibet, Aragatz in Armenia, Gornergrat in Switzerland, Chacaltaya in Bolivia and Mauna Kea in Hawaii. The Sun is being watched for 24 hours using this network.
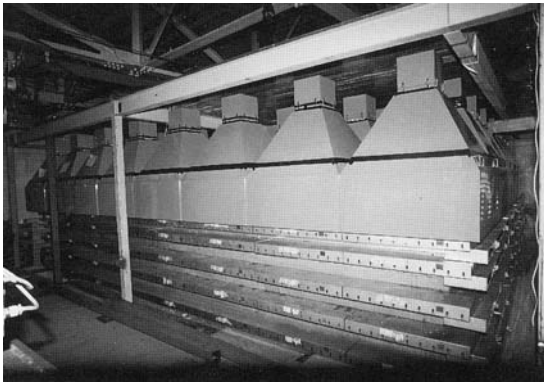


Fig. 2. New Solar-Neutron Telescope of Nagoya Group.

The Sun reached the maximum activity in 2000 and the active phase continued for the next few years. All the telescopes in Norikura Observatory, neutron telescope, neutron monitor, muon telescope and muon hodoscope, have been operated almost continuously through the solar cycle 23 in order to obtain comprehensive information on the solar flare phenomena. Important hints for understanding the mechanism of cosmic-ray acceleration near the solar surface will be obtained by these measurements, especially by energy spectra measured by the timing information of arriving neutrons and muons.

Furthermore, the relation between the electric fields induced by thunderclouds is studied recently[10]. The electric fields with thunderclouds change the intensity of secondary cosmic rays observed on the ground. This effect has been investigated using several detectors located at Norikura Ob-

servatory where excesses of 1 % and more of the average counting rate are observed when the observatory is covered with thunderclouds. A frequency analysis of the time series of days with such excesses for the period 26 October 1990 to 15 January shows the expected summer maximum in the rate of occurrence and, surprisingly, a 26-day variation. An electric field mill was installed to help determine the relationship between the intensity variations and the strength and direction of the field near the detector system: the excess is usually observed when a negative electric field (accelerating negative charges downward) greater than 10 kV/m is present in the atmosphere above the observatory. Based on Monte Carlo simulations, it is predicted that excess counting rates measured without charge discrimination will be expected as a consequence of the excess of positive muons among the secondary cosmic rays.

In addition to the long-term cosmic-ray observations mentioned above, various kinds of short-dated experiments are carried out every year taking an advantage of the high altitude of the observatory. A few examples include a search for super heavy particles with plastic plates, a precise measurement of atmospheric gamma rays and muons, collection of cosmic dusts contained in the snow and the performance study of the balloon borne cosmic ray experiments.

## 3.   Environmental Study

One of the interesting topics is atmospheric environment especially relating with atmospheric aerosol particles and water soluble gases. Because of its height, AC power supply, accommodation facility, and accessibility of cargos, the cosmic ray observatory at Mt. Norikura provides a very unique opportunity for atmospheric observation, especially for free-tropospheric conditions. (The atmosphere lower than a few kilometer is highly affected by the ground. This height level is named as 'atmospheric boundary layer'. The height of the boundary layer is about 4 km in daytime and about 2 km in nighttime around Norikura area. The atmosphere higher than this atmospheric boundary layer is called 'free troposphere'.) Originally, atmospheric observation at the cosmic ray observatory was initiated to study cosmogenic radionuclides with Prof. Suzuki at Shizuoka University. During early stage of the research at Mt. Norikura, a local effect of air contamination was recognized. To reduce air contamination from diesel exhausts and other activities around the observatory, an atmospheric observation hut (6 m$^2$) was installed at the west end (windward) of the observatory in September 1999. From year 2000, continuous monitoring (mostly mid-May to mid-October) of meteorology was started, number-size distribution of aerosols, dew point, aerosol chemical composition, ozone and radon concentrations, and column amount of aerosols from sky radiometer and ceilometer. Monitoring of ozone and radon concentrations was extended during 2 winters from 2001 to 2003. During summer season, also collected were rain, fog, water-condensed aerosol samples. These samples combined with other parameters were used in several the-

sis (master) works and provided useful information about future seeds of hygroscopic study of aerosols. During the past 5 years, the following results[11],[12],[13] were obtained at Mt. Norikura.

(1) Polluted air pumping effects over central Japanese Alps in summer

Under the clear sky conditions in summer, polluted air from mountain valley area is lifted up about 4km of altitude (1km above the mountain top) over Mt. Norikura. The height of observatory is within the atmospheric boundary layer in the daytime, and is out of (higher than) the atmospheric boundary layer in nighttime. The ratio of aerosol volume concentration for daytime (polluted valley wind) to nighttime (clean free-tropospheric) conditions was about 10. The air pumping effects over central Japanese Alps carry about 10 time higher concentration of aerosols to the free-troposphere over Japan in summer. Under the high-pressure system centered over the northwest Pacific in typical summer condition, backward air trajectories were originated from the northwest Pacific to Mt. Norikura and forward trajectories returned to the north Pacific with some deviations to east Russia and the Kurile Islands. The air pumping effects over mountain area provide a strong pollution source mechanism to the free-troposphere over the western Pacific region including East Asia.

(2) Seasonal variation of aerosol chemistry in free troposphere

An automated aerosol sampler was installed at the site in September 2000 to obtain seasonal aerosol samples. The sampler collected aerosols from mid-May to mid-October in 2001 and 2002. Results of its analysis showed seasonal changes in major and minor constituents of aerosols associating with changes of dominant air mass type over Japan.

(3) Vertical profiles of aerosols and clouds near the top of the atmospheric boundary layer

Ceilometer (lidar with small output energy) was installed in summer 2002, and was operated in 4 summer seasons. The aerosol and cloud profiles near the top of the atmospheric boundary layer have been observed. Some events of Asian dust, and of smoke from Siberian forest fire at lower free troposphere have been detected.

## 4. Botanical Study

It is predicted that ecosystems in high-latitudes and alpine regions are sensitive to global climatic warming. The significant increasing trends in air temperature are found in the Hida Mountains, where Mt. Norikura is located. Thus, effects of climatic change caused by global warming on alpine ecosystems must be urgently studied in the alpine region of central Japan. The Hida Mountains, strongly influenced by cold-air masses from Siberia in winter, receive some of the heaviest snowfall in the world. Due to heavy snowfall, dynamics of alpine ecosystems may be peculiar to the Hida Mountains. However, few studies have been made because of difficulty

in approach to the alpine study site. The inter-university research program of ICRR, gave an opportunity to make an intensive study all year around in the alpine region on Mt. Norikura[14],[15].

(1) Tree line dynamics

The tree form of evergreen sub-alpine fir (Abies mariesii) is studied at the upper distribution limit (2500m above sea level) on Mt. Norikura. Leader stems degenerate above the maximum snowpack line (3-4m high) , whereas branches below the snowpack line grow densely. In winter, leaves above snowpack line were severely damaged by environmental stresses, such as abrasion by wind-blown snow particles, desiccation, photoinhibition. Longevity of leaves was shortened to 4-5 years due to high mortality rate in winter. In contrast, leaves below snowpack line were protected from environmental stresses and their longevity was 11 years. As a result, biomass below the snowpack line takes more than 80with climate change should have unfavorable effects on tree line Abies mariesii.

(2) Alpine region

Pinus pumila, an alpine prostrated pine, is dominant in the alpine regions (2500∼3000m above sea level). At wind-protected sites, Pinus pumila grows vigorously with the tree height of 1-2m. They were beried in snowpack throughout the winter. At the wind-exposed ridge, growth is suppressed with the tree height of 0.2-0.5m. Throughout the winter, the surface of the pine community was exposed due to strong wind at the ridge. Leeward leaves were sound, because pine stems with high elasticity were prostrated and buried in snow. Thus, alpine pine can catch and accumulate snow to protect itself. This feature may be advantageous to alpine trees in comparison with sub-alpine trees (Abies mariesii). On the other hand, at the windward side (western), cuticular layer covering epidermal cells of leaf was abraded probably due to wind-blown snow and ice particles. By spring, abraded leaves at the windward side were dead caused by desiccation and photoinhibition. Even Pinus pumila community could reduce its habitat in small snowfall condition caused by global warming.

Impact of global warming due to so-called greenhouse gases like CO2, CH4 and others on vegetation ecology is among the most serious environmental issues. To investigate how plants response to global warming, an experiment of greenhouse effect on vegetation has been continued at a high mountain, Mt. Norikura (3,025 m a.s.l.), central Japan, since 1997. Five open-top chambers which are small greenhouses with a size of maximum open-top diameter, the maximum basal diameter and the height of the chamber were 47 cm, 85 cm and 30 cm, respectively, were set over alpine plant communities consisting of small woody plants and herbaceous vegetation. At places inside and outside of the chambers, seasonal changes in vegetation growth and phenology were observed every month. Using automatic data-recorders, some climate elements such as air and ground temperatures, humidity and rainfall have been observed every hour. Some results through the experiment were quite remarkable. Due to

the temperature enhancement of about 0.8 °C for air temperature and about 0.3°C for ground temperature, plant growth rates and phenological changes showed notable differences between inside and outside of the chambers. The responses to warming, however, were different by different plant species. The results suggest[16],[17] that dominant species in plant community should be replaced by the species with a high physiological response to warming and with a growing form extending tree crown.

## Bibliography

[1] "Precursors of geomagnetic storms observed by the muon detector networ", K. Munakata, J. W. Bieber, S. Yasue, C. Kato, M. Koyama, S. Akahane, K. Fujimoto, Z. Fujii, J. E. Humble, and M. L. Duldig, *J. Geophys. Res.*, Vol. 105, No.A12, pp. 27,457-27,468 (2000).

[2] "Solar cycle variations of modulation parameters of galactic cosmic- rays in the heliospher", K. Munakata, H. Miyasaka, I. Sakurai, S. Yasue, C. Kato, S. Akahane, M. Koyama, D. L. Hall, Z. Fujii, K. Fujimoto, S. Sakakibara, J. E. Humble, and M. L. Duldig, *Adv. Space Res.*, Vol.29, No.10, pp.1527-1532 (2002).

[3] "A 1.7 year quasi-periodicity in cosmic ray intensity variation observed in the outer heliosphere", C. Kato, K. Munakata, S. Yasue, K. Inoue, and F. B. McDonald, *J. Geophys. Res.*, Vol.18, No.A10, p.1367, doi:10.1029/2003JA009897 (2003).

[4] "Exploration of the heliosphere by cosmic rays", K. Munakata, published as the chapter 2 of *Advances in Solar-Terrestrial Physics*, pp.101-116, edited by H. Oya, published by TERRAPUB, Tokyo (2004).

[5] "Cosmic-ray modulation in the heliosphere: global and near-earth measurements and modeling", K. Munakata, Rapporteur paper in 28th *International Cosmic Ray Conference*, Vol.8, edited by T. Kajita et al., pp.251-276, Univ. Acad. Press, Tokyo (2004).

[6] "Geometry of an interplanetary CME on October 29, 2003 deduced from cosmic rays", T. Kuwabara, K. Munakata, S. Yasue, C. Kato, S. Akahane, M. Koyama, J. W. Bieber, P. Evenson, R. Pyle, Z. Fujii, M. Tokumaru, M. Kojima, K. Marubashi, M. L. Duldig, J. E. Humble, M. Silva, N. Trivedi, W. Gonzalez and N. J. Schuch, *Geophys. Res. Lett.*, Vol.31, L19803, doi:10.1029/2004GL020803 (2004).

[7] "A "loss-cone" precursor of an approaching shock observed by a cosmic-ray muon hodoscope on October 28, 2003", K. Munakata, T. Kuwabara, S. Yasue, C. Kato, S. Akahane, M. Koyama, Y. Ohashi, A. Okada, T. Aoki, H. Kojima and J. W. Bieber, *Geophys. Res. Lett.*, Vol.32, L03S04, doi:10.1029/2004GL021469, 2005.

[8] "CME-geometry and cosmic-ray anisotropy observed by a prototype muon detector network", K. Munakata, T. Kuwabara, J. W. Bieber, P. Evenson, R. Pyle, S. Yasue, C. Kato, Z. Fujii, M. L. Duldig, J. E. Humble, M. R. Silva, N. B. Trivedi, W. D. Gonzalez and N. J. Schuch, *Adv. Space Res.*, doi:10.1016/j.asr.2003.05.064, 2005, in press.

[9] "Acceleration below Thunder Clouds at Mount Norikura", by the Tibet hybrid experiment", Y. Muraki *et al.*, Proceedings in the 28th International Cosmic Ray Conference, (31 July - 7 August 2003, Tsukuba, Japan), Vol.7, pp 4177-4180.

[10] "Effects of atmospheric electric fields on cosmic rays", Y. Muraki *et al.*, Phys. Rev. D, **69**, 123010–1-13 (2004).

[11] K. Osada, M. Kido, C. Nishita, K. Matsunaga, Y. Iwasaka, M. Nagatani, H. Nakada, Changes in ionic constituents of free tropospheric aerosol particles obtained at Mt. Norikura (2770 m a. s. l.), central Japan, during the Shurin period in 2000, Atmos. Environ., 36, 5469-5477, 2002.

[12] "Atmospheric diffusion process based on time change of $^{222}$Rn vertical profile", K. Yoshioka, Journal of Aerosol Research, Japan, 17, 267-275, 2002 (in Japanese).

[13] "Free-tropospheric aerosols based on airplane and mountain observations", K. Osada, Journal of Aerosol Research, Japan, 15, 335-342, 2000 (in Japanese).

[14] "Diurnal changes in needle gas exchange in alpine Pinus pumila during snow-melting and summer seasons", A. Ishida, T. Nakano, S. Sekikawa, E. Maruta, T. Masuzawa, Ecological Research 16, 107-116 (2001).

[15] "Effects of high light and low temperature during harsh winter on needle photodamage of Abies Mariesii growing at the forest limit on Mt. Norikura in Central Japan", J. Yamazaki, A. Ohashi, Y. Hashimoto, E. Negishi, S. Kumagai, T. Kubo, T. Oikawa, E. Maruta, Plant Science 165, 257-264, (2003).

[16] "Chemistry of surface water at a volcanic summit area, Norikura, central Japan: Multivariate statistical approach", K. Anazawa and H. Ohmori, Chemosphere, 45, 807-816, (2001).

[17] "Experimental research on vegetation response to artificial warming on a mid-latitude high mountain, central Japan", H. Ohmori, J.H. Iguchi, T. Ohta, A. Terazono and K. Hikita, Geogr. Rev. Japan, 77, 301-320, (2004).

# AKENO Observatory

## Observatory

The Observatory is in Akeno town of Hokuto-city situated 20 km west of Kofu and 130 km west of metropolitan Tokyo. The location is at the longitude of 138.5 °E and the latitude of 35.5°N. The altitude is $\sim$900 m above sea level.

It was established in 1977 as a research center for air shower studies in the very high energy region. The Observatory has been administered by the ICRR as a facility of joint-university-use. An important part of observatory's scientific outputs originates from the university collaborators.

## From 1 km$^2$ Array to AGASA

The Akeno Air Shower Experiment started in 1979 with an array covering 1 km$^2$ area (1 km$^2$ array). The array was enlarged to 20 km$^2$ in 1985 and was gradually expanded to Akeno Giant Air Shower Array (AGASA) of approximately 100 km$^2$ area by 1990. The observation by AGASA continued for 13 years until the beginning of 2004.

One of the distinctive features of Akeno experiments is that the measurement was made over five decades of energies well covering $10^{15}$ eV - $10^{20}$ eV by using both the surface detector (for electromagnetic component) and the shielded detector (for muon component). This feature is well demonstrated in Fig.2; the spectra from Akeno 1 km$^2$ for $10^{14.7}$ eV - $10^{18.7}$ eV [1, 2] and AGASA for $10^{18.6}$ eV - $10^{20.3}$ eV [3] are plotted by open squares and solid circles in red. The wide energy coverage was accomplished by the arrays of scintillation detectors of various inter-detector spacings from 3 m to 1 km and with different triggering conditions.

The analysis had been made with similar algorithm under the same definition of single particle throughout the energy range covered. A difference exists however for the conversion method to the primary energy; the total number of electrons $N_e$ is used for 1 km$^2$ array and the local density at 600 m from the shower core S(600) is used for AGASA. A shift of $\sim$10% in energy is seen between AGASA and 1 km$^2$ array around $10^{18.5}$ eV. This is due to the difference of energy conversion methods employed by two experiments.

The parameter $N_e^{max}$ at the maximum of shower development is well known as one of the best primary energy estimators which does not depend sensitively on the interaction model or primary composition. The observed $N_e$ at Akeno was converted to $N_e^{max}$ experimentally with the longitudinal shower development curves determined with constant intensity cut method of integral $N_e$ spectra measured at Mt. Chacaltaya and at Akeno[1]. The result around the *knee* is consistent with all-particle spectra extrapolated from the direct measurements and those of recent results from Tibet[4] and KASCADE[5].

However, as seen in Fig.2, there are large discrepancies among experiments in the highest energy region. It should be noted that the systematic deviation among experiments already starts at $10^{17}$ eV. New data coming from TA and Pierre Auger will have to be understood in a consistent manner with existing lower energy data.



Fig. 1. Aerial View of Akeno Observatory and 1 km$^2$ Array Area

## Research and Development

Facilities of Akeno Observatory have been used for a variety of air shower studies, detector developments and associated researches. Activities of recent 6 years (2002 - 2007) are listed below.

- Study of EHECRs by AGASA by M.Teshima[a,b], N.Hayashida[a] and AGASA collaboration (2000-2005).

- Research and Development of Telescope Array Detectors by Y.Arai[c], M.Chikawa[d], M.Fukushima[a], K.Hashimoto[e], K.Honda[e], N.Inoue[f], F.Kakimoto[g], S.Ogio[g,h], H.Sagawa[a], M.Sasaki[a], Y.Tanaka[i], S.Yoshida[j] and TA collaboration (2000-2007).

- Observation of UHECRs with Lead-Burger Detector by K.Honda[e] et al. (2000-2003).

- Observation of Air Shower Core for E $> 10^{16}$ eV by H.Sakuyama[k] and N.Suzuki[k] et al. (2000-2004).

- Test Measurement of HE Cosmic Rays using Wide Angle Refractive Optics by H.Shimizu[l], S.Ebisuzaki[l] and EUSO collaboration (2001-2005).

- Energy Calibration of AGASA Event with Schmidt Type Air Fluorescence Telescope (CRIS) by S.Yoshida[j] et al. (2002).

- Measurement of Galactic Cosmic Ray Flux with Large Muon Telescope by S.Kawakami[h] et al. (2000-2007).

- Study of Cosmic Evolution by Quick Observation of GRBs by S.Kawai[g] et al. (2003-2007).

- On-line Observation of GRBs by Wide Angle Optical Telescope by T.Tamagawa[l] et al. (2003-2006).

- Chemical Composition of Primary Cosmic Rays for $10^{17}$eV $<$ E $< 10^{18}$eV by M.Nagano[m] et al. (2003).

- Research and Development for High Resolution All Sky Cosmic Ray Telescope by Y.Arai[c], M.Ieiri[c], R.Ogawa[n], M.Sasaki[a], Y.Tanaka[i], Y.Watanabe[g] et al. (2003-2005).
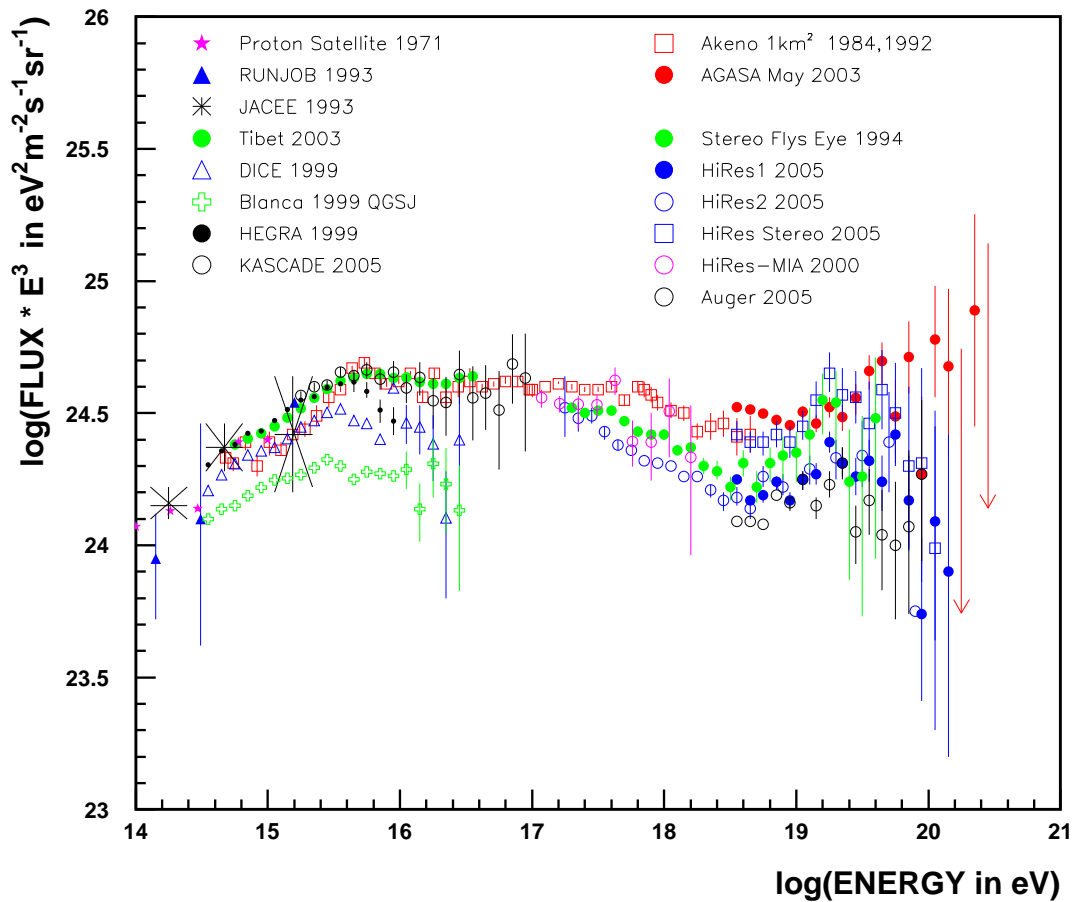
Fig. 2. Energy Spectra of Cosmic Rays between $10^{14}$ eV and $10^{20.3}$ eV. The data marked as "Auger 2005" and "HiRes Stereo 2005" were presented in the 29th ICRC in 2005, Pune.

- Effect of Cloud for Cosmic Ray Observation from Space by M.Nagano[m] et al. (2005).

a: Institute for Cosmic Ray Research, University of Tokyo
b: Max Planck Institute for Physics, Muenchen
c: Institute of Particle and Nuclear Studies, KEK, Tsukuba
d: Kinki University, Osaka
e: Yamanashi University, Kofu
f: Saitama University, Saitama
g: Tokyo Institute of Technology, Tokyo
h: Osaka City University, Osaka
i: Nagasaki Institute of Applied Science, Nagasaki
j: Chiba University, Chiba
k: Meisei University, Tokyo
l: Riken Institute of Physical and Chemical Research, Tokyo
m: Fukui University of Technology, Fukui
n: Toho University, Tokyo

This manuscript was prepared by M.Nagano and M.Fukushima.

## Bibliography

[1] M. Nagano et al., J. Phys. G: Nucl. Phys. **10**, 1295 (1984).

[2] M. Nagano et al., J. Phys. G: Nucl. Phys. **18**, 423 (1992).

[3] M. Takeda et al., Astropart. Phys. **19**, 447 (2003).

[4] M. Takita et al., ICRR Annual Report (2005) p.23.

[5] T. Antoni et al., Astropart. Phys. **24**, 1 (2005)

# KAMIOKA OBSERVATORY

Kamioka observatory is located at 1000m underground (2700 m water equivalent) in the Kamioka Mine, Gifu prefecture, about 200 km west of Tokyo. The observatory was established in 1995 in order to operate Super-Kamiokande. The underground laboratories are located under Mt.Ikeno-yama and accessible to the experimental site through a 1.7 km horizontal tunnel. The observatory also has surface research buildings and a dormitory located at the distance of 15 minutes drive from the entrance of the mine. The Super-Kamiokande experiment had discovered neutrino oscillations through the observations of atmospheric and solar neutrinos (see the section for Neutrino and Astroparticle Division). The atmospheric neutrino oscillation was confirmed by the K2K accelerator neutrino experiment, which was conducted between 1999 and 2004. A new long baseline neutrino oscillation experiment (the T2K experiment) using a high intensity beam, 50 times of the K2K neutrino beam, by the J-PARC proton accelerator, will inject first neutrino beam to the Super-Kamiokande detector in April, 2009.
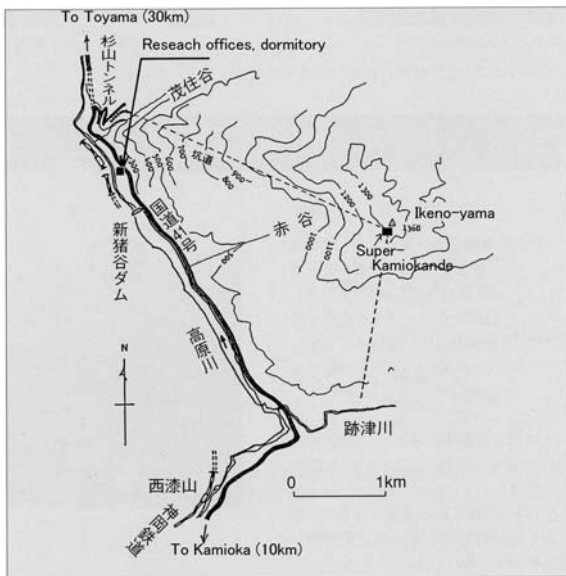


Fig. 1. Map of Kamioka observatory.

The low cosmic ray flux and low seismic noise environment in the underground site enables us to conduct various researches. There is a 100 m long laser interferometer, which is a proto-type of the planned 3 km gravitational wave antenna called LCGT, aiming to detect gravitational waves from extraterrestrial sources (see section of Astrophysics Gravity Division). Using the low radioactive background environment in the Kamioka Mine, A dark matter experiment, called XMASS is being prepared. The XMASS group has performed R&D study using a small proto-type detector and subsequently, the construction of the 800kg liquid xenon detector was started in 2007 and will be ready for data taking by the summer in 2009.

The R&D study of a tracking type detector for dark matter search by the Kyoto University group (the NEWAGE experiment) has also been performed in an underground laboratory. A double beta decay experiment, the CANDLE experiment (Osaka Univ.), is planned to be located in the Kamioka Underground Observatory. In order to support those experiments and also related R&D works, the Observatory is equipped with low background Germanium detector, ICP-MS and so on to measure extremely low radioactive backgrounds.
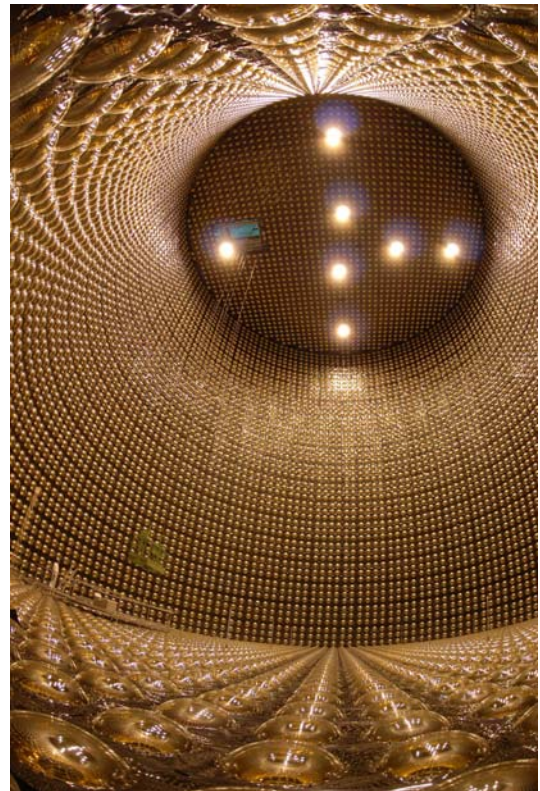


Fig. 2. Super-Kamiokande detector.



Fig. 3. 100 m baseline laser interferometers for gravitational wave and geophysics in Kamioka mine.

# RESEARCH CENTER FOR COSMIC NEUTRINOS

The Research Center for Cosmic Neutrinos was established in April, 1999. The main objective of this Center is to study neutrinos based on data from various observations and experiments. In order to promote studies of neutrino physics, it is important to provide the occasion to discuss theoretical ideas and experimental results on neutrino physics. Therefore, one of the most important practical jobs of this Center is the organization of neutrino-related meetings. On Sep. 30th and Oct.1st,, 2007, we organized 3rd International Workshop on a Far Detector in Korea for the J-PARC Neutrino Beam. This meeting was supported by JSPS (Japan) and KOSEF (Korea), and was held at the University of Tokyo. 47 participants discussed the potential physics of neutrinos by detecting neutrinos in Korea. In addition, members of this Center were the key members on the organization of "Workshop on Next Generation Nucleon Decay and Neutrino Detectors 2007 (NNN07)", which was held at Hamamatsu on Oct.2nd to 5th. The meeting was successful. On Nov. 2nd, 2007, we hosted one domestic neutrino workshop on "Recent neutrino oscillation data and the implications of the large-mixing angles". About 35 physicists participated in this meeting.

Members of this Center have been involved in the Super-Kamiokande, K2K and T2K experiments, carrying out researches in neutrino physics. Atmospheric neutrino data from Super-Kamiokande give one of the most precise pieces of information on neutrino oscillations. With increased data, it is more important to have better predictions of the neutrino flux. Therefore, in addition to data analysis of the above experiments, we work on predicting the atmospheric neutrino flux. In order to accurately predict this flux, it is important to know details of the data based on measurements of primary and secondary cosmic-ray fluxes. For this reason, we have a close collaboration with researchers working on cosmic-ray flux measurements.

It is important that the general public knows about the achievements in the present science. For this reason, we have a public lecture every year. In FY2007, the public lecture was held on April 7 (Sat) at Kashiwa. Two active scientists related to neutrino physics lectured on various aspects of neutrino physics. About 200 people heard the lectures.

This Center, together with the computer committee of ICRR, is in charge of operating the central computer system in ICRR. In FY2007, the computer system was upgraded by about a factor of 5 to 10 in the performance relative to the previous one.

Since 2004, this Center has been acting as the body for accepting the ICRR inter-university programs related to the low-background underground facility in the Kashiwa campus. The facility is currently equipped with 4 Ge detectors mainly for the measurements of cosmic radioactive isotopes. The scientific activities that are related to this facility is described elsewhere.



Fig. 1. Public lecture held in Kashiwa in April 7, 2007.



Fig. 2. New computer facility that have started its operation in FY2007.

# APPENDICES

### A. ICRR International Workshops

### B. ICRR Seminars

### C. List of Publications

 **(a) Papers Published in Journals**

 **(b) Conference Papers**

 **(c) ICRR Report**

### D. Doctoral Theses

### E. Public Relations

 **(a) ICRR News**

 **(b) Public Lectures**

 **(c) Visitors**

### F. Inter-University Researches

### G. List of Committee Members

 **(a) Board of Councillors**

 **(b) Executive Committee**

 **(c) Advisory Committee**

### H. List of Personnel

# A. ICRR International Workshops

## Workshop on Next Generation Nucleon Decay and Neutrino Detector 2007
Date: October 2-5, 2007
Place: Hamamatsu, Japan
(ICRR and KEK, and sponsored in part by Inoue Foundation for Science and HPK.)

### Outline

This series of workshops is organized to discuss about
- Nucleon decay searches
- Accelerator-based neutrino oscillation experiments
- Neutrinos from supernovae, atmosphere, and Sun
- Large detector technology
- Photosensors
... and others

### NNN07 Program Advisory Committee

E. W.Beier (Pennsylvania U.), V. Berger (Wisconsin U.), J.-E. Campagne (LAL Orsay), J. Ellis (CERN), F. von Feilitzsch (TU Munchen), D. Finley (Ferimilab), B. Kayser (Columbia U. and Ferimilab), M. Lindner (MPI Heidelberg), N. K. Mondal (TIFR Mumbai), L. Mosca (CEA Saclay), K. Nishikawa (KEK), A. Rubbia (ETH Zurich), K. Sato (U. of Tokyo), H. Sobel (UC Irvine), A. Suzuki (KEK), Y. Suzuki (ICRR), Y. Totsuka (KEK), J. Wilkes (U. of Washington), T. Yanagida (U. of Tokyo).

### NNN Steering Committee

C. K. Jung (Stony Brook U.), S. Katsanevas (IN2P3), K. Nakamura (KEK) .

### NNN07 Local Organization Committee

H. Aihara (U. of Tokyo), K. Hagiwara (KEK), Y. Hayato (ICRR), J. Hisano (ICRR), T. Kajita (co-chair, ICRR), K. Kaneyuki (scientific-secretary, ICRR), M. Nakahata (ICRR), K. Nakamura (co-chair, KEK), K. Okumura (ICRR), C. Saji (KEK), M. Shiozawa (ICRR).

### Participants

40 from Japan, 48 from USA, 5 from Germany, 3 from Italy, 2 from Korea, 1 from Canada, 1 from Switzerland, 1 from Russia, 1 from Poland.

# B. ICRR Seminars

| Date | Lecturer | Title |
|---|---|---|
| Apr 13, 2007 | Shigeki Matsumoto (Tohoku University) | " Hunting for the Top Partner in the Littlest Higgs Model with T-parity at the LHC " |
| Apr 19, 2007 | Mayumi Aoki (ICRR, University of Tokyo) | " Lepton Flavor Violating Tau Decay in the Left-Right Symmetric Model " |
| Apr 19, 2007 | Sergey Petcov (SISSA/INFN, Itary and IN-RNE, Bulgaria) | " Low-Energy Leptonic CP-Violation and Leptogenesis " |

| | | |
|---|---|---|
| Apr 26, 2007 | Teruaki Suyama<br>(ICRR, University of Tokyo) | " Primordial Non-Gaussianity in Multi-Scalar Slow-Roll Inflation " |
| May 22, 2007 | Jennifer Raaf<br>(Boston University) | " First Oscillation Results from MiniBooNE " |
| May 24, 2007 | Kin-ya Oda<br>(RIKEN) | " Possibility of black hole production at LHC " |
| Jun 1, 2007 | Edwin L. Turner<br>(Princeton University) | " An Astrophysicist's View of the Origin of Life Problem " |
| Aug 1, 2007 | Alexander Dolgov<br>(University of Ferrara, Italy /<br>ITEP, Moscow, Russia / ICRR) | " Antimatter in the Galaxy " |
| Aug 2, 2007 | Kendall Mahn<br>(Columbia Univ) | " Recent results and future plans for the Booster Neutrino Beamline " |
| Sep 10, 2007 | Hiroaki Yamamoto<br>(LIGO, Caltech) | " From Initial LIGO to Advanced LIGO " |
| Sep 10, 2007 | Carsten Rott<br>(Pennsylvania State University) | " Latest Results from the IceCube Experiment " |
| Oct 19, 2007 | Hansjoerg Dittus<br>(ZARM, University of Bremen) | " Gravitational Physics on the Post-Newtonian Level with Satellites " |
| Oct 24, 2007 | Rennan Barkana<br>(ICRR; University of Tel Aviv) | " Cosmology with 21-cm Radio Observations " |
| Oct 25, 2007 | Toshio Namba<br>(ICEPP, University of Tokyo) | " Tabletop experiments –QED, axion, and so on– " |
| Nov 1, 2007 | Kiyotomo Ichiki<br><br>(University of Tokyo) | " Creation of Magnetic Field and Gravitational Waves from Cosmological Density Perturbations, and their Ovservational Implications " |
| Nov 29, 2007 | Tokonatsu Yamamoto<br><br>(Konan University) | " Observation of Highest Energy Cosmic Ray by the Pierre Auger Observatory: status and prospective " |
| Jan 8, 2008 | Jozsef Kota<br><br>(Lunar and Planetary Laboratory, University of Arizona, Tucson, USA / ICRR) | " Acceleration of Energetic Particles at the Solar-wind Termination Shock: Lessons from Voyager 1 and 2 " |
| Jan 22, 2008 | Peter Wessels<br>(LZH, Germany) | " High power lasers for gravitational wave detection " |
| Mar 6, 2008 | Hidekazu Tanaka<br>(Columbia University) | " The SciBooNE neutrino experiment at Fermilab " |
| Mar 14, 2008 | Johannes Bluemer<br><br>(Karlsruhe Institute of Technology KIT / University and Forschungszentrum Karlsruhe) | " The Pierre Auger Observatory: results on ultra-high energy cosmic particles " |

# C. List of Publications — 2007 fiscal year

## (a) Papers Published in Journals

1. "Solar Neutrino Measurements in Super–Kamiokande–II", Super-Kamiokande Collaboration, Submitted to Phys. Rev. D, arXiv:0803.4312[hep-ex]. Additional information in http://www-sk.icrr.u-tokyo.ac.jp/sk/lowe/sk2 data/

2. "Search for Supernova Neutrino Bursts at Super-Kamiokande", Super-Kamiokande Collaboration, Astrophys J. 669 (2007) 519, arxiv:0706.2283[astro-ph].

3. "A measurement of atmospheric neutrino flux consistent with tau neutrino appearance", Super-Kamiokande Collaboration, Submitted to Phys. Rev. Lett., hep-ex/0607059.

4. "Search for Matter-Dependent Atmospheric Neutrino Oscillations in Super-Kamiokande", Super-Kamiokande Collaboration, Phys. Rev. D 77 (2008) 052001.

5. "Experimental study of the atmospheric neutrino backgrounds for proton decay to positron and neutral pion searches in water Cherenkov detectors", K2K Collaboration, *Phys. Rev. D.*, 77, 032003, 2008.

6. "CANGAROO-III Search for Gamma Rays from Centaurus A and the $\Omega$ Centauri Region", S. Kabuki et al., Astrophys. J. **668**, 968 (2007).

7. "CANGAROO-III Search for Gamma Rays from SN 1987A and the Surrounding Field", R. Enomoto et al., Astrophys. J. **671**, 1939 (2007).

8. "CANGAROO-III Observations of the 2006 Outburst of PKS2155-304", Y. Sakamoto et al., Astrophys. J. **676**, 113 (2008).

9. "Observation of an extended VHE gamma-ray emission from MSH $15-52$ with CANGAROO-III", T. Nakamori et al., Astron. Astrophys. **677**, 297 (2008).

10. "Observation of Very High Energy gamma rays from HESS J1804$-$216 with CANGAROO-III Telescopes", Y. Higashi et al., Astrophys. J. **683**, 957 (2008).

11. "CANGAROO-III Search for Gamma Rays from Kepler's Supernova Remnant", R. Enomoto et al., Astrophys. J. **683**, 383 (2008).

12. "Very high energy gamma-ray observations of the Galactic Plane with the CANGAROO-III telescopes", M. Ohishi et al., Astropart. Phys. **30**, 47 (2008).

13. "CANGAROO-III Search for TeV Gamma-Rays from Two Clusters of Galaxies", R. Kiuchi et al., submitted for publication (2008).

14. "Study on Machining of Large Acrylic Lens," Katsuta,T., Yokomizo,S., Sasaki, M., Journal of the Japan Society of Precision Engineering, **73**, No.2, 215-219 (Feb., 2007).

15. "All-sky Survey High Resolution Air-Shower Detector (Ashra)," Sasaki,M., Proceeding of International Workshop on Energy Budget in the High Energy Universe (ICRR, Kashiwa), edit. by Sato, K. and Hisano, J., 197-204 (March, 2007).

16. "Implication of the sidereal anisotropy of 5TeV cosmic ray intensity observed with the Tibet III air shower array", M. Amenomori *et al.*, Proceedings in AIP Conf. **932** 283–289, (2007).

17. "Underground water Cherenkov muon detector array with the Tibet air shower array for gamma-ray astronomy in the 100 TeV region", M. Amenomori *et al.*, Astrophysics and Space Science **309** 435–439, (2007).

18. "Moon Shadow by Cosmic Rays under the Influence of Geomagnetic Field and Search for Antiprotons at Multi-TeV Energies", M. Amenomori *et al.*, Astroparticle Physics **28** 137–142, (2007).

19. "New Estimation of the Spectral Index of High-Energy Cosmic Rays as Determined by the Compton-Getting Anisotropy", M. Amenomori *et al.*, ApJ **672** L53–L56, (2008).

20. "Current status of Japanese detectors", D. Tatsumi *et al*, Class. Quantum Grav. **24**(2007)S399.

21. "Multi-Slit Imaging Spectroscopy Technique: Catalog of Intracluster Planetary Nebulae in the Coma Cluster", Arnaboldi, M., et al., PASJ, 59, 419-425 (2007)

62

22. "The Peculiar SN 2005hk: Do Some Type Ia Supernovae Explode as Deflagrations", Phillips, M. M., et al., PASP, 119, 360-387 (2007)

23. "The kinematics of intracluster planetary nebulae and the on-going subcluster merger in the Coma cluster core", Gerhard, O., et al., A&A, 468, 815-822 (2007)

24. "Rest-Frame R-band Light Curve of a $z \sim 1.3$ Supernova Obtained with Keck Laser Adaptive Optics", Melbourne, J., et al., AJ, 133, 2709-2715 (2007)

25. "The Sloan Digital Sky Survey Quasar Catalog. IV. Fifth Data Release", Schneider, D. P., et al., AJ, 134, 102-117 (2007)

26. "Quantitative comparison between type Ia supernova spectra at low and high redshifts: a case study", Garavini, G., et al., A&A, 470, 411-424 (2007)

27. "A Catalog of Morphologically Classified Galaxies from the Sloan Digital Sky Survey: North Equatorial Region", Fukugita, M., et al., AJ, 134, 579-593 (2007)

28. "Spatial Variations of Galaxy Number Counts in the Sloan Digital Sky Survey. II. Test of Galactic Extinction in High-Extinction Regions", Yasuda, N., et al., AJ, 134, 698-705 (2007)

29. "Wide-Field Survey around Local Group Dwarf Spheroidal Galaxy Leo II: Spatial Distribution of Stellar Content", Komiyama, Y., et al., AJ, 134, 835-845 (2007)

30. "Sloan Digital Sky Survey Standard Star Catalog for Stripe 82: The Dawn of Industrial Optical Photometry", Ivezić, Ž., et al., AJ, 134, 973-998 (2007)

31. "The Fifth Data Release of the Sloan Digital Sky Survey", Adelman-McCarthy, J. K., et al., ApJS, 172, 634-644 (2007)

32. "Life Products of Stars", Serenelli, A. M., Fukugita, M., ApJS, 172, 649-662 (2007)

33. "Exploring the Variable Sky with the Sloan Digital Sky Survey", Sesar, B., et al., AJ, 134, 2236-2251 (2007)

34. "Supernovae in the Subaru Deep Field: an initial sample and Type Ia rate out to redshift 1.6", Poznanski, D., et al., MNRAS, 382, 1169-1186 (2007)

35. "The Sloan Digital Sky Survey-II Supernova Survey: Technical Summary", Frieman, J. A., et al., AJ, 135, 338-347 (2008)

36. "The Sloan Digital Sky Survey-II Supernova Survey: Search Algorithm and Follow-Up Observations", Sako, M., et al., AJ, 135, 348-373 (2008)

37. "The Sloan Digital Sky Survey Quasar Lens Search. III. Constraints on Dark Energy from the Third Data Release Quasar Lens Catalog", Oguri, M., et al., AJ, 135, 512-519 (2008)

38. "The Milky Way Tomography with SDSS. I. Stellar Number Density Distribution", Jurić, M., et al., ApJ, 673, 864-914 (2008)

39. "A New Determination of the High-Redshift Type Ia Supernova Rates with the Hubble Space Telescope Advanced Camera for Surveys", Kuznetsova, N., et al., ApJ, 673, 981-998 (2008)

40. "The Subaru/XMM-Newton Deep Survey (SXDS). VI. Properties of Active Galactic Nuclei Selected by Optical Variability", Morokuma, T., et al., ApJ, 676, 121-130 (2008)

41. "The Subaru/XMM-Newton Deep Survey (SXDS). V. Optically Faint Variable Object Survey'2", Morokuma, T., et al., ApJ, 676, 163-183 (2008)

42. "Lepton Flavour Violating tau Decays in the Left-Right Symmetric Model", A. G. Akeroyd, M. Aoki and Y. Okada, Phys. Rev. D **76** (2007) 013004

43. "Probing Majorana Phases and Neutrino Mass Spectrum in the Higgs Triplet Model at the LHC", A. G. Akeroyd, M. Aoki and H. Sugiyama, Phys. Rev. D **77** (2008) 075010

44. "Unitarity bounds in the Higgs model including triplet fields with custodial symmetry", M. Aoki and S. Kanemura, Phys. Rev. D **77** (2008) 095009

45. "Relic abundance of dark matter in universal extra dimension models with right-handed neutrinos," S. Matsumoto, J. Sato, M. Senami and M. Yamanaka, Phys. Rev. D **76** (2007) 043528 [arXiv:0705.0934 [hep-ph]].

46. "Neutralino Dark Matter in Light Higgs Boson Scenario," M. Asano, S. Matsumoto, M. Senami and H. Sugiyama, Phys. Lett. B **663** (2008) 330 arXiv:0711.3950 [hep-ph].

47. "Primordial Non-Gaussianity in Multi-Scalar Slow-Roll Inflation ", S. Yokoyama, T. Suyama and T. Tanaka, JCAP **07**, 013 (2007) [arXiv:0705.3178 [astro-ph]].

48. "Non-Gaussianity in the modulated reheating scenario", T. Suyama and M. Yamaguchi, Phys. Rev. D **77**, 023505 (2008) [arXiv:0709.2545 [astro-ph]].

49. "Primordial non-Gaussianity in multiscalar inflation,, S. Yokoyama, T. Suyama and T. Tanaka, Phys. Rev. D **77**, 083511 (2008) [arXiv:0711.2920 [astro-ph]].

50. "Non-Gaussianity, Spectral Index and Tensor Modes in Mixed Inflaton and Curvaton Models", K. Ichikawa, T. Suyama, T. Takahashi and M. Yamaguchi, To appear in PRD. (arXiv:0802.4138 [astro-ph]).

51. "Revisiting Signature of Minimal Gauge Mediation", J. Hisano and Yasuhiro Shimizu, Phys. Lett. **B** 655 (2007) 269-279.

52. "'Flavored' Electric Dipole Moments in Supersymmetric Theories", J. Hisano, M. Nagai and P. Paradisi, arXiv:0712.1285 [hep-ph].

53. "Nonthermal dark matter in mirage mediation", M. Nagai and K. Nakayama, Phys. Rev. D **76** (2007) 123501.

54. "Stability of Metastable Vacua in Gauge Mediated SUSY Breaking Models with Ultra Light Gravitino", J. Hisano, M. Nagai, M. Senami and S. Sugiyama, Phys. Lett. B **659** (2008) 361.

55. "Cosmological constraints on neutrino injection", T. Kanzaki, M. Kawasaki, K. Kohri and T. Moroi, Phys. Rev. D **76**, 105017 (2007).

56. "Affleck-Dine leptogenesis via multiscalar evolution in a supersymmetric seesaw model", M. Senami and T. Takayama, JCAP **0711** (2007) 015

57. "Formation of intermediate-mass black holes as primordial black holes in the inflationary cosmology with running spectral index", T. Kawaguchi, M. Kawasaki, T. Takayama, M. Yamaguchi and J. Yokoyama, arXiv:0711.3886 [astro-ph].

58. "Increasing effective number of neutrinos by decaying particles," K. Ichikawa, M. Kawasaki, K. Nakayama, M. Senami and F. Takahashi, JCAP **0705** (2007) 008.

59. "Baryon Asymmetry in Heavy Moduli Scenario," M. Kawasaki and K. Nakayama, Phys. Rev. D **76** (2007) 043502.

60. "Nonthermal dark matter in mirage mediation," M. Nagai and K. Nakayama, Phys. Rev. D **76** (2007) 123501.

61. "Cosmological implications of supersymmetric axion models," M. Kawasaki, K. Nakayama and M. Senami, JCAP **0803** (2008) 009.

62. "Space laser interferometers can determine the thermal history of the early Universe," K. Nakayama, S. Saito, Y. Suwa and J. Yokoyama, arXiv:0802.2452 [hep-ph], to be published in Phys. Rev. D.

63. "Solving Cosmological Problems of Supersymmetric Axion Models in Inflationary Universe," M. Kawasaki and K. Nakayama, arXiv:0802.2487 [hep-ph], to be published in Phys. Rev. D.

64. "Introducing neutrino mass into universal extra dimension models and solving cosmological problem", S. Matsumoto, J. Sato, M. Yamanaka and M. Senami, Int. J. Mod. Phys. E **16** (2007) 1571.

65. "The neutrino masses and the change of allowed parameter region in universal extra dimension models," S. Matsumoto, J. Sato, M. Senami and M. Yamanaka, arXiv:0711.2600 [hep-ph].

## (b) Conference Papers

1. Y. Takenaga, "Search for neutral Q-balls in Super-Kamiokande II", Workshop on Exotic Physics with Neutrino Telescopes, Uppsala, Sweden, Sep 20-22,2006,ISBN 978-91-506-1913-3 astro-ph/0701333 (2007)

2. Y. Obayashi, "SUPER-KAMIOKANDE: The Status of Neutrino Oscillations", in Conference Proceedings Vol. 93 "Frontier Objects in Astrophysics and Particle Physics" (Vulcano, Italy, May 22-27, 2006), F. Giovannelli & G. Mannocchi (eds.), SIF, Bologna 2007, ISBN 978-88-7438-034-3, p571-582

3. T. Kajita "Future neutrino oscillation physics in Japan", Proceedings of the Neutrino Osicllation Workshop (Nucl. Phys. B (Proc. Suppl.) 168, 155-160 (2007).)

4. T. Kajita "Updating the Future Long Baseline Experiment with the Kamioka-Korea two Detector Setup" Proceedings of Twelfth International Workshop on Neutrino Telescopes (2007), pp211-221.

5. M. Fukushima, "AGASA Results and the Status of Telescope Array", International Workshop on Energy Budget in the High Energy Universe, Feb. 22-34, 2006, Kashiwa, Japan.

6. M. Takeda, "The Telescope Array Experiment", Forty Years of the GZK Problem (GZK40), the 3rd International Workshop on the Highest Energy Cosmic Rays and Their Sources, May 16-18, 2006, Moscow.

7. H. Sagawa, "Status of the Telescope Array", 4th Korean Workshop on Origin, Propagation and Interaction of Energetic Particles, May 17-19, Daejon, Korea.

8. S. Yoshida, "The Present Status of the Telescope Array Project", Ultra-High Energy Cosmic Rays: Status and Perspectives (CRIS2006), May 29-June 2, Catania, Italy.

9. N. Sakurai, "Telescope Array Experiment", 14th International Conference on Supersymmetry and the Unification of Fundamental Interactions (SUSY06), June 12-17, Irvine, California.

10. M. Fukushima, "The Status of the Telescope Array", International Workshop "The UHE Universe; a vision for the next decade", June 19-21, Monteporzio Catone (Rome).

11. S. Ogio, "The Telescope Array Experiment", 14th International Symposium on Very High Energy Cosmic Ray Interactions, Weihai, China, August 15-22 2006.

12. K. Kasahara, "Measurement of Photons and Neutrons in the Very Forward Region at the LHC", 14th International Symposium on Very High Energy Cosmic Ray Interactions, Weihai, China, August 15-22 2006.

13. M. Fukushima, "Status of Telescope Array (TA)", International Workshop for Cosmic Ray and High Energy Universe, March 5-6, Aoyama, Tokyo.

14. K. Kasahara. "LHCf: Measuring Zero Degree Photons and Neutrons at LHC for Cosmic Ray Physics", International Workshop for Cosmic Ray and High Energy Universe, March 5-6, Aoyama, Tokyo.

15. S. Ozawa, "The Telescope Array experiment", International Symposium on Astronomy and Astrophysics of Extreme Universe, March 22-23, Riken.

16. M. Amenomori et al., "A large underground water Cherenkov muon detector array with the Tibet air shower array for the Gamma-ray astronomy in the 100 TeV region: detector design and simulation", Nuclear Physics B (Proc. Suppl.), 175-176, 480–483, (2008)

17. M. Amenomori et al., "A large underground water Cherenkov muon detector array with the Tibet air shower array for the Gamma-ray astronomy in the 100 TeV region: Overview and physics goal", Nuclear Physics B (Proc. Suppl.), 175-176, 476–479, (2008)

18. M. Amenomori et al., "Northern Sky Survey for Gamma-ray Point Sources in 100 TeV Region with the Tibet Air Shower Array", Nuclear Physics B (Proc. Suppl.), 175-176, 431–434, (2008)

19. M. Amenomori et al., "Spectral index of high-energy cosmic rays by the Compton-Getting effect at solar time frame with the Tibet air shower array", Nuclear Physics B (Proc. Suppl.), 175-176, 427–430, (2008)

20. "The cosmic-ray energy spectrum around the knee measured by theM. Amenomori et al., Tibet-III air-shower array", Nuclear Physics B (Proc. Suppl.), 175-176, 318–321, (2008)

21. M. Shibata for the Tibet AS$\gamma$ experiment", "Cosmic ray data and their interpretation: about the Tibet Air Shower Array - Chemical Composition of Cosmic Rays at the Knee Viewed from the Tibet Air Shower Experiment -, Nuclear Physics B (Proc. Suppl.), 175-176, 267–272, (2008)

22. D. Tatsumi *et al.*, "TAMA 300 interferometer development", TAUP 2007, September 11-15, 2007, Sendai.

23. K. Arai *et al.*, "Recent Progress of TAMA 300", TAUP 2007, September 11-15, 2007, Sendai; D. Tatsumi *et al* "Current status of Japanese detectors", Class. Quantum Grav. **24**(2007)S399.

24. H. Tagoshi *et al.*, "Results of Searches for inspiraling compact star binaries from TAMA 300fs observation in 2004-2004", TAUP 2007, September 11-15, 2007, Sendai.

25. N. Kanda *et al.*, "Short gravitational wave signal searches in TAMA 300 data: stellar collapse and black hole", TAUP 2007, September 11-15, 2007, Sendai.

26. M. Ohashi *et al.* "Status of LCGT and CLIO", TAUP 2007, September 11-15, 2007, Sendai.

27. K. Kuroda *et.al.*, "Current status of LCGT", Seventh Edoardo Amaldi conference on gravitational waves, Sydney, July 8-14, 2007.

28. S. Matsumoto, J. Sato, M. Senami and M. Yamanaka, "The neutrino masses and the change of allowed parameter region in universal extra dimension models," arXiv:0711.2600 [hep-ph].

29. J. Hisano, S. Matsumoto, M. Nagai, O. Saito and M. Senami, "Non-perturbative effect on thermal relic abundance of dark matter," AIP Conf. Proc. **957** (2007) 401.

30. J. Hisano, M. Nagai, M. Senami, S. Matsumoto and O. Saito, "Detection possibilities of thermally produced wino dark matter", 14th International Conference on Supersymmetry and the Unification of Fundamental Interactions, (SUSY06), (12-17 Jun 2006, Irvine, California), AIP Conf. Proc. **903** (2007) 575.

31. M. Nagai, "New two-loop contributions to hadronic EDMs in the MSSM", 13th International Symposium on Particles, Strings and Cosmology (PASCOS 07), (2-7 Jul 2007, London, England), AIP Conf. Proc. **957** (2007) 245.

32. J. Hisano, S. Matsumoto, M. Nagai, O. Saito and M. Senami, 13th International Symposium on Particles, Strings and Cosmology (PASCOS 07), (2-7 Jul 2007, London, England), "Non-perturbative effect on thermal relic abundance of dark matter", AIP Conf. Proc. **957** (2007) 401.

33. K. Ichikawa, M. Kawasaki, K. Nakayama, M. Senami and F. Takahashi, "Increasing the effective number of neutrinos with decaying particles," 13th International Symposium on Particles, Strings and Cosmology (PASCOS 07), AIP Conf. Proc. **957** (2007) 413.

## (c) ICRR Report

1. ICRR-Report-525-2007-1iFebruary 15, 2008j "Atmospheric neutrino oscillation analysis with solar terms in Super-Kamiokande" Yumiko Takenaga

# D. Doctoral Theses

1. "Atmospheric neutrino oscillation analysis with solar terms in Super-Kamiokande",
   Yumiko Takenaga, Ph.D. Thesis, RCCN, Mar. 2008.

2. "Search for TeV Gamma-ray Emission from Clusters of Galaxies with CANGAROO-III Imaging Atmospheric Cherenkov Telescopes",
   Ryuta Kiuchi, Ph.D. Thesis, CANGAROO, Mar. 2008.

3. "Study of optical properties of $Al_2O_3$ crystal for a gravitational wave telescope",
   Masao Tokunari, Ph.D. Thesis, Gravitational Wave, Mar. 2008.

4. "Search for continuous gravitational waves from PST J0835-4510",
   Tomomi Akutsu, Ph.D. Thesis, Gravitational Wave, Mar. 2008.

# E. Public Relations

## (a) ICRR News

ICRR News is a newspaper published quarterly in Japanese to inform the Institute's activities. This year's editors were K.Okumura and M.Ohashi. It includes :

1. reports on investigations by the staff of the Institute or made at the facilities of the Institute,

2. reports of international conferences on topics relevant to the Institute's research activities,

3. topics discussed at the Institute Committees,

4. list of publications published by the Institute [ICRR-Report, ICRR-Houkoku(in Japanese)],

5. list of seminars held at the Institute,

6. announcements,

7. and other items of relevance.

The main topics in the issues in 2007 fiscal year were :

**No.63** (Nov 30, 2007)

- Report on the Current Status of the Telescope Array (TA) Experiment, Hiroyuki Sagawa.

- Report on the 30th International Cosmic Ray Conference

  1. Ultra High Energy Cosmic Rays, Toshiyuki Nonaka.
  2. Ultra High Energy Gamma Rays, Kyoji Nishijima.
  3. Neutrino, Makoto Miura, Itaru Higuchi.
  4. High Energy Phenomena, .Masato Takita.
  5. SH, Yasushi Muraki.

- ICRR seminars.

- Self-introduction.

- Notice of Call for ICRR inter-University Researches in JFY2008.

**No.64** (Jan 31, 2008)

- Inflation and Initial Fluctuation of the Universe. Teruaki Suyama.

- Report on the ICRR Open House in JFY2007. Makoto Sasaki.

- Report on the Activity of the ICRR Public Relations Office at the Kashiwa Campus Open House in JFY2007 and the Exhibition Related to Neutrino in Nara Women's University, Hideo Itoh.

- Self-introduciton.

- Staff reassignment.

**No.65** (March 31, 2008)

- Didn't the Kepler's Supernova Remnant Produce Cosmic Rays Even If 400 Years passed after its Explosion?. Ryoji Enomoto, Tatsuo Yoshida.

- Recent Report on Tibet Experiment. Masato Takita.

- Report on the Meeting for Presenting the Results of Inter-University Researches in JFY2007. Yoshinari Hayato.

- ICRR-Seminar.

- ICRR-report.

## (b) Public Lectures

- "Public Lecture on Neutrino",
  April 7 2007, Kashiwa, Chiba,
  "Evolution of the Universe, Supernova neutrinos and the chemical elements", Toshitaka Kajino (National Astronomical Observatory of Japan, University of Tokyo).
  "Guft from the cosmos: Cosmic rays and atmospheric neutrinos", Takaaki Kajita (ICRR, University of Tokyo).

## (c) Visitors

KAMIOKA Observatory (Total: 114 groups, 2081 people)

- Yumeno Tamago Jyuku (Science camp for Junior High School Students)

- Yumeno Tamago Jyuku (Hida academy for High School Students)

- MEXT Super Science High School (SSH) project: total 2 schools

# F.   Inter-University Researches

## Researcher Numbers

|  | Application Numbers | Adoption Numbers | Researchers Numbers |
|---|---|---|---|
| Facility Usage |  |  |  |
| Kamioka Observatory | 39 | 39 | 554 |
| Norikura Observatory | 10 | 10 | 73 |
| Akeno Observatory | 4 | 4 | 96 |
| Emulsion and Air Shower Facilities in Kashiwa | 2 | 2 | 19 |
| Low-level Radio-isotope Measurement Facilities in Kashiwa | 6 | 6 | 35 |
| Gravitational Wave Facilities in Kashiwa | 4 | 4 | 94 |
| Over Sea Facilities | 16 | 16 | 153 |
| Other | 18 | 18 | 241 |
|  |  |  |  |
| Collaborative Researches |  |  |  |
| Cosmic Neutrino Researches | 35 | 35 | 502 |
| High Energy Cosmic Ray Researches | 45 | 45 | 516 |
| Theoretical Researches or Rudimental Researches | 9 | 9 | 167 |
| Research Center for Cosmic neutrinos | 10 | 10 | 80 |
|  |  |  |  |
| Others |  |  |  |
| Conferences | 3 | 3 | 55 |
| Special Activity on Abroad | 0 | 0 | 0 |

## Research Titles

1. Energy calibration for Super-Kamiokande

2. Study of solar neutrino energy spectrum

3. Study of simulation for atmospheric neutrino

4. Study of neucleon decay $p \rightarrow \nu K$

5. Study of the low energy solar neutrinos

6. Study of solar neutrino energy spectrum

7. Precise measurement of Day/Night effect for B8 solar neutrinos

8. Sidereal daily variation of 10TeV galactic cosmic-ray intensity observed by the Super-Kamiokande

9. Study for Supernova monitor

10. Development of the new online DAQ system for Super-Kamiokande

11. Study of flavor identification of atmospheric neutrinos

12. Study for the electron neutrino appearance search in the T2K experiment

13. Study in upward-going muons and high energy neutrinos

14. Study of Supernova Relic Neutrinos

15. Search for Nucleon Decay

16. Development of neutrino-nucleus interactions for the precise neutrino oscillation experiment

17. Search for proton decay via $e^+\pi^0$ mode

18. R&D of a 1 Mton water Cherenkov Hyper-Kamiokande

19. Study of atmospheric neutrinos and neutrino oscillations

20. Neutrino interaction study using accelerator data

21. R&D of J-PARC-Kamioka Long Baseline Experiment T2K

22. Study for lowering backgrounds of radioisotopes in large volume detectors

23. Direction-sensitive dark matter search experiment

24. Study of purification system for liquid xenon

25. Development of InP detector for measurement of solar $\nu$

26. Design of detector for dark matter search by using simulation

27. Study on absorption and scattering of vacuum ultraviolet light in liquid xenon

28. A study on emmission spectrum of liquid xenon

29. Study of ambient gamma-ray and neutron flux at Kamioka Observatory

30. Development of low concentration radon detection system

31. R&D for the Astroparticle Detector by using Liquid Xenon

32. 3-flavor Oscillation study in atmospheric neutrinos

33. Scintillation efficiency for the liquid xenon detector

34. Direct dark matter search with liquid xenon detector

35. Study for double beta decay of 48Ca

36. Study of the formation and the evolution of the Universe with prompt observations of gamma-ray bursts

37. Observation of Galactic Cosmic ray by the Large Area Muon Telescope

38. Observation of the highest energy Solar Cosmic Rays

39. Observation of solar neutrons in solar cycle 24

40. Ecophysiological studies of alpine plants

41. A Study of the Radiation Damage to Polyimide film

42. Space weather obsercation using muon hodoscope at Mt.Norikura

43. Continuous observation of microbarographs at high mountains

44. Study of particle acceleration in electric field using X and gamma rays from lightning and thunderclouds

45. Observation of nightglow and its reflected and scattered light on the mountain

46. Adaptive strategies in community structure and leaf characteristics of alpine plants related to snow gradient

47. Field test of natural electric power supply at Mt. Norikura-dake

48. Observation of high-energy cosmic-ray electrons with emulsion chambers

49. A study of cosmic ray interactions by hybrid experiment on Mt. Chacaltaya

50. Study of Galactic Diffuse Gamma Rays

51. Observation of TeV gamma-ray spectra from galactic objects

52. Data Analysis of the UHECR data for the Auger Project

53. Basic Study for Cherenkov Telescopes of Next Generation

54. A R&D for a new atmospheric monitoring system

55. Study of the composition of cosmic-rays at the knee

56. CANGAROO-III Observation of gamma-rays in the southern sky

57. Study of the emission mechanism of unidentified TeV gamma-ray source based on the multi-wavelength spectrum

58. Observation with All-sky Survey High Resolution Air-shower detector Ashra

59. Experimental Study of High-energy Cosmic Rays in the Tibet AS $\gamma$ experiment

60. Development of advanced photon counter for the future IACT

61. Sidereal daily variation of 10TeV galactic cosmic-ray intensity observed by the Tibet air shower array

62. Improvement of characteristics of the image sensor used in Ashra

63. Cosmic ray interactions in the knee and the highest energy regions

64. Bolivian Air Shower Joint Experiment

65. Application of Fast Image-delay Tube to Sky Survey for Cosmic Rays

66. Measurement of the temperature characteristics of YAP for TA fluorescence detectors

67. R&D for the Next Generation VHE Gamma-Ray Telescope

68. Observation of very-high-energy gamma-rays in Australia

69. Composition Study with the Telescope Array Data

70. Development of the optical fiber image transfer system for Ashra

71. A study on variation of interplanetary magnetic field with the cosmic-ray shadow by the sun

72. Workshop on '"High Energy Gamma-ray Astrophysics"

73. Optical observations of transient high-energy sources in the southern sky

74. Search for High Energy Gamma-ray Emission from Star Forming Regions and Theoretical Research

75. Improvement of the CANGAROO-III immediate data analysis system

76. Observation of UHE cosmic rays and TeV gamma rays with Ashra detector

77. Study of absolute energy calibration air shower by compact Electron LINAC

78. Study of radio detection of highest energy cosmic rays

79. Study of Extremely-high Energy Cosmic Rays by Telescope Array

80. Study on High Energy Cosmic-Ray source by Observation Using Long Duration Balloon

81. R&D and Design of large-scale cryogenic gravitational wave telescope (IX)

82. Study of effective thermal shielding method for the LCGT cryostat

83. Development of Sapphire Mirror Suspension for LCGT (IV)

84. Development of a high-power laser system for CLIO

85. Gravitational Wave Detector in Kamioka (VII)

86. digital Control of CLIO and Its Analysis

87. An research of the Earths free oscillations based on simultaneous observations with a laser strainmeter and a superconducting gravimeter

88. Evaluation of a fiber-coupled laser stabilizatino system

89. Evolution of the universe and particle physics

90. Deposition Rate variation of natural activities $^{7}$Be and $^{210}$Pb

91. Continuous Measurement of Underground Laboratory Environment

92. Chemical study for Antarctic micrometeorites

93. Determination of $^{2}$6Al in small Antarctic meteorite samples

94. Comprehensive Researches on Cosmic Dusts

95. Detection of time variations for cosmogenic Be-7, Na-22

96. Detection of low level radioisotopes in tree rings

97. Precise calculation of the atmospheric neutrino flux

98. Monte Calro Simulation Data Generation for the IceCube experiment

99. Neutrino workshop

# G. List of Committee Members

**(a) Board of Councillors**

| | |
|---|---|
| SUZUKI, Yoichiro | ICRR, University of Tokyo |
| KURODA, Kazuaki | ICRR, University of Tokyo |
| KAJITA, Takaaki | ICRR, University of Tokyo |
| FUKUSHIMA, Masaki | ICRR, University of Tokyo |
| YAMAMOTO, Masayuki | University of Tokyo |
| OKAMURA, Sadanori | University of Tokyo |
| TAKASAKI, Tadafumi | KEK |
| EGUCHI, Toru | YITP, Kyoto university |
| MIYAMA, Shoken | National Astronomical Observatory |
| SATO, Fumitaka | Kounan University |
| EJIRI, Hiroyasu | Osaka University |
| MURAKI, Yasushi | Kounan University |
| OHTA, Itaru | The Open University of Japan |
| INOUE, Hajime | Institute of Space and Astronautical Science |
| KOMAMIYA, Yukio | ICEPP, University of Tokyo |

**(b) Advisory Committee**

| | |
|---|---|
| SUZUKI, Yoichiro | ICRR, University of Tokyo |
| TORII, Shoji | Waseda University |
| MURAKI, Yasushi | Kounan University |
| TANIMORI, Toru | Kyoto University |
| KAWAKAMI, Saburo | Osaka City University |
| YANAGIDA, Tsutomu | University of Tokyo |
| NAGAE, Tomohumi | Kyoto University |
| NISHIKAWA Koichiro | KEK |
| NAKAMURA, Takashi | Kyoto University |
| MINOWA, Makoto | University of Tokyo |
| KURODA, Kazuaki | ICRR, University of Tokyo |
| FUKUGITA, Masataka | ICRR, University of Tokyo |
| FUKUSHIMA, Masaki | ICRR, University of Tokyo |
| MORI, Masaki | ICRR, University of Tokyo |
| NAKAHATA, Masayuki | ICRR, University of Tokyo |
| TAKITA, Masato | ICRR, University of Tokyo |

**(c) User's Committee**

| | |
|---|---|
| KAJINO, Fumiyoshi | Konan University |
| NISHIJIMA, Kyoshi | Tokai University |
| TORII, Shoji | Waseda University |
| Ogio, Shoichi | Osaka City University |
| MATSUBARA, Yutaka | Nagoya University |
| YOSHIDA, Shigeru | Chiba University |
| SAKURAI, Takahisa | Yamagata University |
| MUNAKATA, Kazuki | Shinshu University |
| OHASHI, Masataka | ICRR, University of Tokyo |
| HAYATO, Yosinari | ICRR, University of Tokyo |
| SAGAWA, Hiroyuki | ICRR, University of Tokyo |
| KANEYUKI, Kenji | ICRR, University of Tokyo |
| TAKITA, Masato | ICRR, University of Tokyo |
| HISANO, Junji | ICRR, University of Tokyo |

# H.   List of Personnel

| | |
|---|---|
| **Director** | SUZUKI Yoichiro |
| **Vice-Director** | KURODA Kazuaki |

## Kamioka Observatory(Neutrino and Astroparticle Division)

| | | | |
|---|---|---|---|
| Scientific Staff | SUZUKI Yoichiro, | NAKAHATA Masayuki, | MORIYAMA Shigetaka, |
| | TAKEUCHI Yasuo, | SHIOZAWA Masato, | HAYATO Yoshinari |
| | MIURA Makoto, | OBAYASHI Yoshihisa, | KOSHIO Yusuke, |
| | KAMEDA Jun, | TAKEDA Atsushi, | ABE Ko, |
| | SEKIYA Hiroyuki, | YAMADA Satoru, | NAKAYAMA Shoei, |
| | ITOH Yoshitaka, | KOBAYASHI Takashi, | |
| Chief Secretary | AKIMOTO Masatoshi, | | |
| Technical Staff | MIZUHATA Minoru, | KANBE Tomio, | KUMAMARU Seiichi, |
| | NAKAJIMA Tetsue, | | |
| Research Fellows | OGAWA Hiroshi, | WATANABE Hideki, | |
| Secretary | OKURA Youko, | MAEDA Yukari, | OKADA Eri, |

## Research Center for Cosmic Neutrinos(Neutrino and Astroparticle Division)

| | | | |
|---|---|---|---|
| Scientific Staff | KAJITA Takaaki, | KANEYUKI Kenji, | OKUMURA Kimihiro, |
| | SAKURAI Yoshihisa, | TSUKAMOTO Toshifumi, | |
| Technical Staff | SHINOHARA Masanobu, | | |
| Research Fellows | HIGUCHI Itaru, | | |
| Secretary | FUKUDA Yoko, | KITSUGI Atsuko, | |

## High Energy Cosmic Ray Division

| | | | |
|---|---|---|---|
| Scientific Staff | FUKUSHIMA Masaki, | MORI Masaki, | |
| | ENOMOTO Ryoji, | YOSHIKOSHI Takanori, | TAKITA Masato, |
| | SASAKI Makoto, | TAKEDA Masahiro, | HAYASHIDA Naoaki, |
| | OHISHI Michiko, | OHNISHI Munehiro, | |
| | ASAOKA Yoichi, | SAKURAI Nobuyuki, | |
| Technical Staff | AOKI Toshifumi, | KOBAYASHI Takahide, | |
| Research Fellows | OZAWA Shunsuke, | UDO Shigeharu, | TOKUNOU Hisao, |
| | SHIBATA Tatsunobu | SHIOMI Atsushi, | |
| | KONDO Yoshimi, | KAWATA Kazumasa, | HUANG Jing, |
| | WANG Xiao, | NONAKA Toshiyuki, | |
| | YAN Zhitao, | FABRICE Cohen, | |
| Secretary | SAWANO Sumiko, | KOKUBUN Yayoi, | YAMAKAWA Toshie, |
| | TATSUMI Fusako, | | |

## AKENO Observatory(High Energy Cosmic Ray Division)

| | | | |
|---|---|---|---|
| Scientific Staff | SAGAWA Hiroyuki, | | |
| Technical Staff | TORII Reiko, | OHOKA Hideyuki, | KAWAGUCHI Masami, |

## Norikura(High Energy Cosmic Ray Division)

| | | | |
|---|---|---|---|
| Technical Staff | YAMAMOTO Kuniyuki, | AGEMATSU Yoshiaki, | USHIMARU Tsukasa, |
| | ISHITSUKA Hideki, | SHIMODAIRA Hideaki, | |

## Astrophysics and Gravity Division

| | | | |
|---|---|---|---|
| Scientific Staff | FUKUGITA Masataka, | KURODA Kazuaki, | KAWASAKI Masahiro, |
| | OHASHI Masatake, | YASUDA Naoki, | HISANO Junji, |
| | MIYOKI Shinji, | UCHIYAMA Takashi, | |
| Research Fellows | YAMAMOTO Kazuhiro, | OKADA Atsushi, | ICHIKAWA Kazuhide, |
| | SENAMI Masato, | SUYAMA Teruaki, | AOKI Mayumi, |
| Secretary | SAKAI Akiko, | | |

| | | | |
|---|---|---|---|
| Graduate Students (Doctor) | IKEDA Daisuke, | KIDO Eiji, | TAKETA Akimichi, |
| | KIUCHI Ryuta, | YUKAWA Yohei, | SAKO Takashi, |
| | AITA Yuichi, | OKUMURA Akira, | NODA Koji, |
| | CHONAN Tsutomu, | | |
| | MINAMINO Akihiro, | TAKENAGA Yumiko, | UESHIMA Kota, |
| | IIDA Takashi, | MITSUKA Gaku, | NISHINO Haruki, |
| | ISHIHARA Chizue, | IKEDA Ittoku | |
| | TOKUNARI Masao, | AKUTSU, Tomomi, | NAKAGAWA Noriyasu, |
| | AGATSUMA Kazuhiro, | | |
| | NAGAI Minoru, | KANZAKI Toru, | TAKAYAMA Tsutomu, |
| | KONYA Kenichiro, | SEKIGUCHI Toyokazu, | NAKAYAMA Kazunori, |
| | KONISHI Kohki(M2), | | |
| Graduate Students (Master) | YAMAKAWA Yuichi, | | |
| | KUNISAWA Toshiki, | RYOKI Shinichi, | NAGAI Yuichiro, |
| | EGUCHI Makoto, | HIGASHI Yuhei, | |
| | UENO Koh, | NAKAJIMA Yuha, | HAZAMA Shunsuke, |
| | SAITOH Takanori, | MORIOKA Tomoko, | |
| | IMAI Yuta, | SUGIYAMA Shohei, | ARASHIBA Soichi, |
| | OKADA Takashi, | KAWAKAMI Etsuko, | |
| Administration Division Staff | NAGANEO Nobuyoshi, | SASADA Noriaki, | YAMAMOTO Tetsuya, |
| | IIDA Nobuyuki | AKIMOTO Mari, | IRIE Makoto, |
| | TASHIRO Megumi, | AKIYAMA Makiko, | SAITO Akiko, |
| | MATSUMOTO Kenichi | KITA Aiko, | KATO Yasuhiro, |
| | MARUMORI Yasuko | | |